Technical Memorandum 86-68330-2021-7

2020 Annual Report
Paradox Valley Seismic Network
Paradox Valley Unit, Colorado

Colorado River Basin Salinity Control Project
Upper Colorado Region

U.S. Department of the Interior **May 2021**

Mission Statements

The Department of the Interior (DOI) conserves and manages the Nation's natural resources and cultural heritage for the benefit and enjoyment of the American people, provides scientific and other information about natural resources and natural hazards to address societal challenges and create opportunities for the American people, and honors the Nation's trust responsibilities or special commitments to American Indians, Alaska Natives, and affiliated island communities to help them prosper.

The mission of the Bureau of Reclamation is to manage, develop, and protect water and related resources in an environmentally and economically sound manner in the interest of the American public.

Technical Memorandum 86-68330-2021-7

2020 Annual Report Paradox Valley Seismic Network

Paradox Valley Unit, Colorado

Colorado River Basin Salinity Control Project
Upper Colorado Region

Prepared by:

Bureau of Reclamation
Technical Service Center
Denver, Colorado

U.S. Department of the Interior **May 2021**

Acronyms and Abbreviations

dB	decibel
EPA	Environmental Protection Agency
ft	feet
g	standard acceleration of gravity, equivalent to 9.80665 m/s^2
GMPE	ground motion prediction equation
gpm	gallons per minute
km	kilometers
l/min	liters per minute
MASIP	Maximum Allowable Surface Injection Pressure
M_D	duration magnitude
Mgal	millions of gallons
M_L	local magnitude
MPa	MegaPascal
MSL	Mean Sea Level
M_W	Moment magnitude
NGA	Next Generation Attenuation (Model)
NW	Northwest
psi	pounds per square inch
PGA	peak ground acceleration
PVB	Paradox Valley Brine
PVSN	Paradox Valley Seismic Network
PVU	Paradox Valley Unit
SE	Southeast
UIC	Underground Injection Code
USGS	United States Geological Survey

Technical Memorandum 86-68330-2021-7

Technical Approval

The results provided in this report are technically sound and consistent with current Reclamation practice.

LISA BLOCK Digitally signed by LISA BLOCK
Date: 2021.05.18 10:54:41 -06'00'

Lisa Block, Geophysicist — Date

CHRISTOPHER WOOD
2021.05.18 11:01:14 -06'00'

Christopher Wood, Geophysicist — Date

GLENDA BESANA-OSTMAN Digitally signed by GLENDA BESANA-OSTMAN
Date: 2021.05.18 11:33:10 -06'00'

Glenda Besana-Ostman, Geophysicist — Date

JUSTIN SCHWARZER Digitally signed by JUSTIN SCHWARZER
Date: 2021.05.19 20:47:49 -06'00'

Justin Schwarzer, Geophysicist — Date

JUSTIN BALL Digitally signed by JUSTIN BALL
Date: 2021.05.20 06:16:18
-07'00'

Justin Ball, Geophysicist — Date

JONG BEOM KANG Digitally signed by JONG BEOM KANG
Date: 2021.05.18 11:46:31 -06'00'

Jong Boem Kang, Civil Engineer — Date

Peer Review Certification

This document has been reviewed and is believed to be in accordance with the scope of the service agreement and the standards of the profession.

FENG SU

Digitally signed by FENG SU
Date: 2021.05.19 13:41:06 -06'00'

Feng Su, Geophysicist

Date

Acknowledgements

The work described in this report and the continuous operation of the Paradox Valley Seismic Network (PVSN) are made possible through the considerable assistance and support of Andy Nicholas, site Project Manager at the Paradox Valley Unit, Bedrock, CO. We thank Eric Mccaffery for valuable technical support of the PVSN data acquisition computer systems.

Contents

Page

Tables

Page

Figures

Appendices

Technical Memorandum 86-68330-2021-7
2020 Annual Report
Paradox Valley Seismic Network

I. Introduction

The Paradox Valley Seismic Network (PVSN) monitors earthquakes induced by injection operations at the Bureau of Reclamation's (Reclamation) Paradox Valley Unit (PVU) deep disposal well, as well as local naturally occurring earthquakes. This report summarizes PVSN operations and the data recorded during calendar year 2020. We provide project background information in section II, including the history of PVU injection operations and details of the seismic network. In section III, we present PVSN network operations during 2020, including maintenance of the seismic stations and data acquisition systems and annual network performance. The earthquake data recorded during 2020 are discussed in section IV and compared to historical seismicity trends.

II. Project Background

A. Paradox Valley Unit

Reclamation's PVU, a component of the Colorado River Basin Salinity Control Project, intercepts salt brine that would otherwise flow into the Dolores River, a tributary of the Colorado River. PVU is in western Montrose County, approximately 90 km southwest of Grand Junction, Colorado and 16 km east of the Colorado-Utah border (Figure II-1). The Dolores River flows from southwest to northeast across Paradox Valley (Figure II-2), which was formed by the collapse of a salt-cored anticline (Figure II-3). Due to the presence of the salt diapir underlying Paradox Valley, groundwater within the valley is nearly eight times more saline than ocean water. To prevent this highly saline groundwater from entering the Dolores River and degrading water quality downstream, the brine is extracted from nine shallow wells within the valley near the Dolores River. The diverted brine is injected at high pressure into a deep disposal well, designated as PVU Salinity Control Well No. 1. The disposal well is located approximately 1.5 km southwest of Paradox Valley, near the town of Bedrock (Figure II-2).

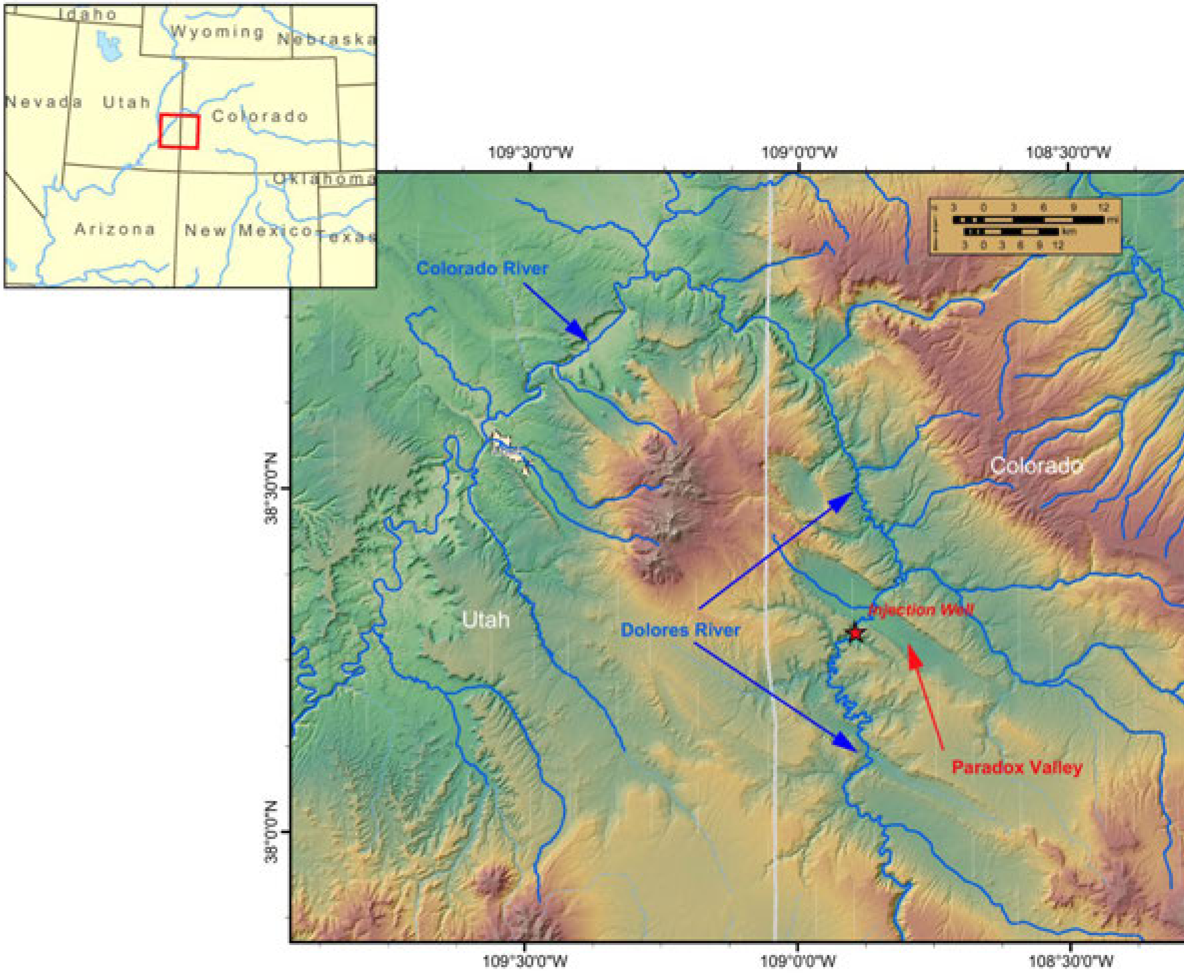

Figure II-1: Location of the deep injection well at Reclamation's Paradox Valley Unit in western Colorado (red star).

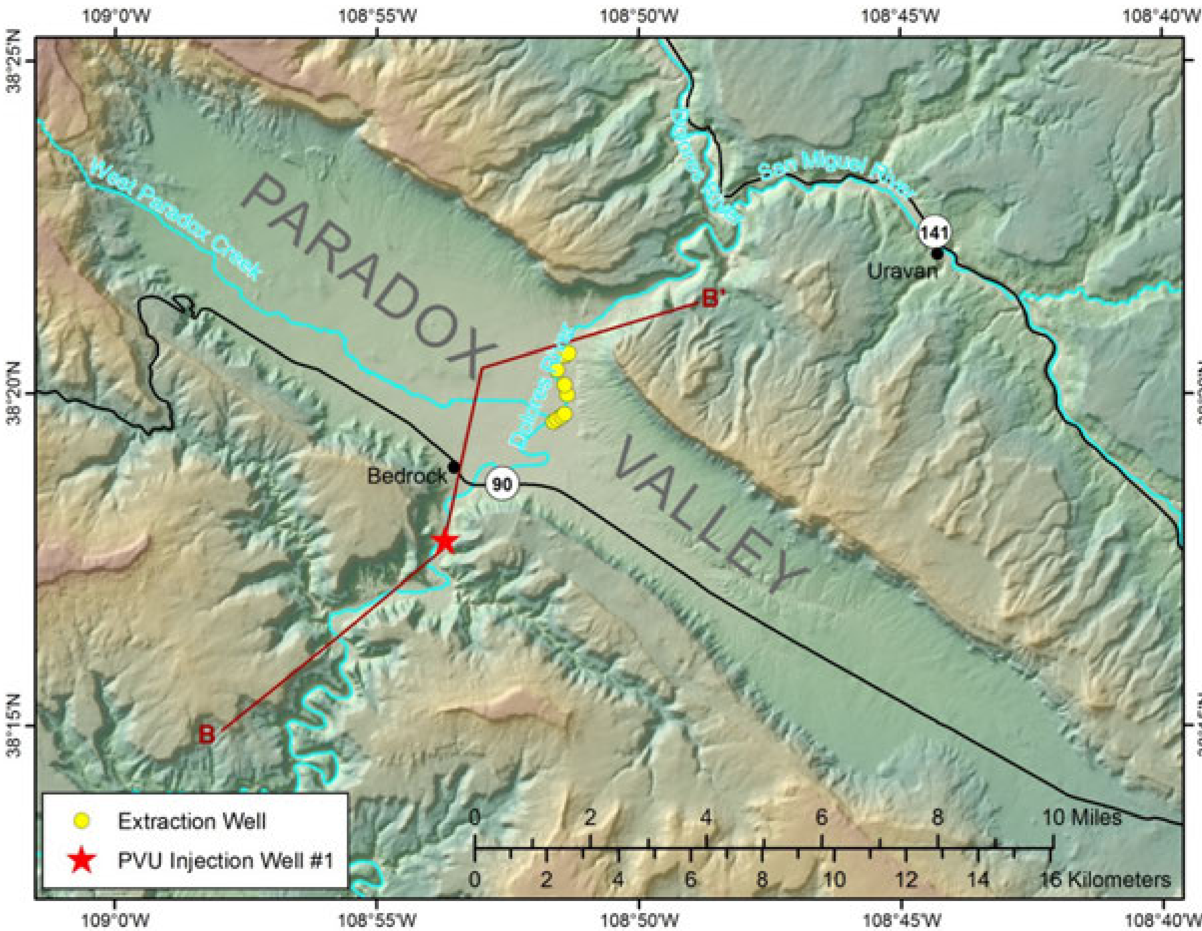

Figure II-2: Location of the Paradox Valley Unit extraction wells (yellow circles) and injection well (red star). Cross section B-B´ is shown in Figure II-3.

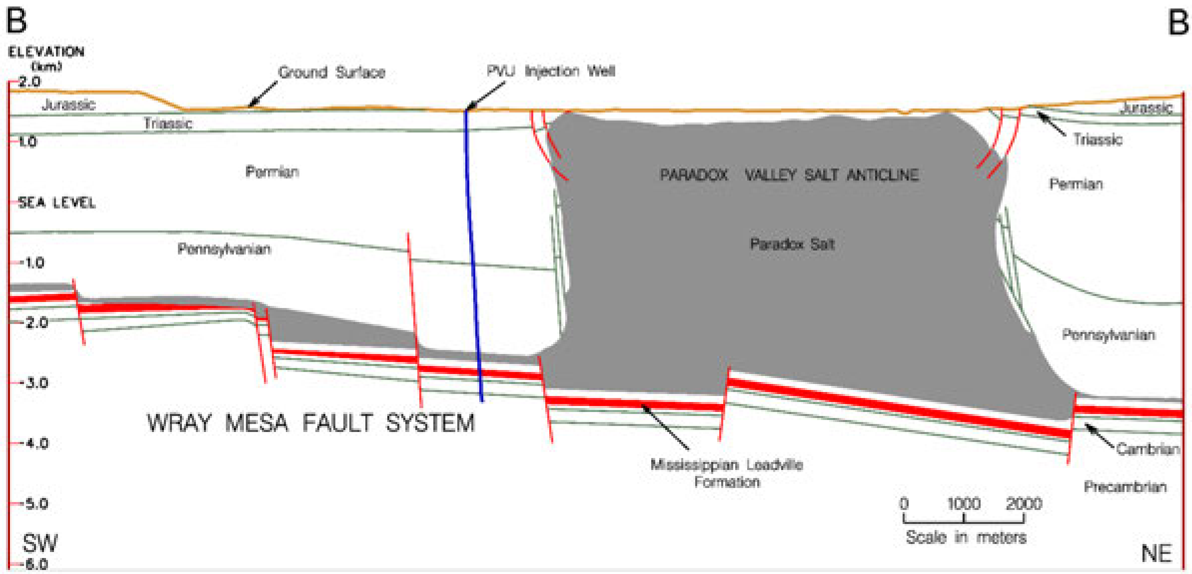

Figure II-3: Vertical cross section roughly perpendicular to Paradox Valley, looking to the northwest. The location of the cross section is shown in Figure II-2. Based on figure from (Bremkamp and Harr, 1988).

PVU Salinity Control Well No. 1 was completed in 1987 to a total depth of 4.88 km (approximately 16,000 ft). The well was built to Environmental Protection Agency (EPA) Underground Injection Code (UIC) Class I standards ("Isolate hazardous, industrial and municipal wastes through deep injection"), but was permitted in 1995 by EPA as a Class V disposal well ("Manage the shallow injection of non-hazardous fluids"). The well penetrates Triassic- through Cambrian-age sedimentary rock layers and granitic Precambrian basement (Figure II-3). Based on interpretation of regional core and log data, the Mississippian Leadville carbonate was selected as the primary injection zone with the upper Precambrian as a secondary zone (Bremkamp and Harr, 1988). The overlying Paradox salt formation acts as a confining layer. The well casing of PVU Well No. 1 (constructed of Hastelloy C- 276, a nickel-molybdenum-chromium alloy) was perforated at a spacing of ~20 perforations per meter in three major intervals between 4.3 km and 4.8 km depth. Plan and vertical views of the wellbore, with near-wellbore stratigraphy and the perforation intervals, are shown in Figure II-4.

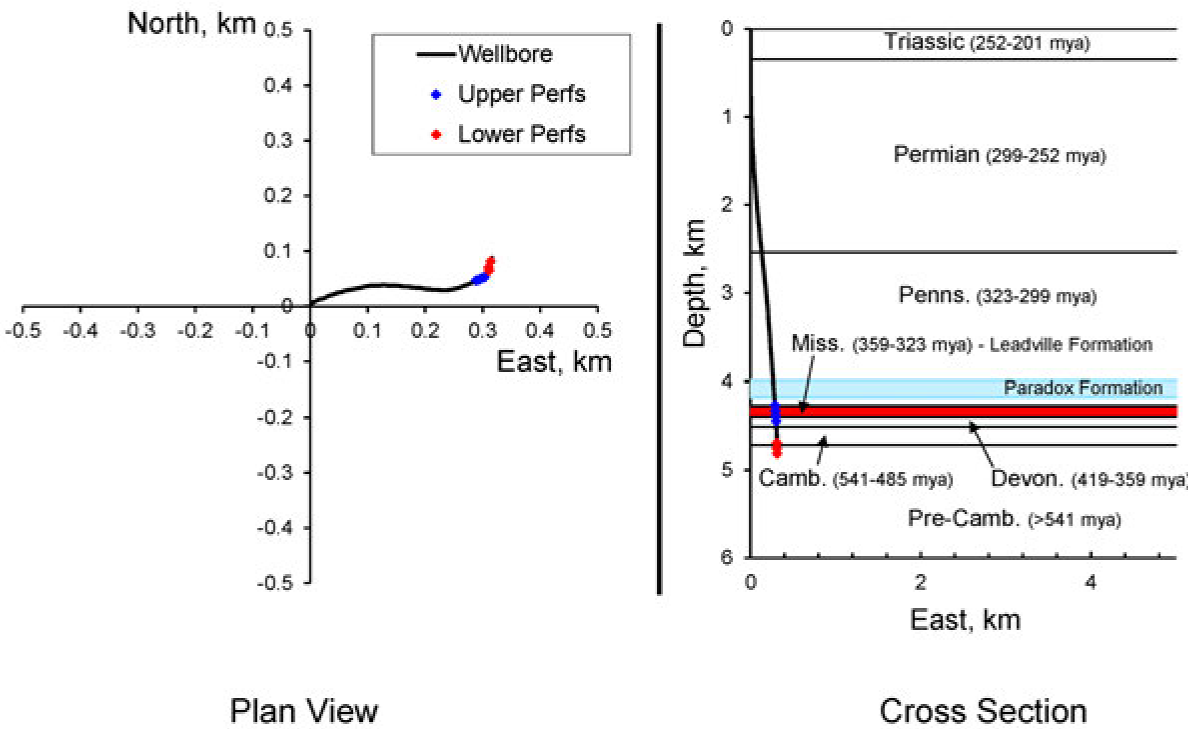

Figure II-4: PVU injection well in plan view (left) and north-viewing vertical cross section (right). Figure includes the near-wellbore stratigraphy and locations of the upper and lower casing perforations. The primary target injection formation, the Leadville, is shown in red, and the Paradox formation confining layer is shown in blue. The ages of the geologic time periods are taken from the Geological Society of America Geologic Time Scale version 4.0 (Walker et al., 2013). The ages shown represent the entire span of any given geologic time period and do not necessarily represent the precise ages of the rocks present at the PVU injection well.

B. PVU Injection Operations

Between 1991 and 1995, Reclamation conducted a series of seven injection tests, an acid stimulation test, and a reservoir integrity test at PVU. The purpose of these tests was to qualify for a Class V permit for deep disposal from the EPA. Near-continuous, long-term disposal of brine began in July 1996, after EPA granted the permit. During long-term injection, Reclamation instituted six major changes in operations. Five of these changes were implemented to mitigate the potential for unacceptable seismicity, and one change was made to improve injection economics. The seven time periods defined by these operational changes are considered separate injection phases and are described below. Plots of the daily average injection flow rates, daily average surface injection pressures, daily average downhole pressures (at a depth of 4.3 km), and cumulative injected fluid volumes during PVU injection operations are shown in Figure II-5. The downhole pressures shown were computed from measured surface pressures using the density of the brine column in the wellbore.

1. Phase I - July 22, 1996 to July 7, 1999

During this initial phase of near-continuous injection, brine was injected at a nominal flow rate of 345 gpm (~1306 l/min), resulting in an average surface pressure of about 4,950 psi (~34.1 MPa). This corresponded to approximately 11,800 psi (~81.4 MPa) downhole pressure at 4.3 km depth. To maintain this flow rate, three constant-rate pumps were used, each operating at 115 gpm. The surface pressure occasionally approached the wellhead pressure safety limit of 5,000 psi. This safety limit was based on the operational specifications of the injection and wellhead equipment. It also corresponded to the maximum allowable surface injection pressure (MASIP) defined in the injection permit issued by EPA, which is intended to prevent breach of the geologic confining layer (the Paradox salt). When the surface pressure approached the MASIP, the injection rate was reduced by shutting down one or two of the injection pumps, allowing the pressure to drop a few hundred psi before returning to a three-pump operation. These partial shutdowns occurred frequently and had typical durations of a few minutes to a few days. This operational protocol resulted in relatively constant surface and downhole pressures (Figure II-5). Periodic maintenance shutdowns of all pumps also occurred and lasted for one to two weeks. In mid-1997, a 71-day total shutdown was needed to replace the operations and maintenance contractors. The *Phase I* protocols resulted in an overall average injection rate of roughly 300 gpm (1136 l/min), and the total volume of fluid injected was 427 Mgal (1.6 x 10^9 liters).

The injectate during *Phase I* was a mixture of 70% Paradox Valley Brine (PVB) and 30% fresh water from the Dolores River. A geochemical study had predicted that if 100% PVB were injected, it would interact with connate fluids and the dolomitized Leadville Limestone at the initial formation temperatures and pressures, resulting in the precipitation of calcium sulfate. This precipitation in turn would lead to reduced permeability (Kharaka et al., 1997).

2. Phase II - July 8, 1999 to May 27, 2000

Following a local magnitude M_L 3.6 earthquake in June 1999 and an M_L 3.5 earthquake in July 1999, PVU altered the injection schedule to include a 20-day total shutdown (shut-in) every six months. Prior to these events, it was noted that the rate of seismicity in the near-wellbore region (i.e., within about a 2-km radius around the wellbore) decreased during and following unscheduled maintenance shutdowns. Similar decreases in seismicity also were observed during the shutdowns following the injection tests of 1991 through 1995. It was therefore hypothesized that the biannual shutdowns might reduce the potential for inducing large-magnitude earthquakes by allowing extra time for the injectate to diffuse from the pressurized fractures and faults into the formation rock matrix. When injecting during this phase, the average flow rate was the same as during Phase I. One hundred and eighteen Mgal (4.5 x 10^8 liters) of fluid were injected during Phase II.

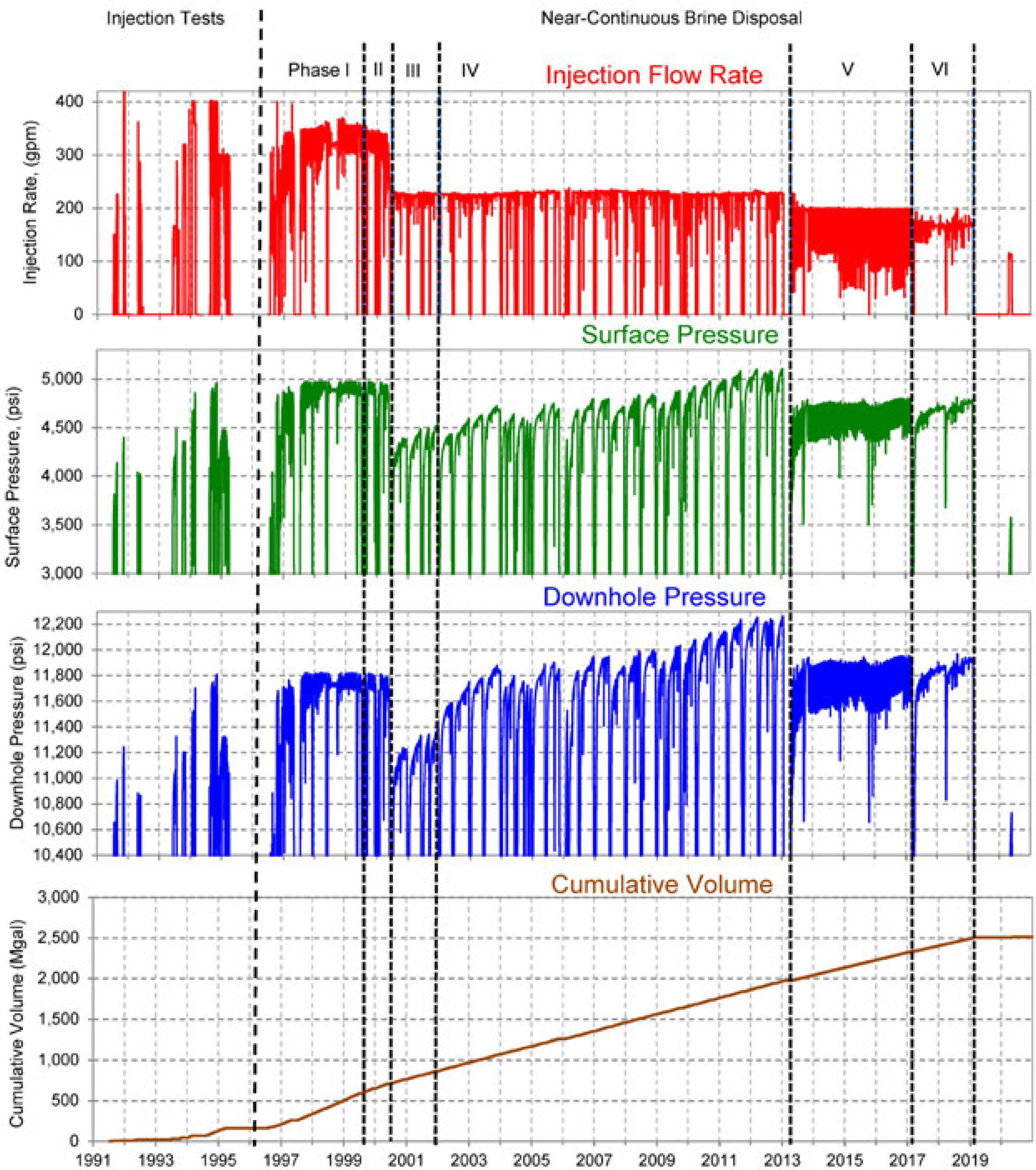

Figure II-5: Daily average injection flow rate, daily average surface injection pressure, daily average downhole pressure at 4.3 km depth, and cumulative volume of brine injected during PVU injection operations. The downhole pressures are computed from the measured surface pressures using the density of the brine column in the well. The vertical dashed lines delineate the injection phases discussed in the text.

3. Phase III - June 23, 2000 to January 6, 2002

Immediately following an M_L 4.3 earthquake on May 27, 2000, injection ceased for 28 days. During this shutdown period, Reclamation evaluated the existing injection protocol and its effect on induced seismicity. The decision was made to reduce the injection flow rate in the expectation that this change would likely reduce the potential for inducing large-magnitude earthquakes. On June 23, 2000, PVU injection resumed using two pumps rather than alternating between two and three pumps. The biannual 20-day shutdowns were maintained. The nominal flow rate during *Phase III,* while injecting using two pumps, was 230 gpm (~871 l/min). Accounting for the two 20-day shut-ins per year, the average injection flow rate was approximately 205 gpm (776 l/min), a decrease of about 32% compared to *Phase I*. During this phase, 156 Mgal (5.9 x 10^8 liters) of fluid were injected.

4. Phase IV - January 7, 2002 to January 24, 2013

During October 2001, the need to dilute PVB with fresh water prior to injection was re-evaluated. Lab testing of drill cores conducted in 1993 detected no evidence of precipitation or plugging for either a 70 % brine / 30 % freshwater mixture or for a 100 % brine mixture, at temperatures of 270 °F or 300 °F (Envirocorp Services and Technology Inc., 1993). In addition, temperature logging had been performed multiple times between 1992 and June 2001 and recorded substantial near-wellbore cooling at the depth of the Leadville Formation (~70° to ~130° F decrease) (Subsurface Technology, 2001). The temperature measurements recorded in the upper Leadville in 2001 indicted "a super-cooled buffer zone, some distance from the well, which will prevent the creation of conditions favorable to calcium sulfate precipitation" (Subsurface Technology, 2001, pg. 18). Hence, if precipitation were to occur, it would not be near the wellbore perforations where clogging might be a concern (Nicholas, 2001). In addition, the high PVU injection pressures would likely act to keep fractures open within the target injection formations, even if some precipitation were to occur (McKinley, 2001). Further analyses indicated that, if precipitation occurs, its maximum expected rate is ~8 tons of calcium sulfate per day (Mahrer et al., 2003). To put this amount into perspective, injecting at ~230 gpm and assuming a brine density of 9.86 lbs/gal (17% more dense than fresh water) results in a daily injection mass of ~1633 tons. The maximum expected precipitate therefore is only ~0.5% of the daily injection mass.

After considering this new information, the decision was made to begin injecting 100% PVB, to partially offset the reduction in salt disposal rates resulting from the decreased injection rate implemented in *Phase III.* Injection of 100% PVB began on January 7, 2002, following the December-January 20-day shutdown, and has been maintained since. The injection rate implemented in *Phase III* (230 gpm) and biannual 20-day shutdowns were continued. The volume of fluid injected during *Phase IV* was 1,110 Mgal (4.2 x 10^9 liters).

Because of the decreased flow rate in *Phase III* and *Phase IV* compared to the earlier phases, the surface pressure remained below the MASIP of 5,000 psi for over a decade (mid-2000 to 2011). Hence, there was no need to frequently alter flow rates, as had been done during *Phases I* and *II*. Nevertheless, the continued injection during *Phases III* and *IV* resulted in a trend of increasing maximum surface and downhole pressures (Figure II-5). In addition, because of the increased density of the 100% PVB injected during *Phase IV* over the 70% PVB / 30% fresh water mix injected previously, the computed downhole pressures increased by ~300 psi immediately following the change to 100% brine in January, 2002.

In response to the increasing surface injection pressures, Reclamation submitted a request to EPA in 2004 to increase the MASIP. EPA approved the request, pending infrastructure upgrades to increase the injection equipment pressure safety limit. In 2009, the PVU injection wellhead equipment was upgraded to a pressure safety limit of 10,000 psi. An increase in the MASIP to 5350 psi was formally incorporated into the injection permit reauthorization issued by EPA in August 2011.

5. Phase V - April 17, 2013 to March 12, 2017

An induced earthquake with M_L 4.4 (corresponding to moment magnitude M_W 4.0) occurred ~8 km northwest of the PVU injection well on January 24, 2013 (Block et al., 2014). In response to this earthquake, injection was halted while a reassessment of the seismic hazard associated with PVU injection was performed. Analyses of the seismic and injection data indicated that the potential for inducing large felt events would be reduced by decreasing the long-term average injection pressures (Block and Wood, 2009; Wood et al., 2016). Pressure-flow modeling indicated that reducing the flow rate would lead to a corresponding reduction in wellhead pressures. Forward modeling was used to evaluate the effect of different flow rates on wellhead pressures (Wood et al., 2016). In addition, the pressure-flow modeling indicated that changing the injection well shut-in schedule to one with shorter, more frequent shut-ins would result in a reduction in the average wellhead pressure, compared to the biannual 20-day shut-ins previously used.

As a result of these analyses, the decision was made in April 2013 to reduce the injection flow rate and increase the frequency of injection well shut-ins. Due to the lag time in obtaining pump plungers that would allow injection at a lower flow rate, injection was initially resumed on April 17, 2013, maintaining the flow rate at 230 gpm and implementing a 36-hour shut-in every week. On June 6, 2013, following the installation of the new plungers, the flow rate was reduced to 200 gpm and the shut-in length was reduced to 18 hours, maintaining the frequency of one shut-in per week. A shut-in duration of 18 hours was chosen so that the total annual shut-in time would be approximately equivalent to that scheduled previously with the biannual 20-day shut-ins. Hence, the nominal flow rate during *Phase V* (200 gpm) was decreased by 13 % from that during *Phase IV* (230 gpm), and the total duration of planned shut-ins remained the same.

Because of the frequency of the new shut-in schedule, the durations of any unplanned shut-ins (such as those periodically required for equipment maintenance) were tracked, and those hours were subtracted from the weekly scheduled 18-hour shut-ins. The durations of unplanned shut-ins had not been tracked and subtracted from the biannual 20-day shut-ins during earlier injection phases, and hence the total shut-in time during previous years had sometimes varied substantially, depending on the number and duration of unplanned shut-ins required. Hence, while the nominal flow rate during *Phase V* was decreased by 13% from that during *Phase IV*, the effective decrease in flow rate was less than this value due to the difference in total shut-in time. The average flow rate during *Phase V* was 177 gpm, which is ~9.7 % less than the average flow rate of 196 gpm during the preceding three years (2010-2012). Three hundred and sixty-four Mgal (1.4 x 10^9 liters) of fluid were injected during this phase.

6. Phase VI - April 8, 2017 to March 4, 2019

Beginning on March 12, 2017, the injection well was shut in for 27 days. Injection was resumed on April 8, at a ~5 % reduced effective flow rate. These changes were made partially in response to the observation that the rates and magnitudes of PVU-induced earthquakes had been increasing for ~1.5 years. The occurrence of an M_D 2.9 earthquake nearly 13 km from the injection well (on 3/12/17) further influenced the decision to reduce the effective flow rates.

The reduced effective flow rate was initially achieved by changing the size of the plungers from 2.000" to 1.875", which reduced the nominal flow rate from 200 gal/min to 174 gal/min. At the same time, the duration of the weekly shut-ins was reduced from 18 hours to 6 hours. Two pumps were run continuously, except for the weekly plant shutdowns. Considering the weekly shut-ins, the effective average flow rate was 168 gal/min.

In September 2017, premature wear of the new 1.875" plungers forced reinstallation of larger plungers in two of the three pumps (one 2.125" plunger and one 2.000" plunger). As a result, injection operations were changed to accommodate the larger plungers (and corresponding rate increase) by eliminating the six-hour weekly plant shutdown and starting daily pump shutdowns on the pumps with larger plungers. Weekly shutdown of the single pump with the 1.875" plunger continued. Injection was then continuous, with either one or two pumps running at any given time. The target daily injection volume was 242,000 gallons, corresponding to a target average injection rate of 168 gpm. Hence, the effective average flow rate remained the same as with the smaller plungers. The total volume of fluid injected during *Phase VI* was 167 Mgal (6.3 x 10^8 liters).

An induced earthquake with moment magnitude M_W 4.5 occurred ~1.6 km southwest of the PVU injection well on March 4, 2019 (Block et al., 2020b). This earthquake was the largest PVU-induced earthquake to date and was substantially larger than the M_W 4.0 earthquake of January 2013. More than 2,000 aftershocks occurred in the first five months following the main shock, resulting in the highest near-well seismicity rates in 20 years. Analyses indicate that aftershocks will continue to occur for several years, at gradually decreasing rates (Block et al., 2020b). The PVU injection well had been shut down for a few hours at the time of the M_W 4.5 earthquake, to accommodate equipment maintenance activities. The well remained shut down for more than a year, while detailed analyses of the M_W 4.5 earthquake and its numerous aftershocks were conducted. This extended shutdown also allowed formation pressures and aftershock rates to decay substantially.

7. Operations since March 2019

Injection resumed on April 21, 2020 for a planned six-month test period. The purpose of the test was to evaluate how the well would perform after being shut in for more than a year. Specifically, the pressure response of the well was monitored to determine whether any potential near-wellbore precipitation in the injection formations during the extended shutdown has altered the injection pressure response. In addition, seismicity was closely monitored for any changes in induced seismicity response to injection. Injection during this test was at a near-constant rate of 115 gpm, a 32% reduction compared to the flow rate during *Phase VI.*

The injection test was prematurely terminated on May 29, 2020, in response to a request by Reclamation management for an external peer review of injection operations. Preliminary analyses of data acquired during the 5 ½ weeks of injection suggest that the pressure response to injection may have degraded as a result of the prolonged injection well shut-in, but more thorough analyses are needed before conclusions can be drawn. In addition, a longer-term test may still be needed to thoroughly assess reservoir conditions. No change in the induced seismicity attributable to the injection test was observed. The well has remained shut down since May 29, 2020, while analyses of the injection and seismic data are continuing.

C. Seismic Monitoring

1. Paradox Valley Seismic Network

During the planning for PVU it was recognized that earthquakes could be induced by the high-pressure, deep-well injection of brine. This was based on comparison to other deep-well injection projects in Colorado, including the Rocky Mountain Arsenal, near Denver, and oil and gas extraction projects near Rangley (Gibbs et al., 1973; Hsieh and Bredehoeft, 1981; Nicholson and Wesson, 1990; Raleigh et al., 1976).

In 1983, eight years before the first injection at PVU, Reclamation commissioned a seismic monitoring network to characterize the pre-injection, naturally occurring seismicity in the Paradox Valley region, and to monitor earthquakes that might be induced once injection operations began. The Paradox Valley Seismic Network (PVSN) was the product of these efforts. Field equipment for an initial 10-station network was acquired and installed in 1983 by the U.S. Geological Survey (USGS), under a Memorandum of Agreement with Reclamation. Nine of these original seismic stations were vertical-component, and the remaining station (PV08) was three-component. All stations used short-period seismometers (natural frequency of 1 Hz), and analog telemetry. Continuous data recording and archiving began in 1985. For the first several years of monitoring, seismic data from this network were acquired and processed by the USGS at their facilities in Golden, Colorado. In 1990, responsibility for data acquisition and analysis was assumed by Reclamation. The USGS continued to assist Reclamation with the maintenance of the field instrumentation and radio telemetry.

PVSN has been upgraded and expanded several times, both to modernize its instrumentation and to improve coverage of seismically active areas. In addition, some stations have been de-commissioned, either due to repeated vandalism or changing telemetry requirements. The locations of the original and current PVSN seismograph stations are shown in Figure II-6. Details about the stations are provided in Table II-1, including dates of operation, station type, and number of components. Table II-2 lists the station location names.

Upgrade and expansion of the original 10-station continuously telemetered, high-gain seismic network began in 1989. First, a three-component station (PV11) was installed on the mesa just south of the injection well in order to provide better focal depth control and to allow for more sensitive event detection. Three vertical-component stations (PV12-PV14) were also added in 1989 to increase the density of stations surrounding the well. Station PV08 was downgraded in 1989 from a three-component station to a vertical-component only station, because it was determined that the equipment could be better used at the new stations closer to the injection well. Station PV15 was installed in 1995 to replace PV06, which had been vandalized in 1991, 1992, and 1994, when it was finally abandoned. A second three-component station (PV16) was installed on the mesa north of the injection well in 1999 to further improve near-well coverage.

In October 2000, a major upgrade to the data telemetry and acquisition was implemented. Up until this time, analog data from all stations had been radio-telemetered through PV08, which then relayed the data stream to Reclamation offices in Montrose, where it was transmitted via microwave and analog telephone links to Denver. In Denver, the analog data from all stations were digitized (using 12-bit digitizers) and processed. In October 2000, a wide-area network (WAN) link was established at the Hopkins Field Airport, near Nucla, Colorado, and new 16-bit digitizers were installed there. All analog radio links from the stations were reconfigured to terminate at Hopkins Field, and the use of analog telephone circuits to relay data was discontinued. Station PV08 was no longer used as a radio-telemetry relay. Station PV08 was temporarily removed in October 2003 to accommodate nearby construction activities and reinstalled in October 2007, at which time it was returned to a three-component configuration.

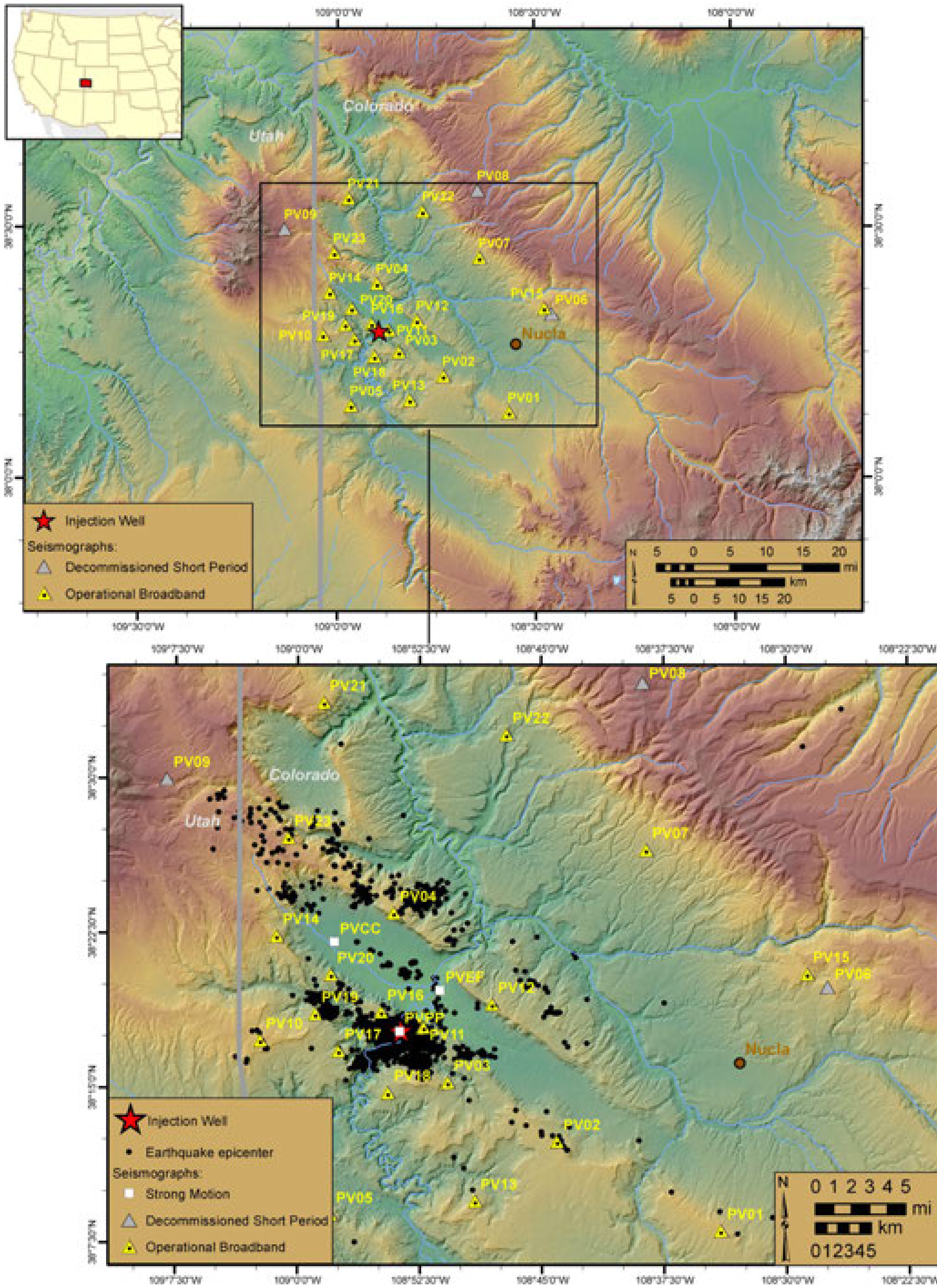

Figure II-6: Locations of the PVSN seismic stations, PVU injection well, and epicenters of earthquakes ≤ 10 km deep. PVCC, PVEF, & PVPP are the strong motion stations. Station PV06 was replaced by PV15. Stations PV08 and PV09 were decommissioned when the network was upgraded to broadband digital instrumentation.

Table II-1: PVSN Station Locations and Characteristics

Station Name	Latitude deg., N	Longitude deg., W	Elev. m	Dates of Operation	Station Type	Sensor Direction
PV01	38.13	108.57	2191	5/83-7/16/15 5/10-present	short-period broadband	vertical triaxial
PV02	38.21	108.74	2177	5/83-8/27/11 10/08-present	short-period broadband	vertical triaxial
PV03	38.25	108.85	1972	5/83-7/16/15 10/08-present	short-period broadband	vertical triaxial
PV04	38.39	108.90	2176	5/83-6/06 5/07-present	short-period broadband	vertical triaxial
PV05	38.15	108.97	2142	5/83-7/16/15 5/10-present	short-period broadband	vertical triaxial
PV06	38.33	108.46	2243	5/83-8/94	short-period	vertical
PV07	38.44	108.64	2040	6/83-8/27/11 5/10-present	short-period broadband	vertical triaxial
PV08	38.58	108.65	2950	6/83-9/89 9/89-10/03 10/07-7/12/11	short-period short-period short-period	triaxial vertical triaxial
PV09	38.50	109.13	2662	6/83-7/16/15	short-period	vertical
PV10	38.29	109.04	2266	6/83-7/16/15 10/08-present	short-period broadband	vertical triaxial
PV11	38.30	108.87	1882	12/89-10/13 10/08-present	short-period broadband	triaxial triaxial
PV12	38.32	108.80	2092	12/89-7/05 11/05-present	short-period broadband	vertical triaxial
PV13	38.16	108.82	2158	12/89-7/16/15 5/10-present	short-period broadband	vertical triaxial
PV14	38.37	109.02	2234	12/89-4/02 6/07-present	short-period broadband	vertical triaxial
PV15	38.34	108.48	2234	6/95-8/27/11 7/11-present	short-period broadband	vertical triaxial
PV16	38.31	108.92	2025	7/99-7/16/15 5/10-present	short-period broadband	vertical triaxial
PV17	38.28	108.96	1991	11/05-present	broad-and	triaxial
PV18	38.25	108.91	1999	7/11-present	broadband	triaxial
PV19	38.31	108.98	2041	7/11-present	broadband	triaxial
PV20	38.34	108.97	1852	7/11-present	broadband	triaxial
PV21	38.56	108.97	2235	7/11-present	broadband	triaxial
PV22	38.54	108.79	1925	7/11-present	broadband	triaxial
PV23	38.45	109.01	2456	11/11-present	broadband	triaxial

Station Name	Latitude deg., N	Longitude deg., W	Elev. m	Dates of Operation	Station Type	Sensor Direction
PVPP	38.30	108.90	1524	12/97-present	strong motion	triaxial
PVEF	38.33	108.85	1513	10/03-present	strong motion	triaxial
PVCC	38.37	108.96	1617	6/05-present	strong motion	triaxial
Notes: Elevations are relative to mean sea level (MSL). The surface elevation of the injection well is 1540 m above MSL. Stations with vertical sensor direction are single-component; triaxial are 3-component (vertical, north, and east).						

Table II-2: Location Names of PVSN High-Gain Sites

Station	Station Location Name
PV01	The Burn
PV02	Monogram Mesa
PV03	Wild Steer
PV04	Carpenter Flats
PV05	E. Island Mesa
PV07	Long Mesa
PV08	Uncompahgre Butte
PV09	North LaSalle
PV10	Wray Mesa
PV11	Davis Mesa
PV12	Saucer Basin
PV13	Radium Mtn
PV14	Lion Creek
PV15	Pinto Mesa
PV16	Nyswonger Mesa
PV17	Wray Mesa East
PV18	Skein Mesa
PV19	Morning Glory Mine
PV20	W. Nyswonger Mesa
PV21	Cone Mountain
PV22	Blue Mesa
PV23	Carpenter Ridge
PVPP	Paradox Valley Pumping Plant
PVEF	Paradox Valley Extraction Field
PVCC	Paradox Valley Community Center

Starting in 2005, upgrades to the high-gain seismic network focused on replacing the analog short-period seismic instrumentation with digital broadband instrumentation. The short-period instrumentation had become obsolete both in terms of the data quality needed for ongoing analyses, and in terms of maintaining equipment that was no longer manufactured. Two key characteristics of the instrumentation constrain data quality: bandwidth and dynamic range. The short-period instrumentation had an effective seismic signal bandwidth of 1-20 Hz. The low end of this range was determined by the natural frequency (1 Hz) of the seismometers used (Geotech model S-13), and the high end by the analog low-pass filter setting (nominally 25 Hz). The bandwidth of the analog stations was insufficient for many analysis purposes, such as accurately identifying complex seismic phases, accurately computing seismic moments of induced earthquakes (which require determination of long-period spectral levels), waveform modeling, or extracting time-domain Green's functions from ambient noise. Furthermore, the effective dynamic range of the analog stations constrained the ratio of the largest to smallest seismic signal that could be recorded on-scale to only a factor of about 1000, which corresponds to approximately two earthquake magnitude units. This resulted in seismic signals of earthquakes greater than about M 1.5 being clipped, which limited the use of this important data for magnitude and moment calculations, waveform cross-correlation, and identification of the S-wave arrival. Although 16-bit digitizers (with a dynamic range of 90 dB) were used after 2000, the effective dynamic range of the analog stations remained much less, approximately 10 or 11 bits (60 dB), because of the limited sensitivity of the voltage-controlled oscillators (VCOs) used at the stations to modulate the seismic signals onto the carrier tones used for analog radio telemetry. Modern broadband instrumentation provides much better characteristics, with typical bandwidths of 0.03 to 50 Hz, 24-bit digitizers providing a dynamic range of 135 dB or more, and seismometers typically packaged as a single unit with internal three-component sensors.

In November 2005, the first three-component broadband seismometer (Guralp model CMG-40TD) was installed at a new station southwest of the injection well (PV17). This instrument uses a 24-bit digitizer integrated within the seismometer case to minimize potential cable noise (digitizers and seismometers separated by a long analog cable can be sensitive to cross-talk at the microvolt level, which is difficult to protect against). Station PV12 was similarly upgraded at about the same time, and stations PV04 and PV14 were converted in May and July of 2007. These first-generation digital stations used digital radios that effectively behaved as a remote RS232 serial data link and which required the use of "combiner-repeater" modules (Guralp model CRM-6) to combine the serial signals from multiple stations. The first-generation stations exhibited a number of data quality problems, the most severe of which was crosstalk between the GPS antenna cabling (which provided timing for the internal digitizer) and the system providing power to the seismometer (O'Connell, 2008). The crosstalk inherent in the first-generation design resulted in significant spectral spikes in the data at frequencies of 1 Hz and greater, as illustrated in Figure II-7.

A new station design was developed in 2007 and 2008 based on experience from the first generation stations and from similarly instrumented seismic networks deployed at B.F. Sisk and Hungry Horse Dams (O'Connell, 2008). The new stations incorporated features to minimize the GPS antenna cable crosstalk problem, as well as to make the system more modular and robust. It included entirely new seismometer vaults, station enclosures, antennas, solar panels, and Ethernet packet radios. Deployment of the new instrumentation began in 2008, with upgrades of PV02, PV03, PV10, and PV11. In May 2010, stations PV01, PV05, PV07, PV13, and PV16 were upgraded. In July 2011, station PV15 was upgraded. In addition, six broadband digital seismic stations (PV18 to PV23) were installed at new sites in 2011. Two of these stations, PV22 and PV23, are replacements for old analog stations PV08 and PV09, which were decommissioned because they were noisy sites founded on thick alluvial deposits (all other sites are on rock). The other four new seismic stations (PV18, PV19, PV20, and PV21) were installed to improve coverage in seismically active areas of interest (including seismicity occurring within 9 km of the injection well and at the northern end of Paradox Valley).

The digital broadband upgrade of PVSN seismic stations was completed in late 2011. Consequently, Reclamation discontinued maintenance of the obsolete analog seismic stations. Four of those stations permanently went offline during 2011 (PV02, PV07, PV08, and PV15), and an additional analog station (PV11) ceased functioning in late 2013. The remaining analog stations were decommissioned in July 2014, when the data acquisition center at Hopkins Field was relocated into a new building.

During 2018, we began replacement of the Guralp model CMG-40TD broadband seismometers with Guralp model 3ESPCDE seismometers, as some of the original seismometers began to fail and were no longer supported. For example, compatible GPS antennas could no longer be obtained for the oldest CMG-40TDs in the network, making continued maintenance of the stations with these old instruments impractical. The 3ESPCDE seismometers have several advantages over the CMG-40TD seismometers, including substantially less self-noise, considerably less power usage than the oldest CMG-40TDs, and Ethernet capability for future communications upgrades. In April 2018, the CMG-40TD seismometers at stations PV02, PV10, PV18, PV20, and PV23 were replaced with new 3ESPCDE seismometers. The seismometers at stations PV12 and PV19 were upgraded in May 2019. The seismometers at the remaining stations were upgraded in September 2020 (PV03, PV04, PV05, PV11, PV13, PV14, PV15, PV17, PV21, PV22) and October 2020 (PV01, PV07, PV16).

In addition to the continuously telemetered high-gain seismic array, three event-triggered strong-motion instruments were added to PVSN. The first strong-motion instrument (station name PVPP) was installed near the PVU injection wellhead in December 1997. A second strong-motion instrument was installed near the PVU extraction facilities (PVEF) in January 1998, and the third was installed at the nearby community of Paradox, Colorado (PVCC) in June 2005. Telemetry for the strong-motion instruments was provided by dial-up phone line. The strong-motion array is designed to measure earthquake ground motions that are large enough to be felt or cause damage and which could saturate high-gain array stations closest to the epicenter.

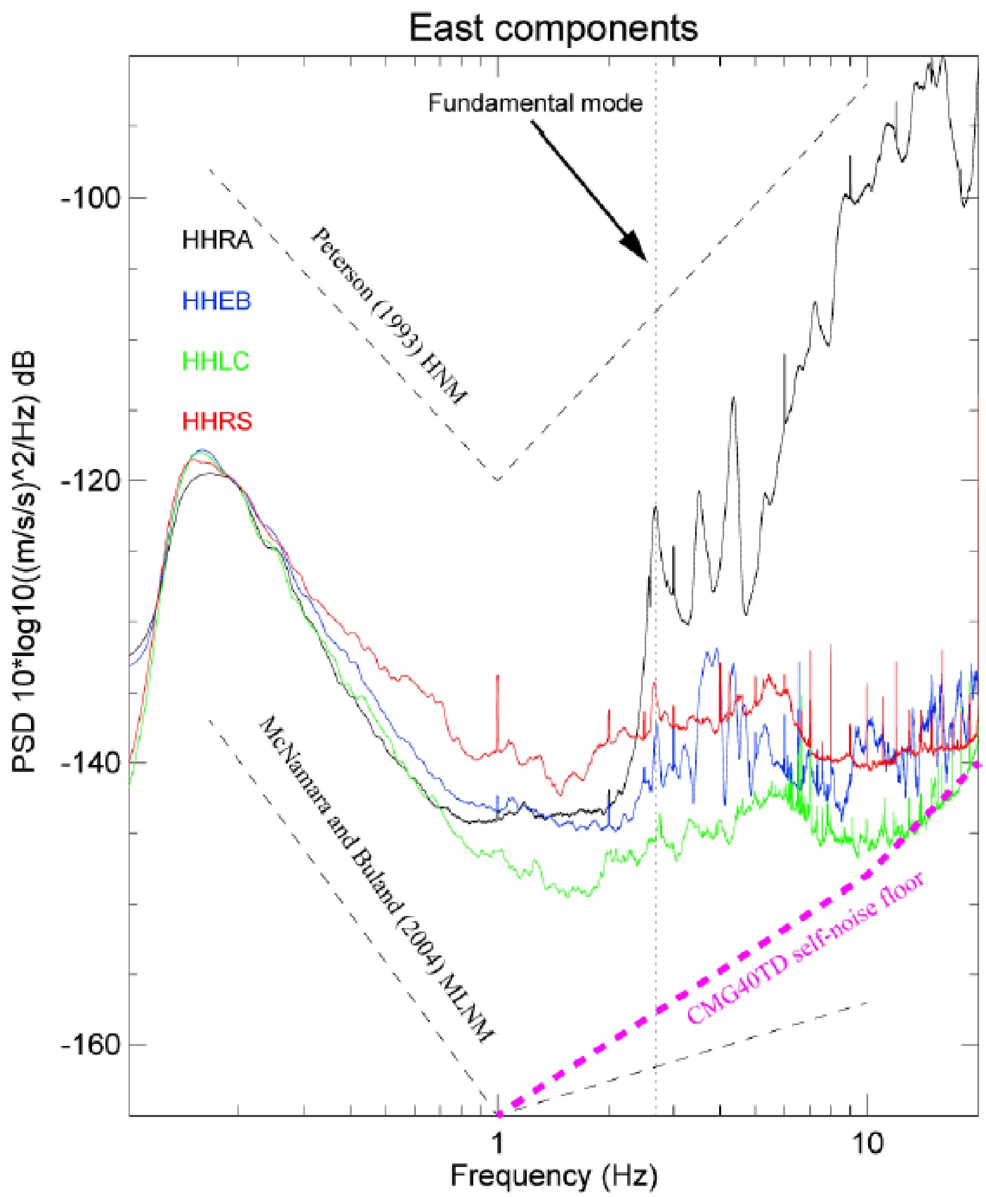

Figure II-7: Stacked multi-taper acceleration power spectra from the east-west components of Guralp model CMG40TD seismometers installed at four first-generation stations (HHRA, HHEB, HHLC, and HHRS) near Hungry Horse Dam, Montana. Windows were 400 seconds in length and represented ambient conditions (station HHRA was located close to power generation plant at the dam, and therefore exhibited much higher ambient noise levels at frequencies above 2 Hz). The obvious spikes in the spectra at frequencies of 1 Hz and higher were caused by GPS antenna crosstalk problems inherent in the first-generation stations. A new station design was implemented at PVSN to substantially reduce these crosstalk problems. Figure from (O'Connell, 2008).

The original instruments at PVPP and PVEF consisted of 12-bit data loggers (Kinemetrics model SSA-2 and Syscom model MR2002) and three-component force-balance accelerometers (FBAs), with the digitizers only approximately synchronized to Coordinated Universal Time (UTC). In November 1999, station PVEF was upgraded to use an 18-bit digitizer (Kinemetrics model K2), which was synchronized to UTC using a GPS receiver. Station PVPP was similarly upgraded in October 2003. Station PVCC had used a K2 data logger since its original installation in 2005.

On February 28, 2019, the K2 was removed from station PVEF, and three different data loggers and accelerometers were installed for a temporary side-by-side comparison study. These included the following instruments: (1) Reftek model RT130 data logger with Silicon Audio model 203V accelerometer, (2) Reftek RT130 data logger with Nanometrics model Titan accelerometer, and (3) Guralp model Minimus data logger with Guralp model Fortis accelerometer. A wireless TCP/IP bridge was installed to provide continuous real-time radio telemetry. In May 2019, the Silicon Audio sensor and Reftek digitizer were removed, and the Titan sensor was replaced with a similar unit with an internal digitizer. From May 2019 to October 2020, the Guralp instruments and the Nanometrics Titan with internal digitizer were run side-by-side at PVEF, with continuous telemetry.

Following the testing of strong motion sensors and digitizers in 2019-2020, the decision was made to upgrade all strong motion sites using a Silicon Audio model 203V accelerometer and a Guralp Minimus digitizer. These upgrades were implemented in October 2020. At the same time, real-time radio telemetry was established for stations PVPP and PVCC. The real-time data from all three strong motion sites are integrated with the data from the high-gain broadband sites at the PVSN communication center at Hopkins Field in Nucla, Colorado.

2. Induced Seismicity

Nearly 10,600 relatively shallow (≤ 10 km deep) earthquakes have been recorded in the vicinity of Paradox Valley since injection began in 1991. No shallow earthquakes were detected in six years of seismic monitoring prior to the start of injection operations. Most of these events have focal depth estimates between approximately 2.5 and 6.5 km (relative to the ground surface elevation at the PVU injection wellhead), close to the depth of the injection interval (4.3 to 4.8 km). The seismicity has been observed at increasing distance from the injection well over time (Figure II-8). The initial earthquakes were detected just four days after the start of the first injection test in July 1991 and occurred very close to the injection well. As injection continued, earthquakes occurred at progressively increasing radial distances. By 2002, earthquakes were occurring as far as 16 km from the well. The lack of shallow seismicity detected during six years of pre-injection seismic monitoring, the general correlation of the depths of the earthquakes and the depth of injection, and the spatiotemporal evolution of the seismicity since the start of injection demonstrated in Figure II-8 indicate that these earthquakes have been induced by PVU fluid injection.

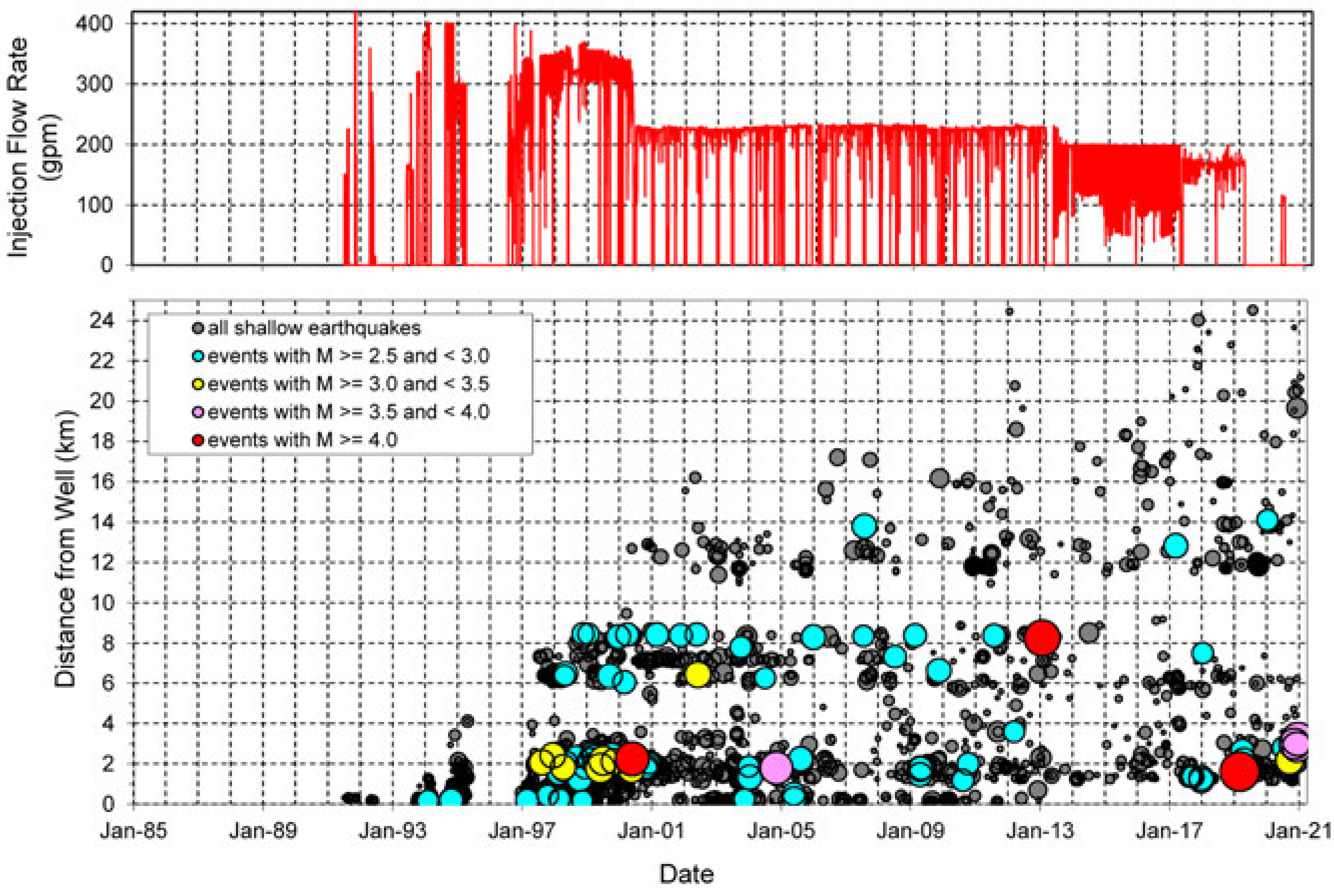

Figure II-8: Lower plot: scatter plot of earthquakes having magnitude ≥ 0.5 and depth ≤ 10 km (relative to the ground surface elevation at the injection wellhead), plotted as a function of date and distance from the PVU injection well. Each circle represents a single earthquake, with the width of the circle scaled by the event magnitude. The magnitudes shown are duration magnitudes for earthquakes with M_D < 3.0 and moment magnitudes for larger events. Upper plot: daily average injection flow rate.

Several distinct groups, or clusters, of induced seismicity have developed over the history of PVU injection operations. By the end of the injection tests in 1995, earthquakes were occurring to radial distances of roughly 4 km from the well (Figure II-9a). This area of induced seismicity immediately surrounding the injection well is referred to as the "near-well" region. In 1997, about one year after the start of continuous injection, earthquakes began occurring 6 to 8 km northwest of the injection well (Figure II-9b). This group of induced seismicity is called the "northwest (NW) cluster". In mid-2000, earthquakes were first detected 12 to 14 km from the injection well, along the northern edge of Paradox Valley (Figure II-9b). Several distinct clusters of earthquakes soon formed along the northern edges of the valley (Figure II-9c). The earthquakes occurring in all these groups are referred to as "northern valley events". Following the formation of these clusters (and a 32% decrease in the injection rate in mid-2000), the geographical expansion of induced seismicity greatly slowed for nearly a decade (Figure II-9c, d) but was renewed in 2010. For example, a single earthquake was first detected about 6 km southeast of the injection well in 2004 (Figure II-9c), but the seismicity rate in this area markedly increased beginning in 2010 (Figure II-9e). This tight group of earthquakes is referred to as the "southeast (SE) cluster". Earthquakes also began occurring in north-central Paradox Valley in 2010. (Figure II-9e). In the last several years, the rate of induced seismicity at the northern end of Paradox Valley has increased and its geographical extent has expanded (Figure II-9e, f, g, and h). Earthquakes likely related to PVU brine injection are now occurring at distances up to ~27 km northwest of the injection well and up to ~7 km outside the northwest perimeter of the seismic network (Figure II-9g). In addition, seismicity potentially related to PVU brine injection has occurred in several previously aseismic areas, including: toward the southeast to a distance of ~37 km from the injection well, east to a distance of ~24 km from the well, and west to a distance of ~14 km from the well (Figure II-9f, g, h).

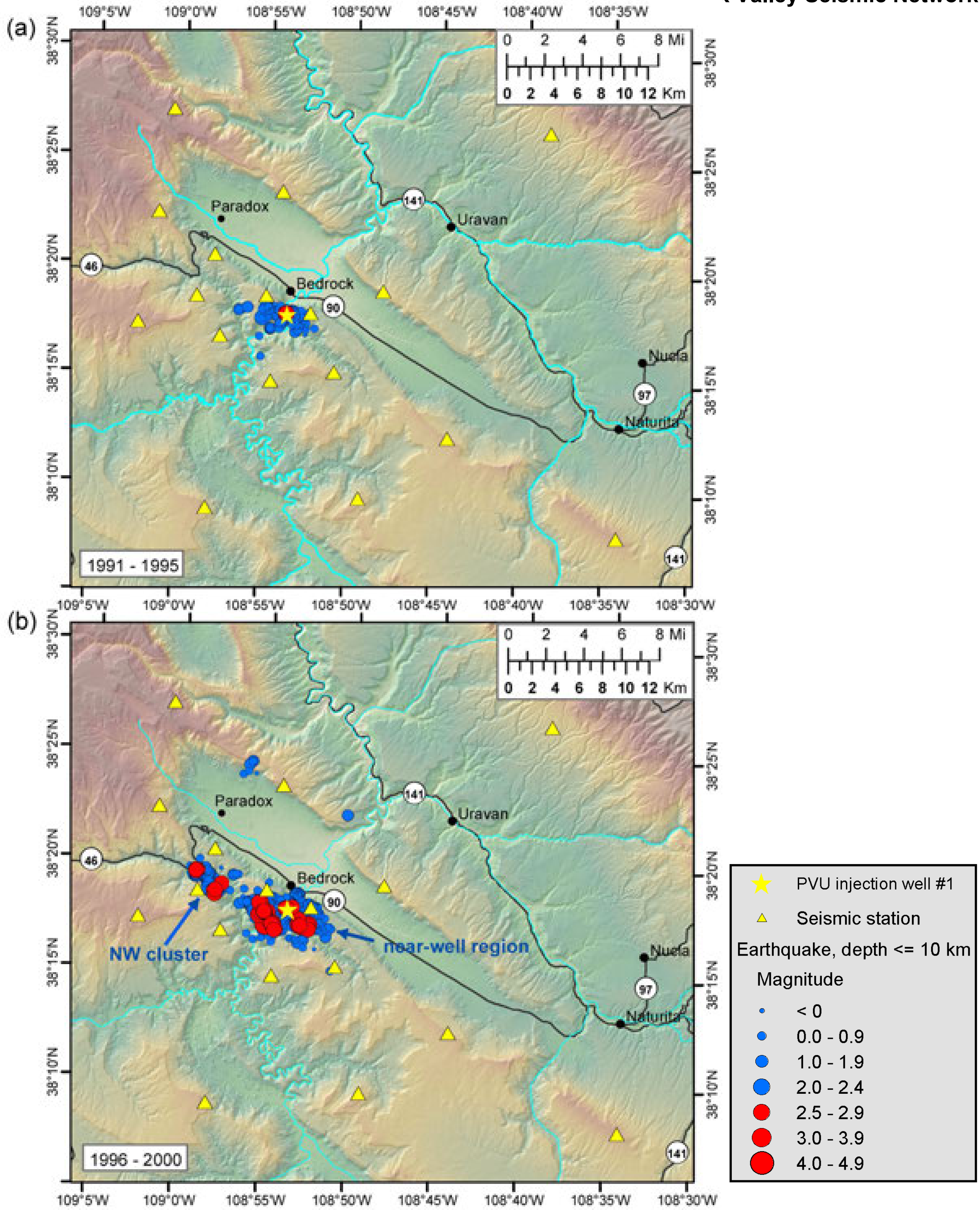

Figure II-9: Maps showing the spatial distribution of shallow seismicity (depth ≤ 10 km) over time: (a) 1991-1995 (b) 1996-2000 (c) 2001-2004 (d) 2005-2008 (e) 2009-2012 (f) 2013-2016 (g) 2017-2019 (h) 2020. Earthquake symbols are sized according to magnitude, and earthquakes with magnitudes ≥ 2.5 are shown in red.

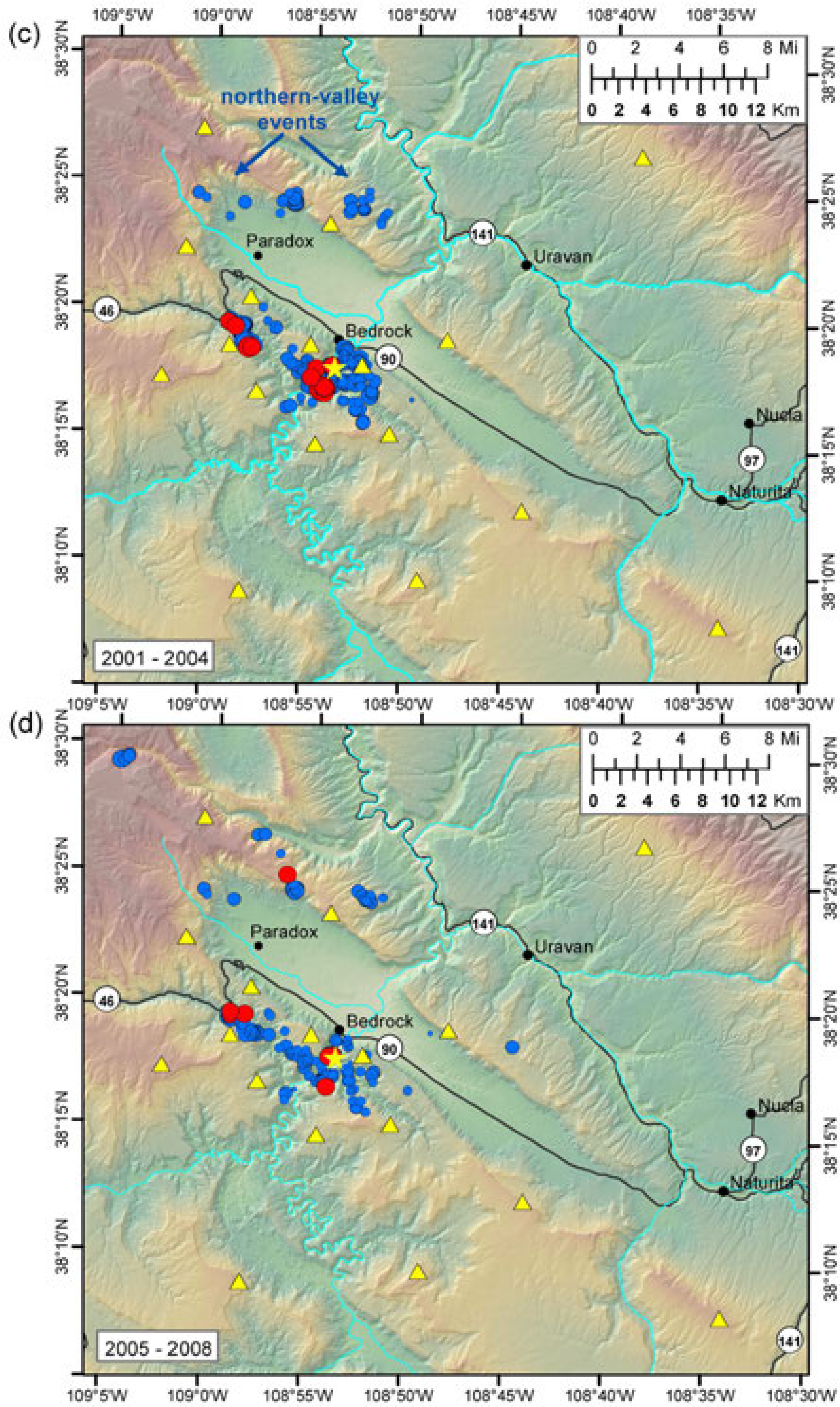
(c)
northern-valley
events
Paradox
Uravan
Bedrock
Nucla
Naturita
141
46
90
97
0 2 4 6 8 Mi
0 2 4 6 8 10 12 Km
2001 - 2004
(d)
Paradox
Uravan
Bedrock
Nucla
Naturita
2005 - 2008
109°5'W
109°0'W
108°55'W
108°50'W
108°45'W
108°40'W
108°35'W
108°30'W
38°30'N
38°25'N
38°20'N
38°15'N
38°10'N

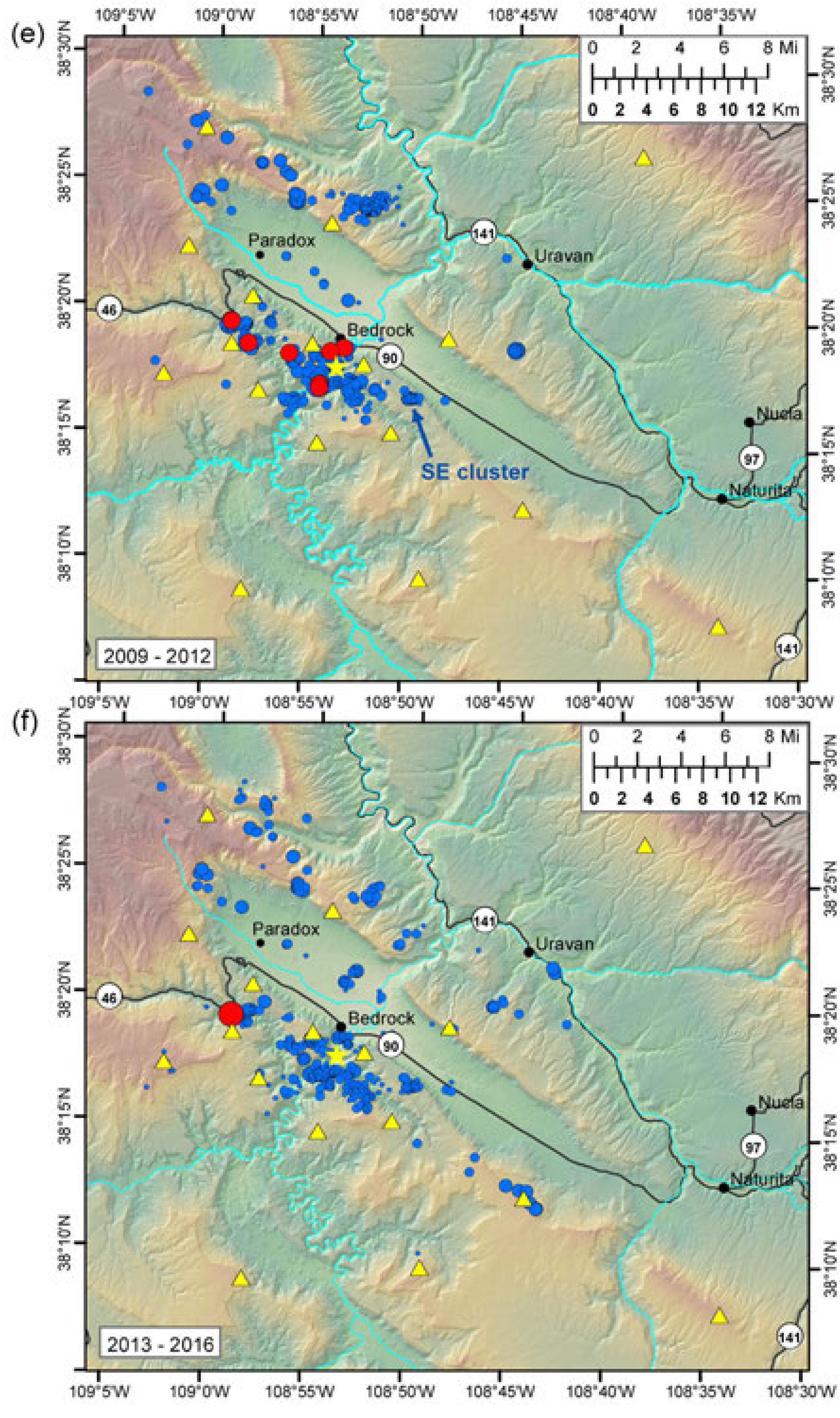
(e)
2009 - 2012
Paradox
Bedrock
Uravan
Nucla
Naturita
SE cluster
0 2 4 6 8 Mi
0 2 4 6 8 10 12 Km
(f)
2013 - 2016

(g)

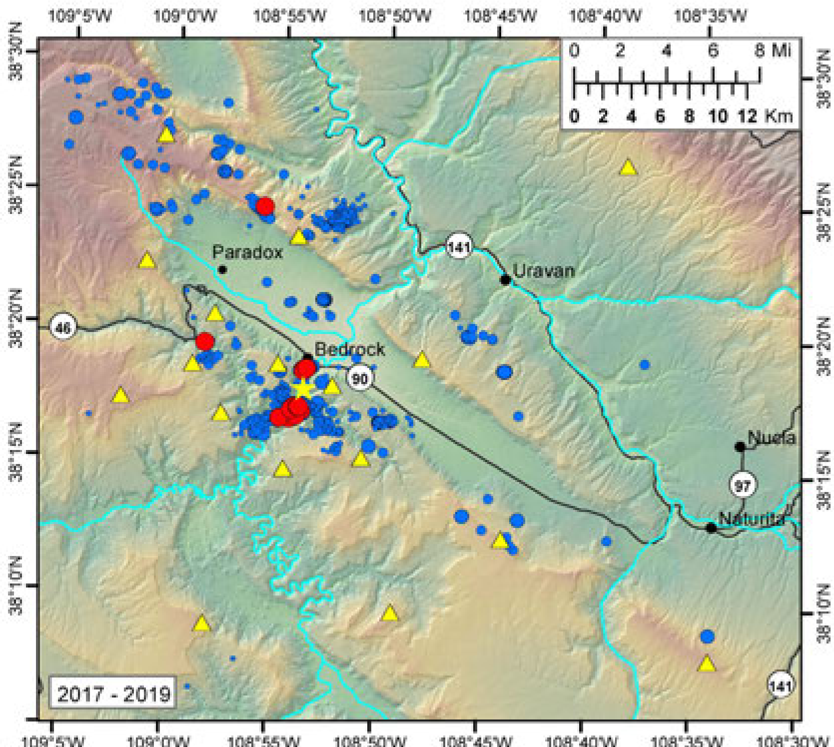
109°5'W
109°0'W
108°55'W
108°50'W
108°45'W
108°40'W
108°35'W
108°30'W
38°30'N
38°25'N
38°20'N
38°15'N
38°10'N
0 2 4 6 8 Mi
0 2 4 6 8 10 12 Km
Paradox
Uravan
Bedrock
Nucla
Naturita
141
46
90
97
2017 - 2019

(h)

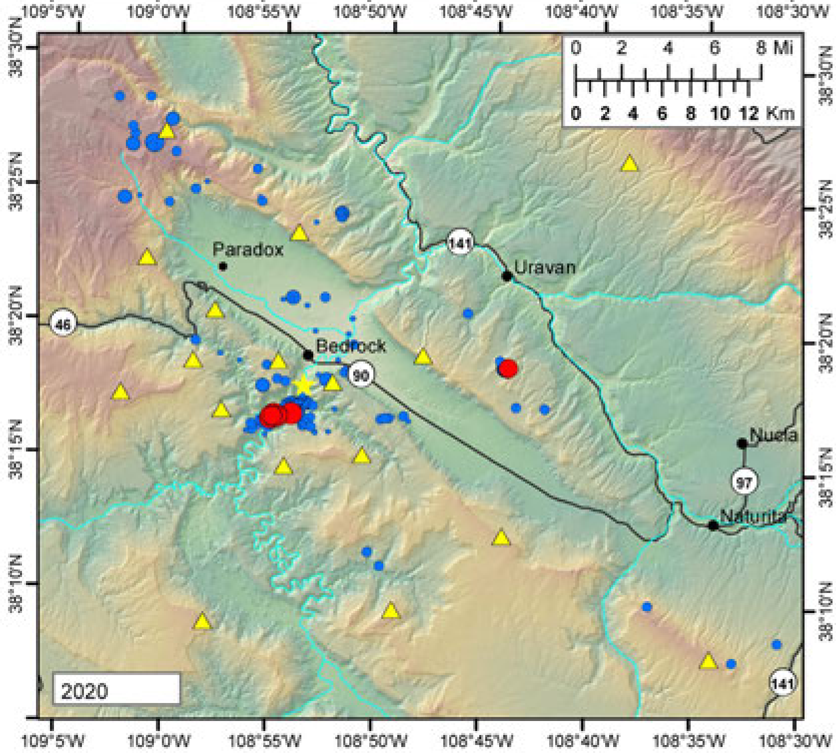
109°5'W
109°0'W
108°55'W
108°50'W
108°45'W
108°40'W
108°35'W
108°30'W
38°30'N
38°25'N
38°20'N
38°15'N
38°10'N
0 2 4 6 8 Mi
0 2 4 6 8 10 12 Km
Paradox
Uravan
Bedrock
Nucla
Naturita
141
46
90
97
2020

III. Network Operations during 2020

A. Network Maintenance and Upgrades

Because of COVID-19 concerns and travel restrictions, only two site visits were conducted during 2020. During these site visits, preventive maintenance and equipment upgrades were implemented at the 20 remote broadband seismic stations, the three strong motion sites, and the data communication center at Hopkins Field in Nucla, Colorado. A summary of the activities performed at the sites is given below. Additional details of the work performed at each site are included in the site visit reports in Appendix B.

The work performed at the 20 broadband seismic stations included both preventive maintenance activities and implementation of significant equipment upgrades. The preventive maintenance activities included: checking station power systems, replacing aging batteries, testing cables and antennas and replacing any degraded components, testing radios, and inspecting seismometer vaults. Equipment upgrades included installation of new seismometers, station electronics, and firmware. New Guralp model 3ESPCDE broadband seismometers were installed at 13 stations: PV01, PV03, PV04, PV05, PV07, PV11, PV13, PV14, PV15, PV16, PV17, PV21, and PV22. This work completed the network-wide broadband seismometer upgrade that was begun in 2018. The new seismometers have improved sensitivity and noise characteristics compared to the previously-installed Guralp model CMG-40T seismometers. Redesigned station electronics break-out-boxes (DM24-BOBs), which supply conditioned power to the seismometers, were replaced at all 20 broadband stations. These new DM24-BOBs have a more power-efficient design than the older units and are expected to reduce station power consumption. Lastly, the firmware which monitors GPS antenna function and initiates a reboot of the GPS antenna if timing is lost (located in the GPS-BOB) was upgraded at all sites to improve performance.

The three strong motion sites underwent major upgrades in October 2020. The seismic instrumentation at all sites were replaced with Silicon Audio 203V sensors and Guralp Minimus digitizers, and real-time data telemetry links were established. These upgrades followed more than 1.5 years of field and lab testing of various strong motion sensors and digitizers. Antennas and radios were installed at stations PVPP and PVCC, to incorporate the real-time data from these stations into the PVSN radio telemetry network for the first time. A temporary antenna mast at station PVEF, which had been installed in 2019 for equipment testing, was replaced with a permanent mast. Other improvements to these sites included installation of antenna cable surge-suppressors, a new grounding system, and a new charging and battery-backup system. The obsolete K2 digital accelerometers were removed, along with all dial-up communications equipment. Orientations of the new and old sensors were measure to an accuracy of better than 0.5° using a fiberoptic gyroscope system (iXblue Quadrans).

B. Network Performance

PVSN network performance depends on the performance of the hardware at individual seismic stations, the robustness of the radio data communication between the stations and the communication hub at Hopkins Field, and the reliability of the data acquisition computer systems. The performance of each of these components during 2020 is discussed below.

Four of the 20 PVSN broadband seismic stations experienced hardware problems in 2020 (Table III-1). Station PV04 lacked GPS timing from July 14th to September 11th, due to failure of the GPS antenna. Communication was lost to station PV19 on November 11th. This station is expected to be brought back online during a site visit scheduled for late April 2021. Numerous reboots of the seismometer occurred at station PV21 between late January and mid-September, resulting in intermittent station downtime (Figure III-1). The resulting data loss from this station was generally minor, but ~20% of the data was lost during July. The problem was corrected during a site visit in September 2020. The GPS antenna at station PV12 experienced intermittent reboots from January to March and late September to December, suggesting a temperature-sensitive hardware problem at this site. During the September 2020 site visit, the GPS antenna and the circuit board in the GPS-BOB were both replaced, and a cable test was performed, showing no indication of problems with the station wiring. However, the GPS antenna reboots persisted. Further testing will be performed during the 2021 field season to try to resolve the issue. In the meantime, station PV12 is otherwise operating normally and providing useable data.

In contrast to the last several years, no station experienced night-time power failures during 2020. Recently installed new GPS antennas and station electronics (DM24-BOBs) that use less power than the old units likely contributed to the good station power performance during 2020.

Most stations experienced robust radio communications during 2020, which maintained the network’s ability to continuously transmit the seismic data. Station PV07 experienced minor data loss late in the year (3% - 4%), due to slightly degraded radio communications (Figure III-1).

Table III-1: Performance of PVSN Seismic Stations During 2020

Station	Performance
PV01	Online and functioning normally throughout the year.
PV02	Online and functioning normally throughout the year.
PV03	Online and functioning normally throughout the year.
PV04	Online and functioning normally during most of the year. Had no GPS timing from 7/14 4:35 (UTC) to 9/11 23:00 (UTC) due to a failed GPS antenna.
PV05	Online and functioning normally throughout the year.
PV07	Online and functioning normally throughout the year.
PV10	Online and functioning normally throughout the year.
PV11	Online and functioning normally throughout the year.
PV12	Online and providing data throughout the year. The GPS antenna rebooted dozens of times during January to March and September to December, suggesting a temperature-sensitive problem. Extensive testing performed at this site in September 2020 could not identify the cause of the rebooting, and replacement of several station components did not resolve the issue. Further testing is planned for April 2021.
PV13	Online and functioning normally throughout the year.
PV14	Online and functioning normally throughout the year.
PV15	Online and functioning normally throughout the year.
PV16	Online and functioning normally throughout the year.
PV17	Online and functioning normally throughout the year.
PV18	Online and functioning normally throughout the year.
PV19	Went offline on 11/3 at 4:16 UTC and remained offline through the rest of the year. Currently have no radio communication to the site.
PV20	Online and functioning normally throughout the year.
PV21	Online and providing data during most of the year. Dozens of reboots of the seismometer occurred from late January to mid-September, resulting in intermittent station downtime. The resulting data loss from this station was generally minor, but ~20% of the data was lost during July.
PV22	Online and functioning normally throughout the year.
PV23	Online and functioning normally throughout the year.

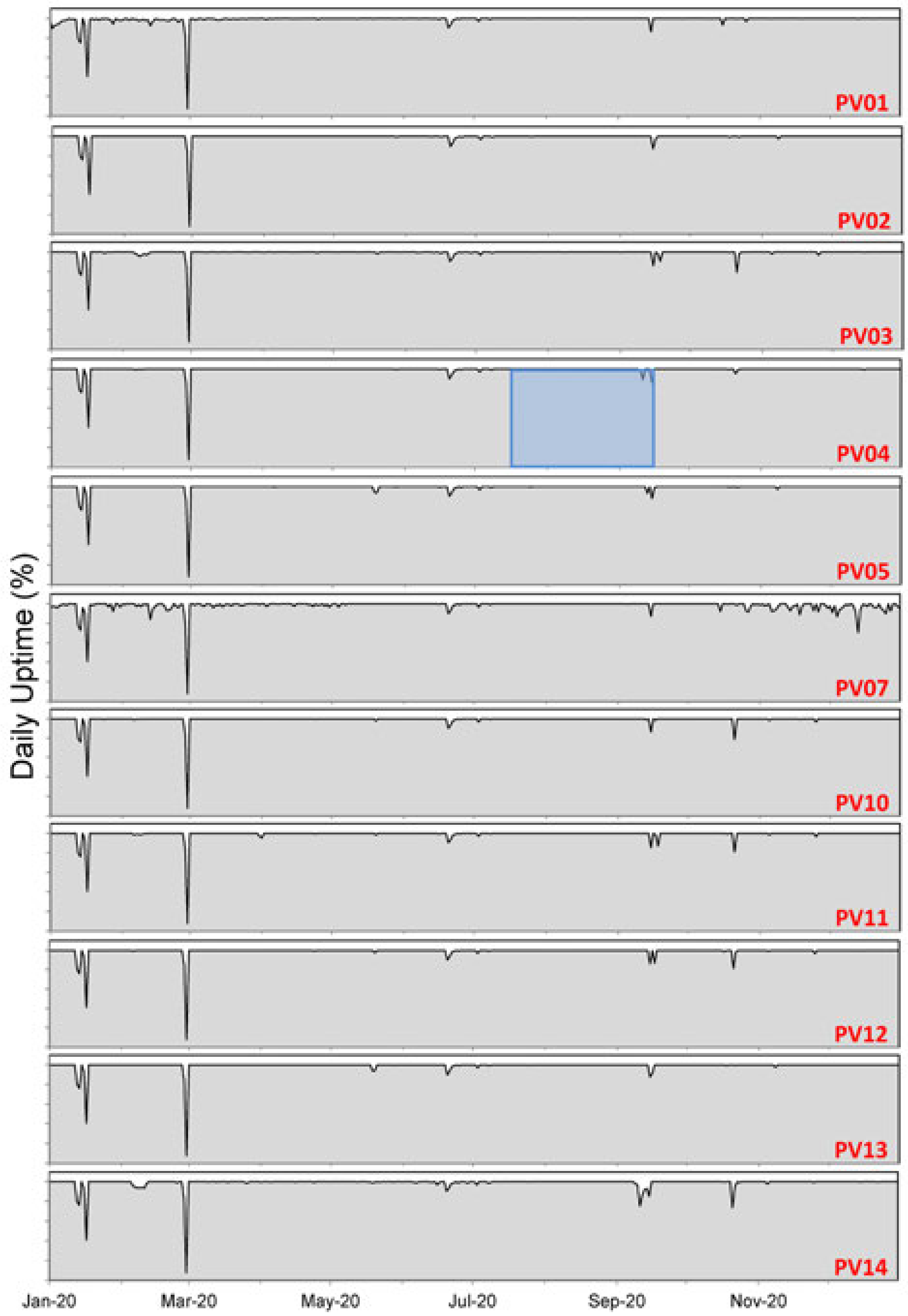

Figure III-1: Daily uptime (%) for the PVSN broadband seismic stations during 2020. The uptime values represent the percent of the day for which data from a given station were recorded. The vertical axes on the plots are scaled from 0 to 110%. Filled gray areas represent daily uptime, while dips in the filled volume show decreases in uptime (lack of data). Shaded blue areas indicate time periods with unreliable station timing.

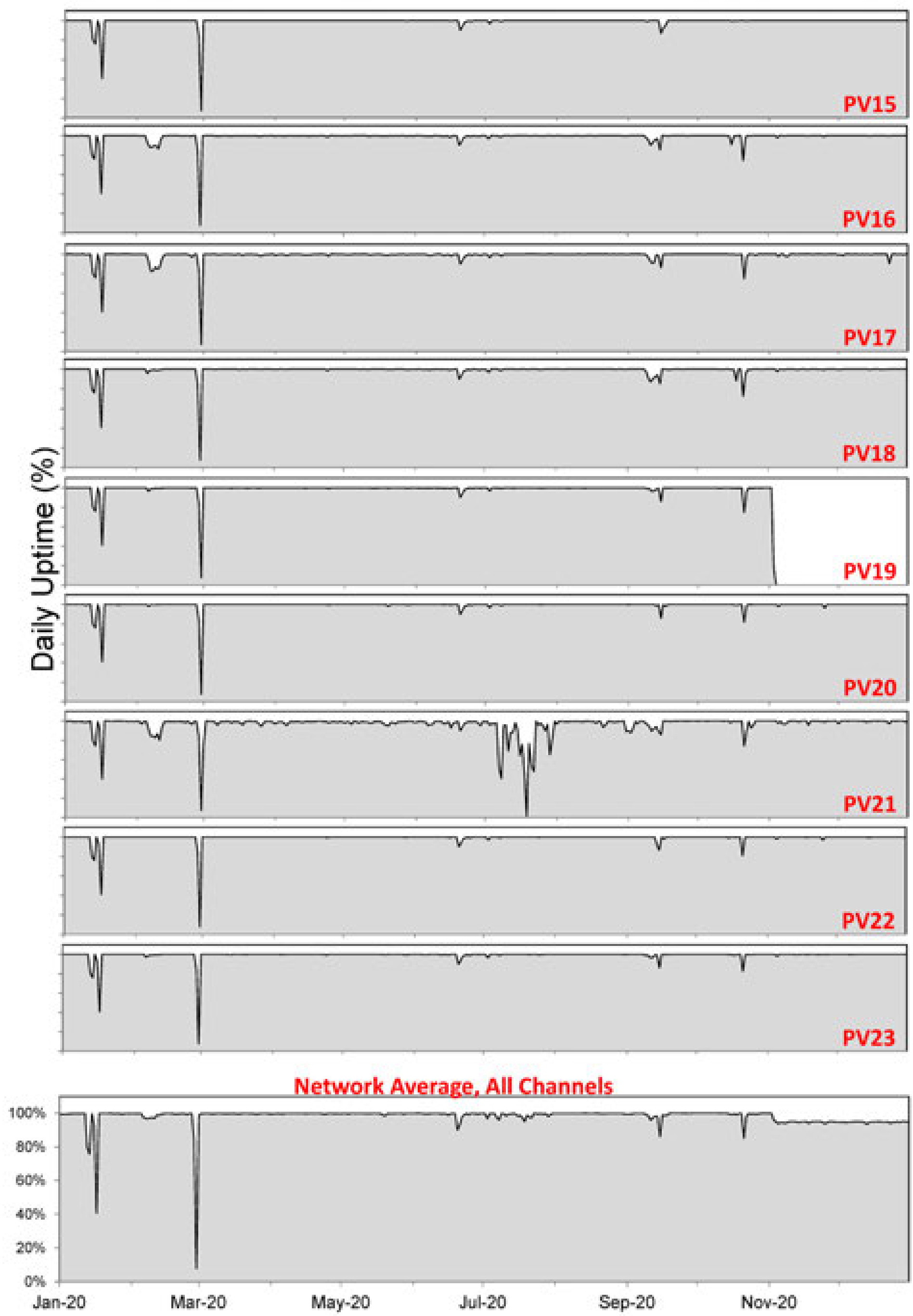

Figure III-1, continued. The bottom plot shows the daily average performance for all PVSN broadband channels.

The PVSN data acquisition computer systems were online and functioning normally during most of the year. Four data acquisition system downtimes occurred during 2020, lasting from 3 to 26 hours each (Table III-2). Two of these downtimes occurred in January and were due to mandatory computer security updates. The acquisition systems were offline for a total of 25.5 hours during the deployment of these updates. The seismic network was down for about 26 hours at the end of February (2/28/2020 20:09 to 2/29/2020 22:04 UTC), due to a malfunction of the *Scream* data acquisition software. The systems were also offline for about 3 hours on September 15th to accommodate maintenance activities at the Hopkins Field Data Communication Center.

Considering data loss from hardware failures at individual seismic stations, radio communication data drop-outs, and PVSN system downtimes, the 2020 annual uptimes for the PVSN high-gain seismic stations range from 83% to 99%, with 18 of the 20 stations having uptimes ≥ 98% (Figure III-2; Table III-3). These uptimes represent the percent of the year for which data from a given station were recorded.

We have been computing and tracking the overall annual uptimes of PVSN since 2000. These annual uptimes are estimates of the percent of each year during which PVSN was reliably detecting and recording earthquakes. They generally represent the percent of the year during which the PVSN data acquisition systems were operating. The sum of the time periods when PVSN was down during 2020 is 2.3 days, corresponding to an annual uptime of 99.4% (Table III-4).

Table III-2: Times When PVSN Was Down in 2020

Approximate Time Period (UTC)	Reason
1/13 19:41 to 1/14 6:13 (~10.5 hours)	Implementation of mandatory IT security updates
1/16 22:56 to 1/17 14:13 (~15 hours)	Implementation of mandatory IT security updates
2/28 20:09 to 2/29 22:04 (~26 hours)	Malfunction of *Scream* data acquisition software
9/15 15:43-19:00 (~ 3 hours)	Preventive maintenance activities at the Hopkins Field Data Communication Center

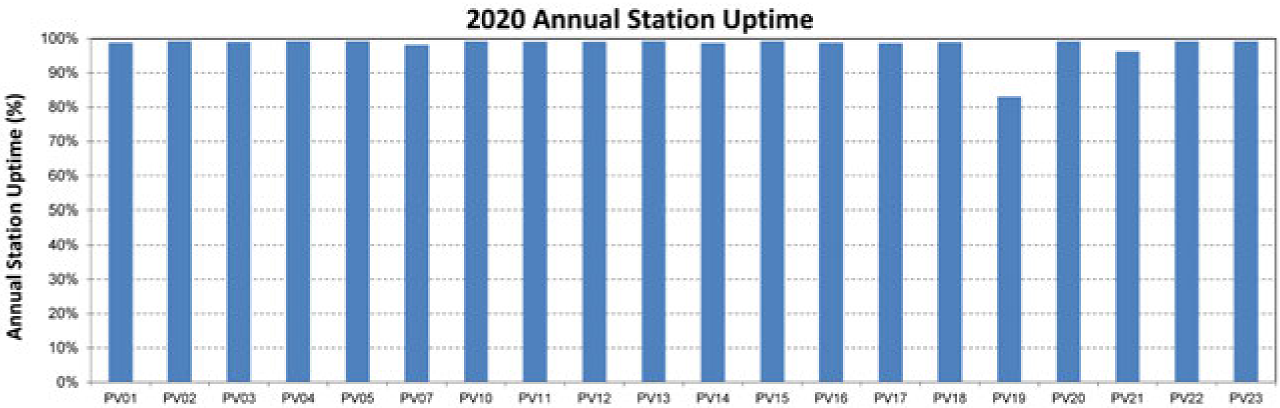

Figure III-2: Graph of annual (2020) uptime for each PVSN telemetered high-gain seismic station.

Table III-3: Annual PVSN Station Uptimes in 2020

Station	Annual Station Uptime in 2020
PV01	99%
PV02	99%
PV03	99%
PV04	99%
PV05	99%
PV07	98%
PV10	99%
PV11	99%
PV12	99%
PV13	99%
PV14	99%
PV15	99%
PV16	99%
PV17	99%
PV18	99%
PV19	83%
PV20	99%
PV21	96%
PV22	99%
PV23	99%

Table III-4: Annual PVSN Uptimes

Year	Annual Number of Days with Monitoring Absent or Degraded	Percent Uptime
2000	24	93.4%
2001*	**	**
2002	5	98.6%
2003	14.5	96.0%
2004	16	95.6%
2005	34	90.7%
2006	47	87.1%
2007	37	89.9%
2008	10	97.2%
2009	6.5	98.2%
2010	0	100.0%
2011	12.2	96.7%
2012	2.2	99.4%
2013	4.6	98.8%
2014[1]	10.3	97.2%
2015[2]	8.7	97.6%
2016[3]	17.3	95.3%
2017[4]	1.2	99.7%
2018	2.4	99.3%
2019	0.03	100.0%
2020	2.3	99.4%

**not tabulated in 2001
[1] includes 40.5 hours of downtime in September 2014 when network was operating but event detection was severely degraded due to malfunctioning of the data acquisition software
[2] includes 50% rating for 12 days in February and 5 days in December when network was operating but monitoring was substantially degraded due to absence of data from 8-12 stations simultaneously.
[3] includes 50% rating for 9 days in August and 22 days in September when network was operating but monitoring was substantially degraded due to absence of data from 14 stations simultaneously.
[4] includes 50% rating for 31 hours in January when network was operating but monitoring was substantially degraded due to absence of data from ≥ 5 stations simultaneously.

IV. Seismic Data Recorded in 2020

A. Annual Summary

During 2020, there were 549 earthquakes recorded within or near the perimeter of PVSN. The map in Figure IV-1 shows the epicenters of these events (colored circles), as well as the epicenters of all earthquakes recorded in previous years (gray and white circles). The local earthquakes recorded during 2020 are classified into four categories based on their depths (relative to the ground surface elevation of 1.524 km above MSL at the PVU injection well) and distances from the injection well:

1. Shallow near-well: depth ≤ 10 km, distance from injection well ≤ 5 km
2. Shallow intermediate: depth ≤ 10 km, distance from injection well > 5 km and ≤ 10 km
3. Shallow distant: depth ≤ 10 km, distance from injection well >10 km
4. Deep: depth > 10 km, any distance from injection well

The earthquakes are color-coded using these categories in the map presented in Figure IV-1. The numbers and magnitudes of the earthquakes recorded during 2020 in each of the location categories are summarized in Table IV-1. The 2020 local earthquake catalog is included in Appendix B.

Table IV-1: Summary of Earthquakes Recorded During 2020 by Location Category

Location Category	Depth	Distance from well	Number of Earthquakes	Number of Earthquakes with M_D ≥ 0.5	Magnitude Range[1]
shallow near-well	≤ 10 km	0 to 5 km	464	102	-1.6 – 3.9
shallow intermediate		> 5 to 10 km	16	5	-0.4 – 1.0
shallow distant		> 10 km	64	30	-0.6 – 2.5
TOTAL SHALLOW			**544**	**137**	**-1.6 – 3.9**
Deep	> 10 km	all distances, within or near perimeter of PVSN	5	1	0.1 – 0.5
TOTAL			**549**	**138**	**-1.6 – 3.9**

[1] Duration magnitudes (M_D) are used for events with M_D < 3.0, and moment magnitudes (M_W) are used for larger events.

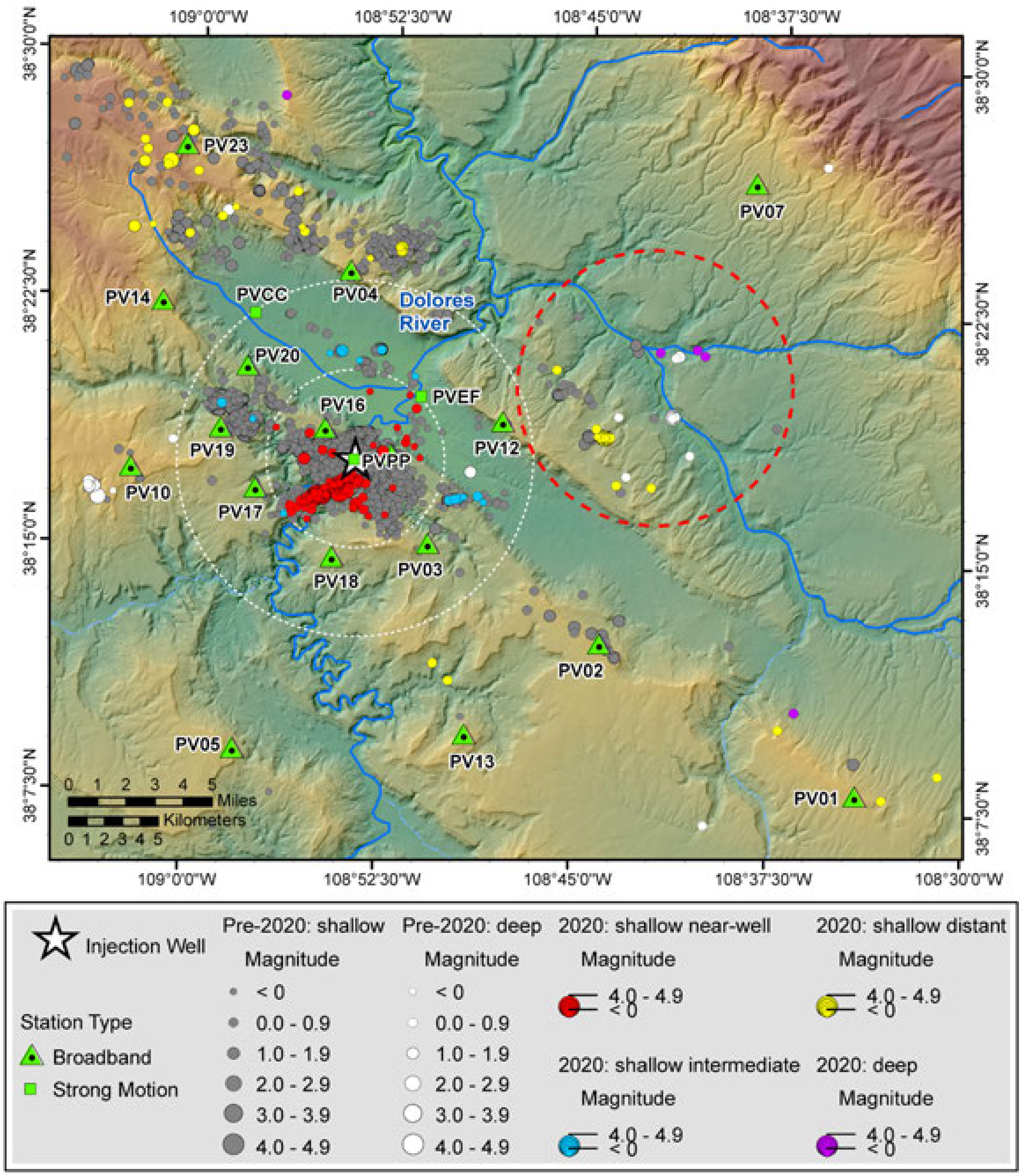

Figure IV-1: Locations of local earthquakes recorded by PVSN during 2020 (colored circles) and previous years (gray and white circles). The events that occurred during 2020 are color-coded using the event location categories described in the text. Events identified as "shallow" have depths ≤ 10 km (relative to the ground surface elevation at the injection well); those identified as "deep" have depths > 10 km. The white dashed circles represent radial distances of 5 and 10 km from the injection well. The occurrence of seismicity over time within the red dashed circle is presented in Figure IV-2.

All but five of the 549 local earthquakes recorded during 2020 have depths ≤ 10 km. Of these relatively shallow earthquakes, 464 occurred within 5 km of the injection well, 16 occurred at distances between 5 and 10 km from the well, and 64 occurred > 10 km from the well. Based on the relatively shallow depths of these earthquakes and the geographical expansion of the seismicity since injection began, we interpret most, and potentially all, of these earthquakes as being induced by PVU brine injection.

Three of the relatively deep earthquakes recorded during 2020 occurred 18.1 to 20.4 km east-northeast of the PVU injection well (Figure IV-1, purple circles). The depths of these three earthquakes are 10.6-10.7 km, only slightly greater than our 10-km depth threshold. No seismicity was detected in this general area east of seismic station PV12 (delineated by the red dotted circle in Figure IV-1) prior to 2007. Since 2007, earthquakes have been observed in this area at generally increasing rates (Figure IV-2). The depths of most of these events range between 5 and 12 km (Figure IV-2a). No improvement in PVSN event detection capabilities accounts for the onset of seismicity in 2007. More than one-third of the 82 earthquakes that have been detected in this area have magnitudes ≥ M_D 1.0 (Figure IV-2b), and the PVSN magnitude completeness threshold has been ≤ M_D 1.0 nearly continuously since 1985. The lack of seismicity in this area during 22 years of seismic monitoring prior to 2007 and its continued occurrence and generally increasing rate since then suggest that these earthquakes are related to PVU brine injection.

The relationship of the other two deep earthquakes to PVU injection, if any, is not clear. One of these events is an M_D 0.1 earthquake that occurred 20.7 km north-northwest of the injection well (Figure IV-1). This event has an estimated depth of 14.3 km, relative to the ground surface at the injection well. Currently available information suggests that this earthquake is naturally occurring. A single earthquake was detected ~2 km from this event's epicenter during the six years of pre-injection monitoring (1985-1990). The estimated depth of the pre-injection earthquake (using the most recent velocity model) is 14.2 km, nearly identical to the depth of the earthquake recorded in 2020. The other deep earthquake recorded during 2020 occurred 28.5 km southeast of the injection well, at the southeastern end of Paradox Valley (Figure IV-1). This event has a magnitude of M_D 0.1 and estimated depth of 10.5 km. Only a handful of earthquakes have occurred within ~10 km of this event's epicenter. However, all of these earthquakes have occurred since 2018, including three other earthquakes in this area in 2020 with depths less than the 10-km depth threshold (Figure IV-1, yellow circles). We currently interpret the earthquakes in this area as potentially induced by PVU injection. Continued monitoring should help confirm whether these earthquakes are induced by pore pressure diffusion from PVU injection. If so, then their occurrence rate would be expected to increase over the next several years (even if the injection well remains shut in).

Ten earthquakes with duration magnitude (M_D) ≥ 2.5 occurred during 2020 (Figure IV-3). This magnitude threshold is significant because it is the approximate minimum magnitude for ground shaking to be felt in the Paradox Valley area. One of these earthquakes occurred on January 12th, 12.1 km east of the PVU injection well (Figure IV-3). This earthquake occurred at a depth of 6.3 km (relative to the ground surface at the

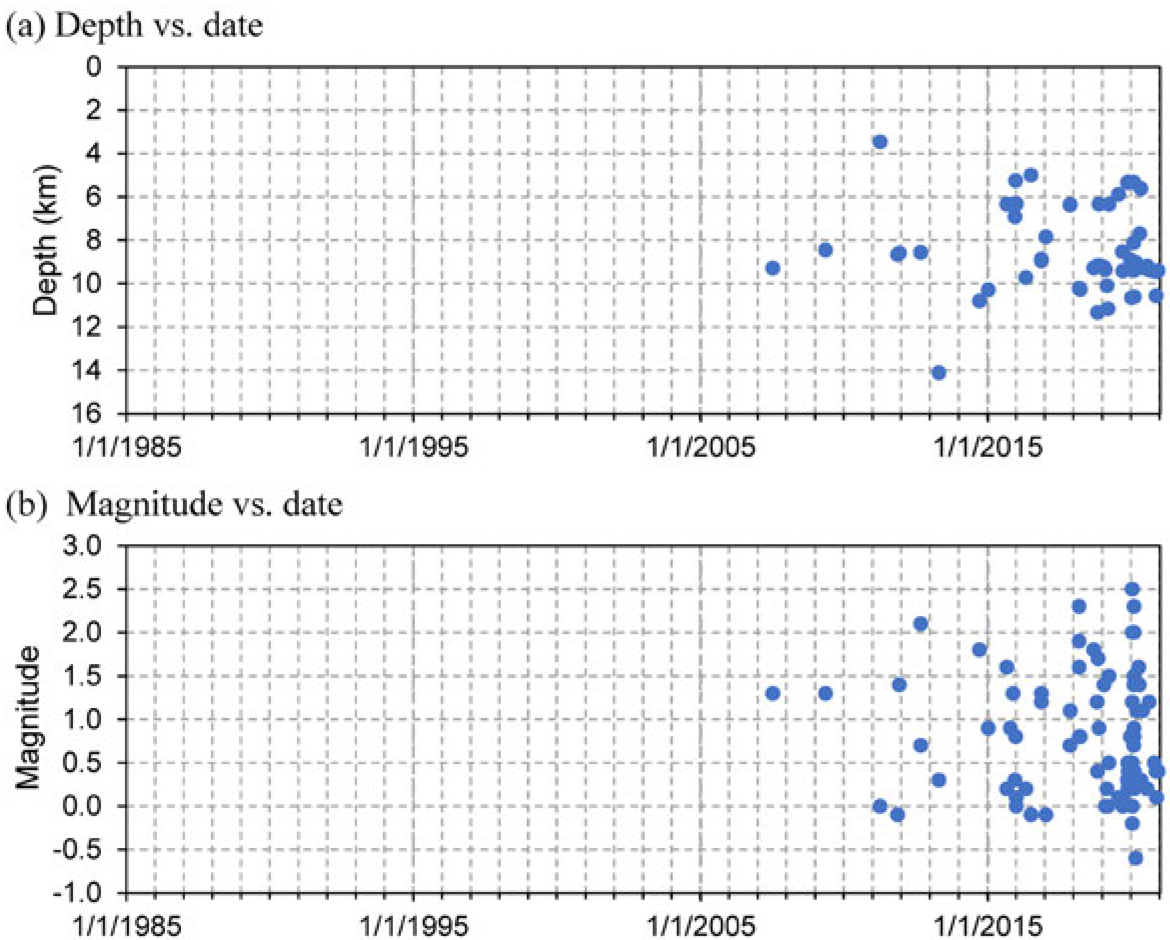

Figure IV-2: Occurrence of the earthquakes east of Paradox Valley within the red dashed circle in Figure IV-1 over time: (a) depth vs. date (b) magnitude vs. date. Depths are relative to the ground surface elevation at the PVU injection well (1.524 MSL), and magnitudes are from the duration magnitude scale.

PVU injection well), in a small cluster that began developing in 2007. This earthquake has a duration magnitude of M_D 2.5 and moment magnitude of M_W 2.3. The other nine 2.5+ earthquakes occurred within 3.5 km of the injection well (Figure IV-3). One of these earthquakes occurred 2.2 km southwest of the injection well, in the immediate vicinity of the rupture plane of the M_W 4.5 March 2019 earthquake. This event occurred on Sept. 16th and is clearly an aftershock of the M_W 4.5 earthquake based on its location. It has a duration magnitude of M_D 3.1 and moment magnitude of M_W 3.3. The remaining eight M_D 2.5+ earthquakes occurred 2.8 to 3.2 km southwest of the injection well and approximately 700 to 1200 m southwest of the M_W 4.5 earthquake rupture plane. One of these earthquakes occurred on July 12th, and the other seven earthquakes occurred during a swarm of increased seismic activity between November 8th and December 20th. These

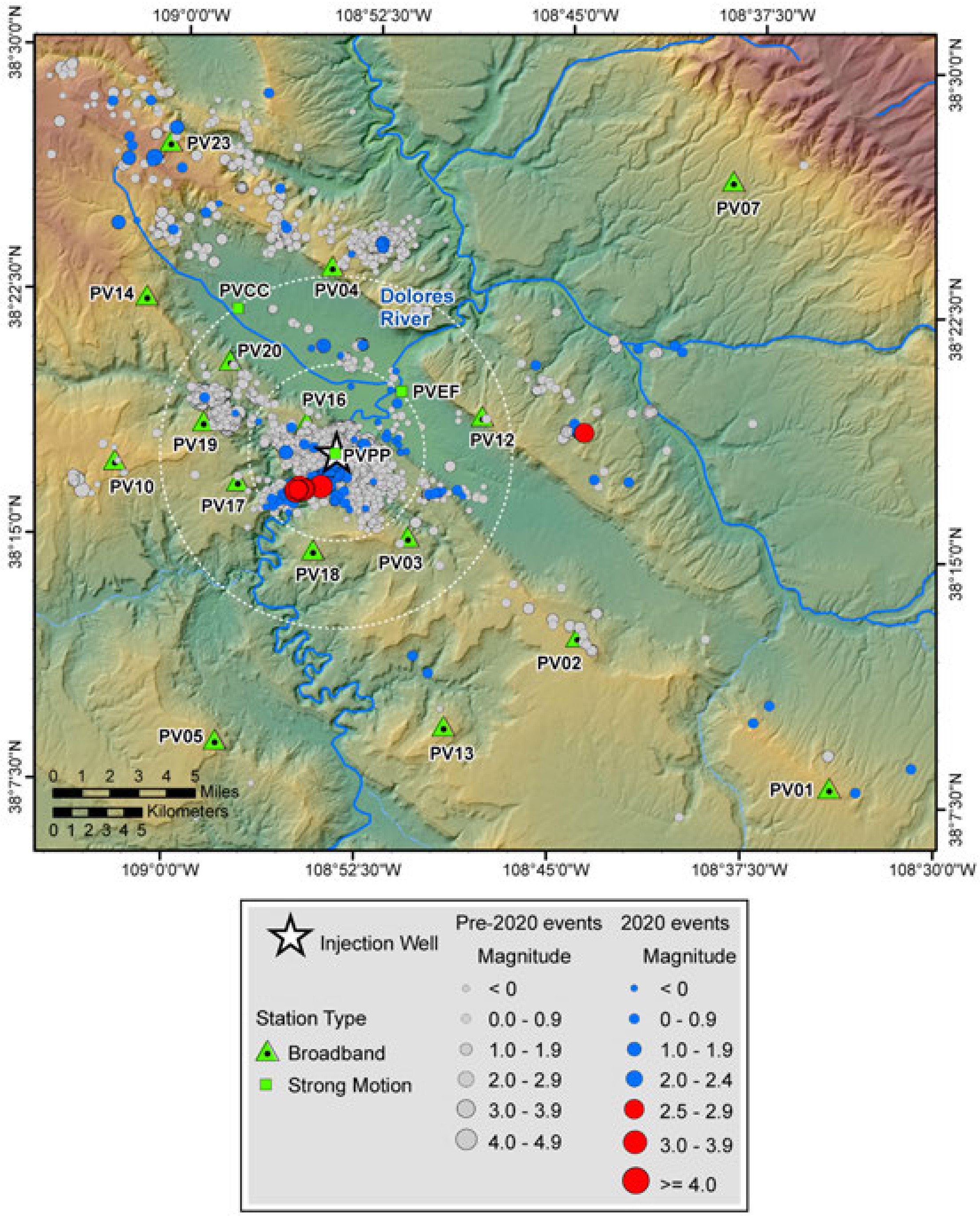

Figure IV-3: Locations of local earthquakes recorded by PVSN during 2020 by magnitude. The earthquakes in 2020 with $M_D \geq 2.5$ are shown in red; those with smaller magnitudes are shown in blue. The epicenters of earthquakes recorded prior to 2020 are shown in gray for reference.

eight earthquakes have duration magnitudes between M_D 2.5 and M_D 3.2 and moment magnitudes between M_W 2.5 and M_W 3.9. (The PVSN duration magnitude scale begins to saturate above ~M_D 3, and therefore moment magnitude estimates are more reliable for earthquakes in this range.) The occurrence of these earthquakes appears to be related to the M_W 4.5 earthquake fault rupture but their occurrence rate is higher than expected for an aftershock sequence. Analyses are ongoing to try to better understand the relation of these events to the M_W 4.5 main shock.

The local earthquakes recorded by PVSN during 2020 are plotted as a function of date, earthquake magnitude, and location category in Figure IV-4. The rates and magnitudes of shallow near-well events increased during the last two months of the year, due to the seismicity swarm discussed above (Figure IV-4, pink squares). Earthquakes at intermediate distances from the well (5 to 10 km) occurred at low rates throughout the year (Figure IV-4, blue circles). The occurrence of the distant seismicity (more than 10 km from the well) was somewhat sporadic, with the highest rates and magnitudes in January and February (Figure IV-4, yellow diamonds).

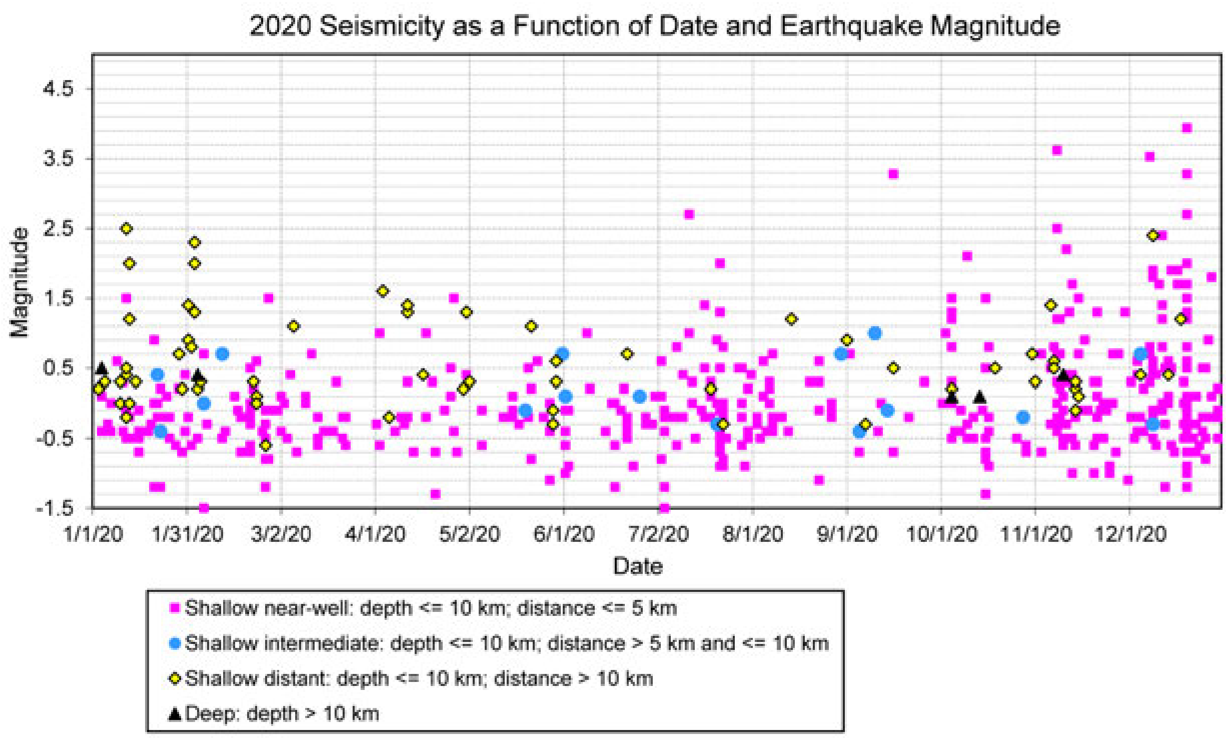

Figure IV-4: Earthquakes recorded by PVSN during 2020 plotted as a function of date, magnitude, and event location category. Duration magnitudes are used for events with M_D < 3.0, and moment magnitudes are used for larger events.

B. Seismicity near the Injection Well

Hypocenters of the earthquakes that occurred in 2020 within 7 to 9 km of the injection well are compared to those from previous years in the map in Figure IV-5 and in the vertical cross sections in Figure IV-6. In these figures, the earthquakes that occurred during 2020 and those that occurred in previous years are each separated into two categories based on how precise the computed hypocenters are relative to the other events. The best earthquake locations were computed using a relative earthquake location method employing precise arrival time differences between pairs of earthquakes (computed using waveform cross-correlation). The poorer earthquake locations were computed independently using manually determined absolute arrival times, because their waveform data were either not of sufficient quantity or quality to include these events in the relative location. The hypocenter of the March 2019 M_W 4.5 earthquake is represented by the yellow square in Figure IV-5 and Figure IV-6 for reference.

As seen in the map and cross sections, most of the earthquakes induced within ~7-9 km of the injection well during 2020 occurred in or near areas of previous seismic activity, with one exception. The near-well seismicity swarm that occurred in November-December 2020 substantially expanded a small seismicity cluster that had started forming after the March 2019 M_W 4.5 earthquake. The location of this cluster is labeled in Figure IV-5 and Figure IV-6b (dotted blue circle). Although many earthquakes had previously occurred at this position in map view (Figure IV-5), the pre-2019 earthquake hypocenters are 1 to 3 km shallower than the cluster that began forming in 2019 and expanded in 2020 (Figure IV-6b).

The formation of this new seismicity cluster appears to be related to stress redistribution from the fault plane rupture associated with the March 2019 M_W 4.5 earthquake. The first earthquake at this location occurred on March 7, 2019, three days after the March 4th main shock. Furthermore, the cluster lies in an area where aftershocks of the M_W 4.5 earthquake are expected, based on simple Coulomb models of the redistribution of stress from the main shock fault rupture (Block et al., 2020b). By early May 2019, 13 earthquakes had been detected in this cluster, the largest having a magnitude of M_D 2.7 (M_W 2.5). These earthquakes were interpreted as aftershocks of the March 2019 main shock. Only two additional events were detected in this cluster from mid-May 2019 through June 2020. Seismicity rates within the cluster began increasing in July 2020, with 8 additional earthquakes occurring between July and mid-October. The seismicity rate increased substantially more in November 2020, and 115 events were detected here between early November and the end of 2020. Rates subsequently declined in January 2021. As discussed in section IV-A, eight earthquakes with magnitude $\geq M_D$ 2.5 occurred within this cluster during 2020. Of these, four earthquakes have magnitude $\geq M_W$ 3.0; the maximum magnitude is M_W 3.9. Although the formation of this cluster appears to have been triggered by stress redistribution following the March 2019 M_W 4.5 earthquake, the increased seismicity rate observed in November 2020 to January 2021 is not typical for aftershock sequences. Additional analyses may help determine whether other factors

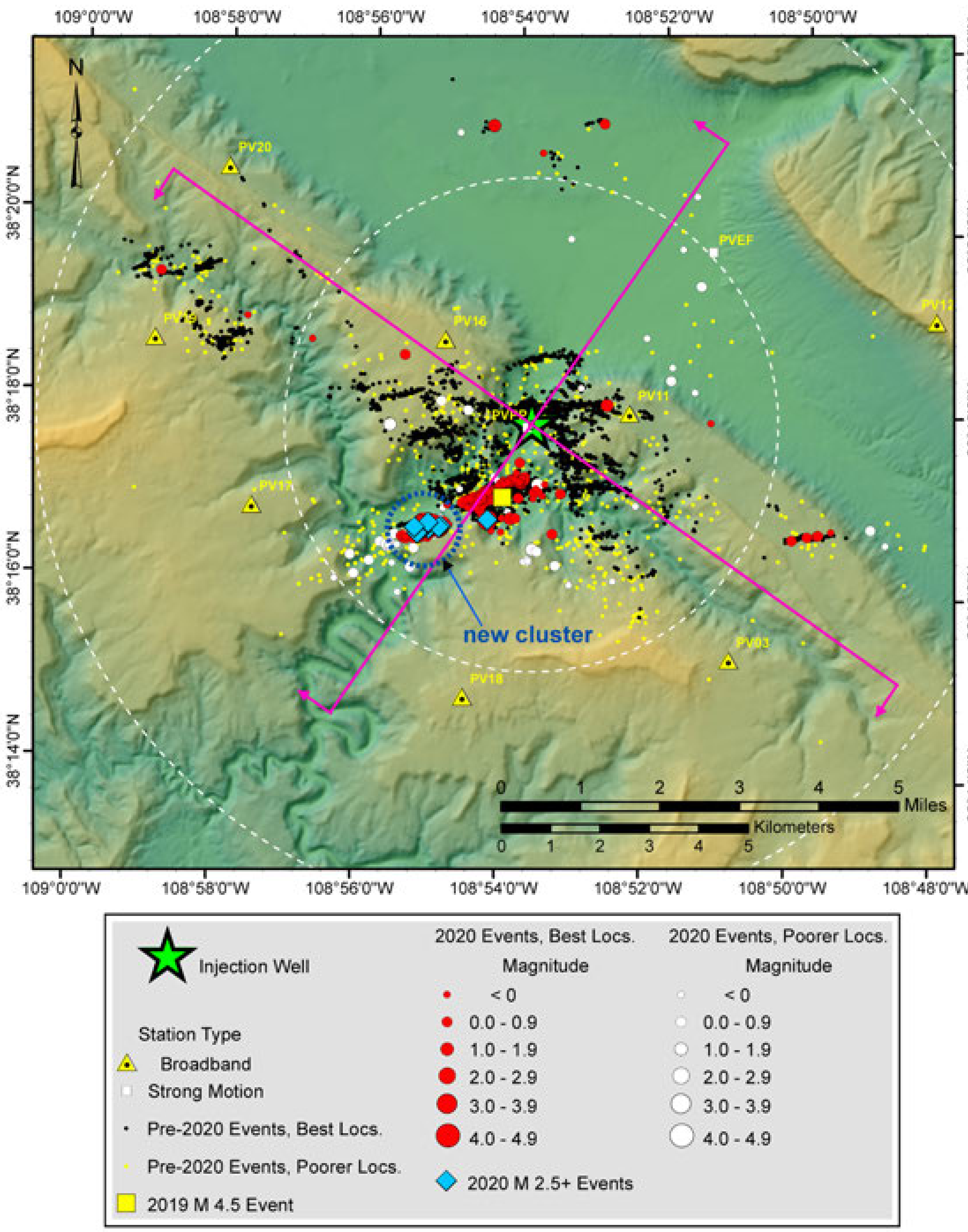

Figure IV-5: Map showing the epicenters of earthquakes (≤ 10 km depth) in the vicinity of the injection well in 2020, compared to the locations of previously-induced events. The white dashed circles indicate radial distances of 5 and 10 km from the injection well. The magenta lines indicate the orientations of the cross sections presented in Figure IV-6.

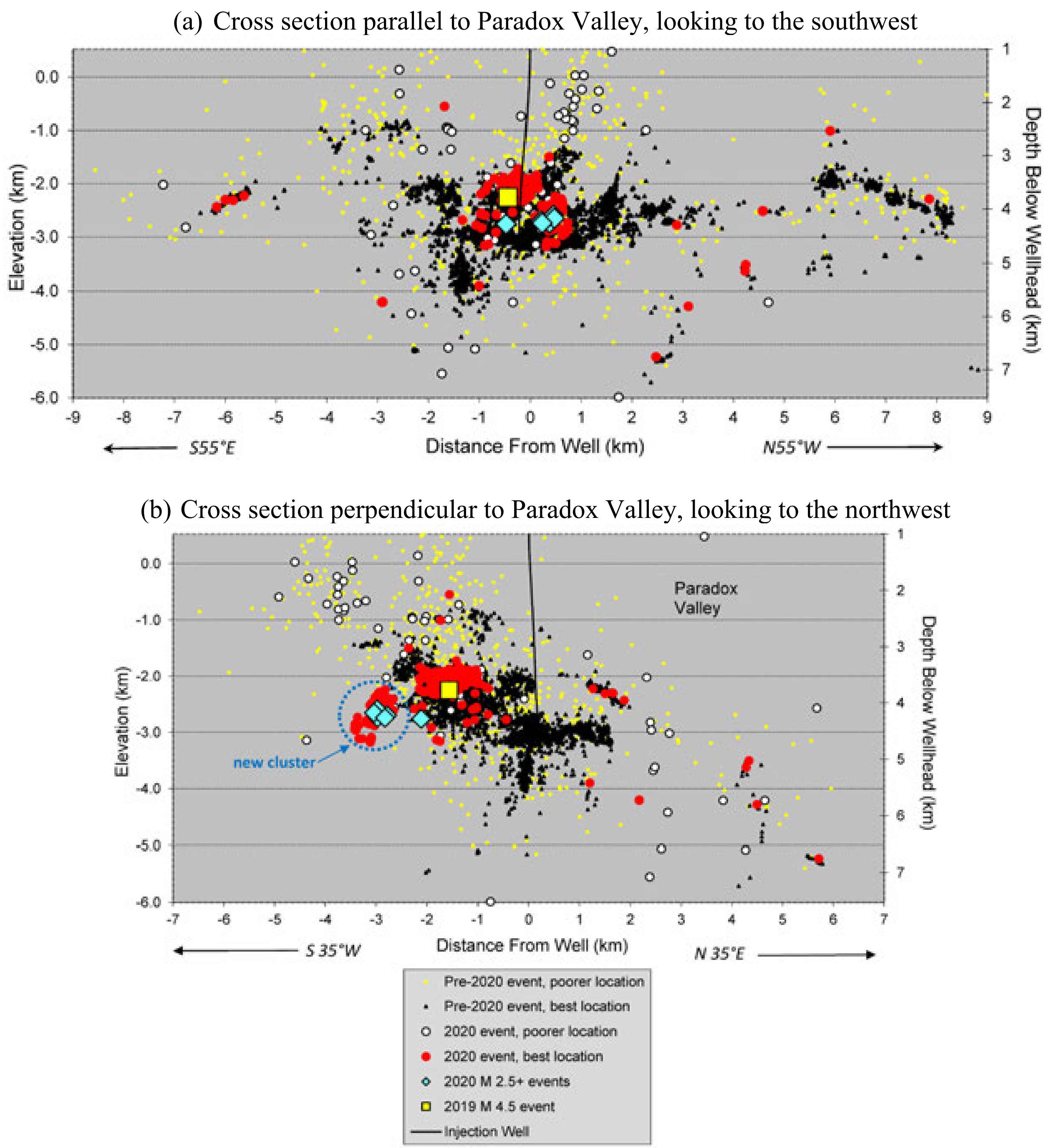

Figure IV-6: Vertical cross sections showing the hypocenters of earthquakes occurring within approximately 7-9 km of the injection well in 2020, compared to the locations of previously-induced events: (a) section parallel to Paradox Valley (b) section perpendicular to Paradox Valley. The orientations of the cross sections are indicated by the magenta lines in Figure IV-5.

contributed to the increased seismicity rate (such as stress changes related to reservoir de-pressurization during the continuing injection well shut-in).

C. Distant Earthquakes

During 2020, 64 shallow local earthquakes (depths ≤ 10 km) were detected at distances greater than 10 km from the injection well. In addition, four of the five deeper earthquakes recorded during 2020 have depths only slightly greater than our 10-km depth threshold (10.5-10.6 km; section IV-A). Based on the spatiotemporal evolution of the earthquakes in these areas observed since monitoring began in 1985, we interpret these 68 distant earthquakes as likely induced by PVU brine injection.

Of these 68 distant earthquakes, 30 occurred at or near the northern end of Paradox Valley (Figure IV-1), where seismicity has been detected every year since 2000. For comparison, 725 events occurred in this northern-valley region in 2019, 119 in 2018, 59 in 2017, and 29 in 2016. Hence, the number of earthquakes that occurred in the northern valley area during 2020 was the lowest number since 2016. Historically, the annual number of northern-valley events has varied widely, ranging from 2 to 725 events per year from 2000 to 2019. The northern-valley earthquakes recorded during 2020 range in magnitude from M_D -0.3 to M_D 2.4. Depth estimates of these earthquakes range from 3.2 to 7.8 km (relative to the ground surface at the PVU injection well), consistent with depth estimates of previous northern-valley events.

The seismicity in the northern-valley area is expanding to the northwest, beyond the northwestern perimeter of the Paradox Valley Seismic Network (Figure IV-1). Uncertainties in the computed locations and depths of earthquakes greatly increase when they occur outside the perimeter of the seismic network. Earthquakes are already occurring up to roughly 7 km outside the northwestern perimeter of PVSN. Hence, it will be difficult to monitor the further expansion of the seismicity to the northwest with the current network configuration.

During 2020, 29 shallow earthquakes (depth ≤ 10 km; Figure IV-1, yellow circles east of seismic station PV12) and three slightly deeper events (Figure IV-1, purple circles) occurred east of Paradox Valley and south of the Dolores River, at distances of ~12 km to ~20 km from the well. The magnitudes of these events range from M_D -0.6 to M_D 2.5, and their depth estimates range from 5.3 to 10.7 km. Earthquakes have occurred in this area since 2007, and seismicity rates here have generally increased over time (Figure IV-2). During 2020, this area had a slightly higher rate of seismicity than the northern-valley area.

The remaining six earthquakes occurred southeast of the injection well, as distances ranging from ~12 to ~37 km (Figure IV-1, yellow and purple circles southeast of the injection well). Five of these events occurred at depths < 10 km, and the remaining event has a slightly greater depth estimate of 10.5 km. The magnitudes of these events range from M_D 0.1 to M_D 0.9. As discussed previously (section IV-A), these earthquakes are considered likely induced by PVU injection but additional monitoring is required to confirm the seismicity trends in this area.

D. Strong Ground Motions

Peak ground accelerations recorded at station PVPP (near the injection well-head) for the five induced earthquakes in 2020 with magnitudes ≥ M_W 3.0 are listed in Table IV-2. The table lists the raw peak ground accelerations (PGA) for each component (E – east, N – north, and Z – vertical), which represent the maximum of the absolute value of the as-recorded acceleration time histories, corrected only for instrument sensitivity, but which have not been baseline-corrected (Boore, 2001; Boore et al., 2002). As-recorded PGA values depend on the orientation of the accelerometer relative to the fault plane of an earthquake, and the local geology. A different accelerometer orientation would result in different PGA values. Orientation-independent measures therefore have been developed for the routine analysis of strong-motion data (Boore, 2010; Boore et al., 2006). We compute two such measures from the sensitivity-corrected and baseline-corrected records: (1) GMRotI50, which represents the median value of the period-independent geometric mean of the as-recorded horizontal components, mathematically rotated through all possible angles; and (2) RotD50, which represents the median value of the period-dependent horizontal components, rotated through all possible angles. In general, these values are similar. GMRotI50 was used for the ground-motion prediction equations (GMPEs) of the original Next Generation Attenuation (NGA) project (Power et al., 2008), and RotD50 was used for the NGA-West2 project (Bozorgnia et al., 2014). The accelerations recorded at station PVPP (the closest strong-motion station) from these earthquakes were less than 0.03 g.

Table IV-2: Peak Ground Motion Accelerations Recorded by Station PVPP During 2020

Earthquake			Strong Motion Data				
Date (UTC)	Time (UTC)	Mag.	Sta.	Comp.	Raw PGA (g)	GMRotI50 (g)	RotD50 (g)
9/16/2020	15.26.40	M_W 3.3	PVPP	E	0.036	0.024	0.028
				N	0.011		
				Z	0.008	-	-
11/8/2020	11:19:57	M_W 3.6	PVPP	E	0.029	0.022	0.024
				N	0.021		
				Z	0.009	-	-
12/8/2020	22:53:42	M_W 3.5	PVPP	E	0.017	0.017	0.016
				N	0.017		
				Z	0.007	-	-
12/20/2020	01:53:43	M_W 3.3	PVPP	E	0.021	0.020	0.021
				N	0.022		
				Z	0.008	-	-
12/20/2020	02:11:06	M_W 3.9	PVPP	E	0.020	0.019	0.020
				N	0.021		
				Z	0.012	-	-

E. Comparison to Seismicity from Previous Year

The numbers of earthquakes observed within 5 km of the injection well and at distances greater than 10 km from the well decreased markedly in 2020 compared to 2019, while the number of earthquakes in the intermediate distance range (5-10 km) decreased only slightly (Table IV-3). During 2020, 464 earthquakes were detected within 5 km of the injection well, compared to 2230 events in 2019, a decrease of 79%. Such a decrease in near-well seismicity rates was expected because the rates of aftershocks of the near-well March 2019 M_W 4.5 earthquake are decaying over time. At distances > 10 km, the number of local earthquakes likely related to PVU injection (at all depths) decreased from 741 in 2019 to 68 in 2020, a decrease of 91%. In the intermediate distance range (5-10 km), the number of earthquakes decreased from 20 in 2019 to 16 in 2020, a decrease of 20%.

Because the ability to detect very small earthquakes can vary over time, depending on both the operating status of the seismic network and background seismic noise levels, more robust estimates of the variation in seismicity rate are determined by comparing the occurrence of earthquakes with magnitude ≥ M_D 0.5 (PVSN's approximate magnitude completeness threshold). These values are presented in Table IV-4. Substantial decreases in seismicity rates are still observed within 5 km of the well (64%) and at distances greater than 10 km (83%). The rate of events with $M_D \geq 0.5$ at intermediate distances (5-

Table IV-3: Number of Earthquakes of All Magnitudes Recorded in 2019 and 2020

Distance Range (km)	Number of Events Recorded in 2019	Number of Events Recorded in 2020	Percent Change
0 to 5	2230	464	-79%
> 5 to 10	20	16	-20%
> 10	741	68	-91%

Table IV-4: Number of Earthquakes With Magnitude ≥ M_D 0.5 Recorded in 2019 and 2020

Distance Range (km)	Number of Events Recorded in 2019	Number of Events Recorded in 2020	Percent Change
0 to 5	283	102	-64%
> 5 to 10	4	5	25%
> 10	178	31	-83%

10 km) increased 25% from 2019 to 2020, but the absolute number of events is so small (5 in 2020) that the statistics are not robust.

The numbers of earthquakes recorded during 2019 and 2020 are plotted as a function of magnitude in Figure IV-7. Individual histograms are shown for earthquakes within 5 km of the injection well, for those at distances of 5 to 10 km from the well, and for events > 10 km from the well. (These radial distances are indicated by the white dashed circles on the map in Figure IV-5.) Because of the decreased rate of aftershocks of the March 2019 M_W 4.5 earthquake, seismicity rates in the 0-5 km distance range were lower for most magnitude intervals in 2020 compared to 2019 (upper plot in Figure IV-7). The maximum earthquake magnitude decreased from M_W 4.5 in 2019 to M_W 3.9 in 2020. For the 5-10 km distance range, seismicity rates were comparable for most magnitudes in 2019 and 2020 (middle plot in Figure IV-7), with the absolute numbers of events in both years being small. The maximum earthquake magnitude for this distance range decreased from M_D 1.7 in 2019 to M_D 1.0 in 2020. For earthquakes occurring more than 10 km from the injection well (including those with both shallow and slightly deeper hypocenters), seismicity rates decreased substantially for nearly all magnitudes in 2020 compared to 2019 (lower plot in Figure IV-7). The maximum earthquake magnitude for this distance range increased slightly from M_D 2.4 in 2019 to M_D 2.5 in 2020.

Normalized cumulative magnitude vs. log-frequency plots of the same data are presented in Figure IV-8. These are normalized Gutenberg-Richter magnitude relations ($\log_{10}(N) = a - bM$, where N = the percent of earthquakes with magnitude ≥ M). For both the near-well (≤ 5 km) and distant (> 10 km) regions, the fraction of larger-to-smaller-magnitude earthquakes increased in 2020 compared 2019. This is seen as a

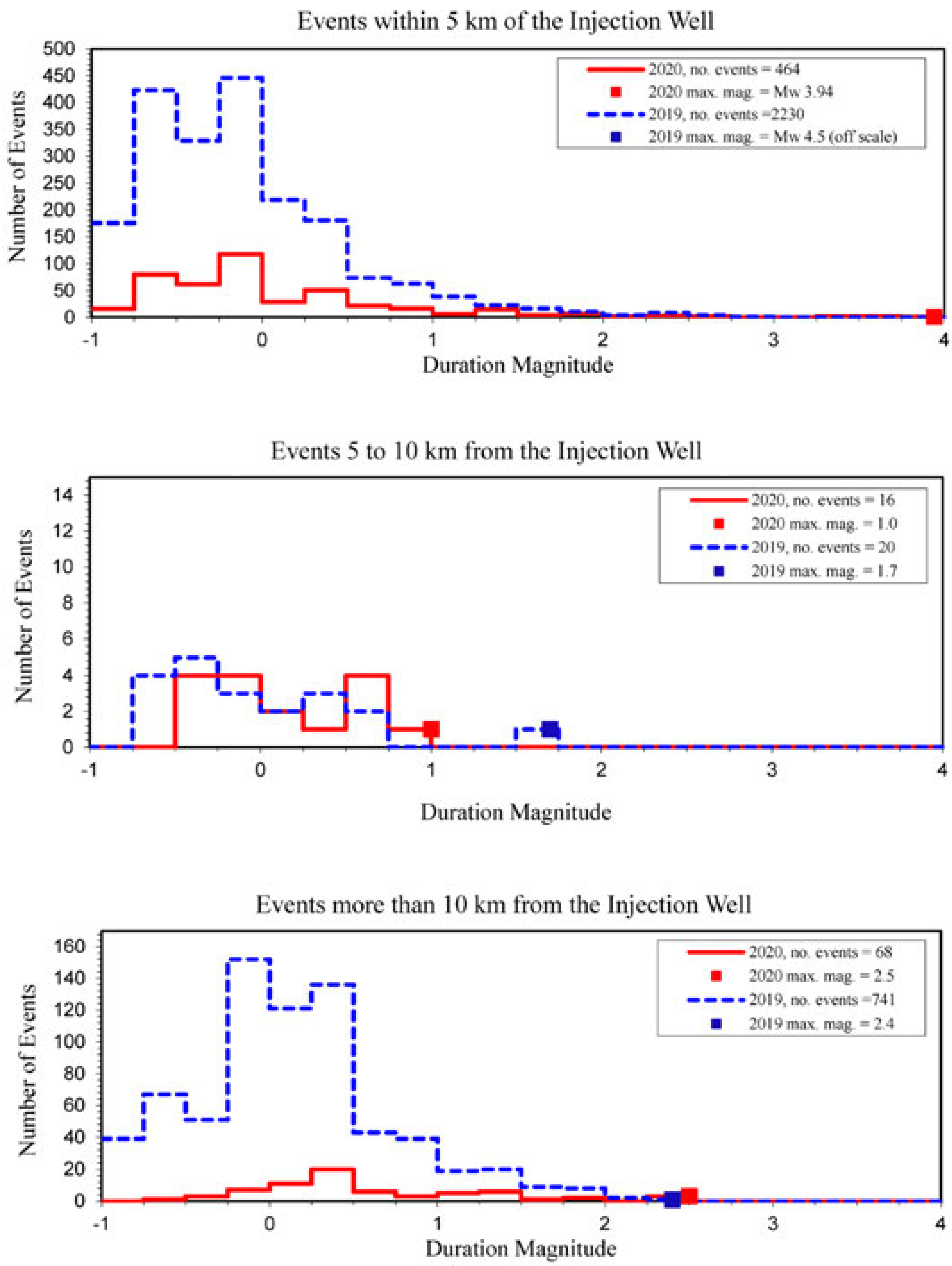

Figure IV-7: Magnitude histograms of events within 5 km of the injection well (top), at distances of 5 to 10 km from the well (middle), and more than 10 km from the well (bottom) during 2020 (solid red lines) and 2019 (dashed blue lines). Duration magnitudes are used for events with M_D < 3.0, and moment magnitudes are used for larger events. The squares indicate the maximum earthquake magnitude for a given distance range and year. The maximum earthquake magnitude for events within 5 km of the well in 2019 is off the scale of the plot (M_W 4.5).

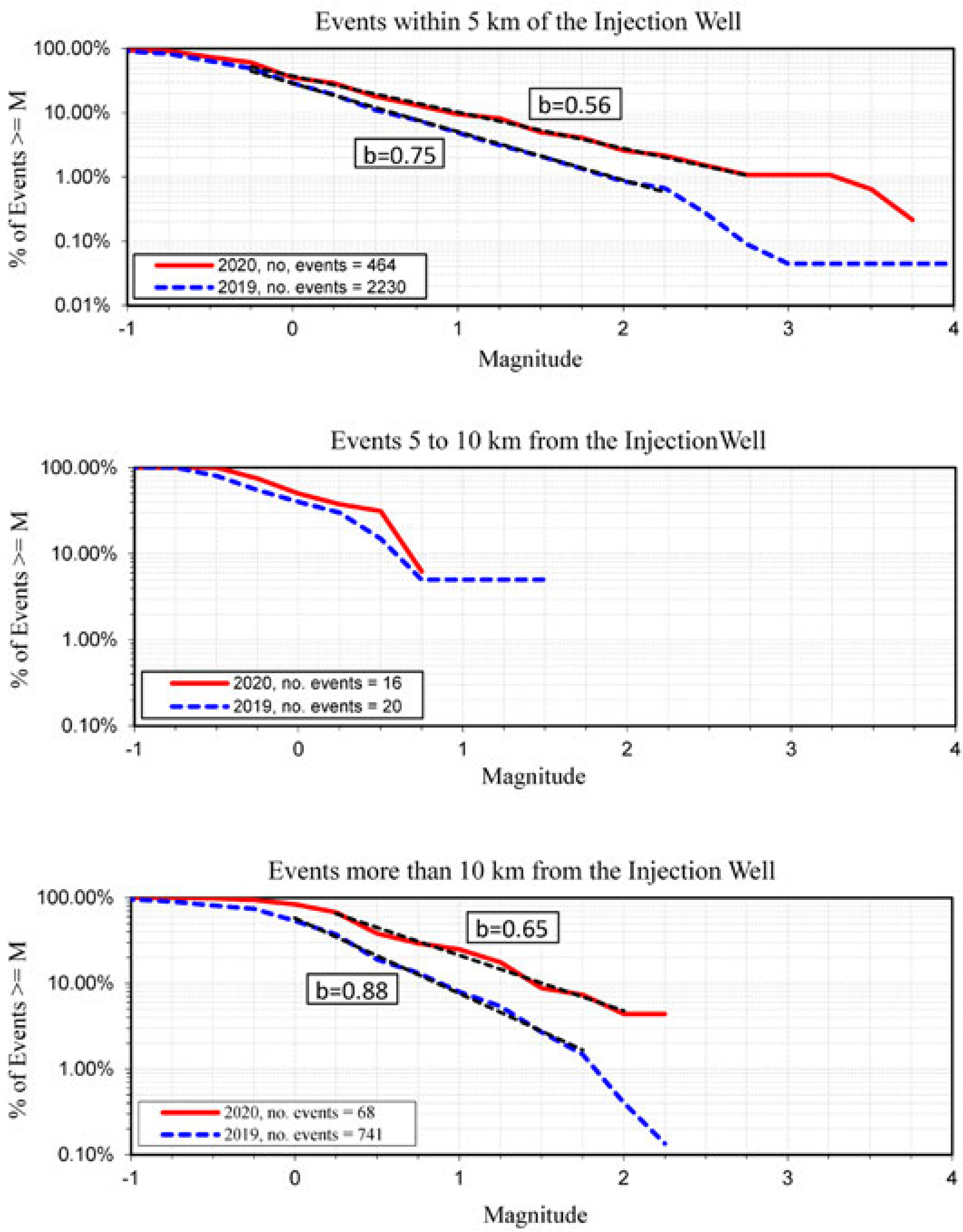

Figure IV-8: Normalized cumulative magnitude-(log)frequency plots of events within 5 km of the injection well (top), at distances of 5 to 10 km from the well (middle), and more than 10 km from the well (bottom) during 2020 (solid red lines) and 2019 (dashed blue lines). Duration magnitudes are used for events with M_D < 3.0, and moment magnitudes are used for larger events. The dashed black lines indicate linear fits to straight portions of the magnitude distributions; the b-values shown are from the slopes of these linear fits.

decrease in the absolute slopes (b-values) of the magnitude relations in the upper and lower plots in Figure IV-8. The reason for this apparent change in b-value between 2019 and 2020 has not yet been investigated but could potentially be related to changing spatial pore pressure gradients or the fraction of seismicity occurring in the Precambrian basement. The magnitude relations for the intermediate distance range are comparable in 2019 and 2020 (Figure IV-8, middle plot).

F. Historical Seismicity Trends

The rates and magnitudes of earthquakes that occurred during 2020 are compared to the historical seismicity trends in three plots described below. Only events with $M_D \geq 0.5$ are included in these plots, since the detection capability for earthquakes with magnitudes less than this threshold has varied considerably over the history of PVSN. First, the bubble plots in Figure IV-9 show the historical occurrence of seismicity (depth ≤ 12 km) as a function of date and earthquake magnitude during long-term injection at PVU (1996-2020). The area of each circle in these plots is scaled by the number of earthquakes in a given quarter-year and magnitude range. Individual bubble plots are included for earthquakes occurring within 5 km of the injection well, between 5 and 10 km from the well, and more than 10 km from the well. The daily average injection rates are included in Figure IV-9 for reference. In order to better observe the trends in recent years, similar plots that only include data from 2010-2020 are presented in Figure IV-10. Lastly, we show the annual seismicity rates for 2010-2020, for the different distances from the well, in Figure IV-11.

These plots show that the seismicity rate for the near-well area (within 5 km of the well) was fairly high in the last quarter of 2020 compared to historical levels (Figure IV-9b and Figure IV-10b). Although much of the near-well seismicity that occurred during 2020 is continuing aftershock activity from the March 2019 main shock, the anomalously high rate in the fourth quarter is related to the unusual seismicity swarm that occurred in November-December (section IV-B). According to these data, more earthquakes with magnitudes between M_w 3.5 and 4.0 occurred in the last quarter of 2020 than during any previous quarter.

The seismicity rates at distances of 5 to 10 km from the injection well in 2020 were relatively low compared to historical trends. The 2020 annual rate of M_D 0.5+ earthquakes in this distance range was about the same as the rate in 2019 but 60% lower than the average rate for the last ten years (2010-2019) (Figure IV-11b). The maximum earthquake magnitude in this intermediate distance range in 2020 was low compared to long-term historical trends (Figure IV-9c). Figure IV-9c and Figure IV-10c indicate that the maximum earthquake magnitude in this distance range was between M_D 1.0 and M_D 1.5 in 2020; this is the smallest maximum magnitude for this distance range for any calendar year except 2015.

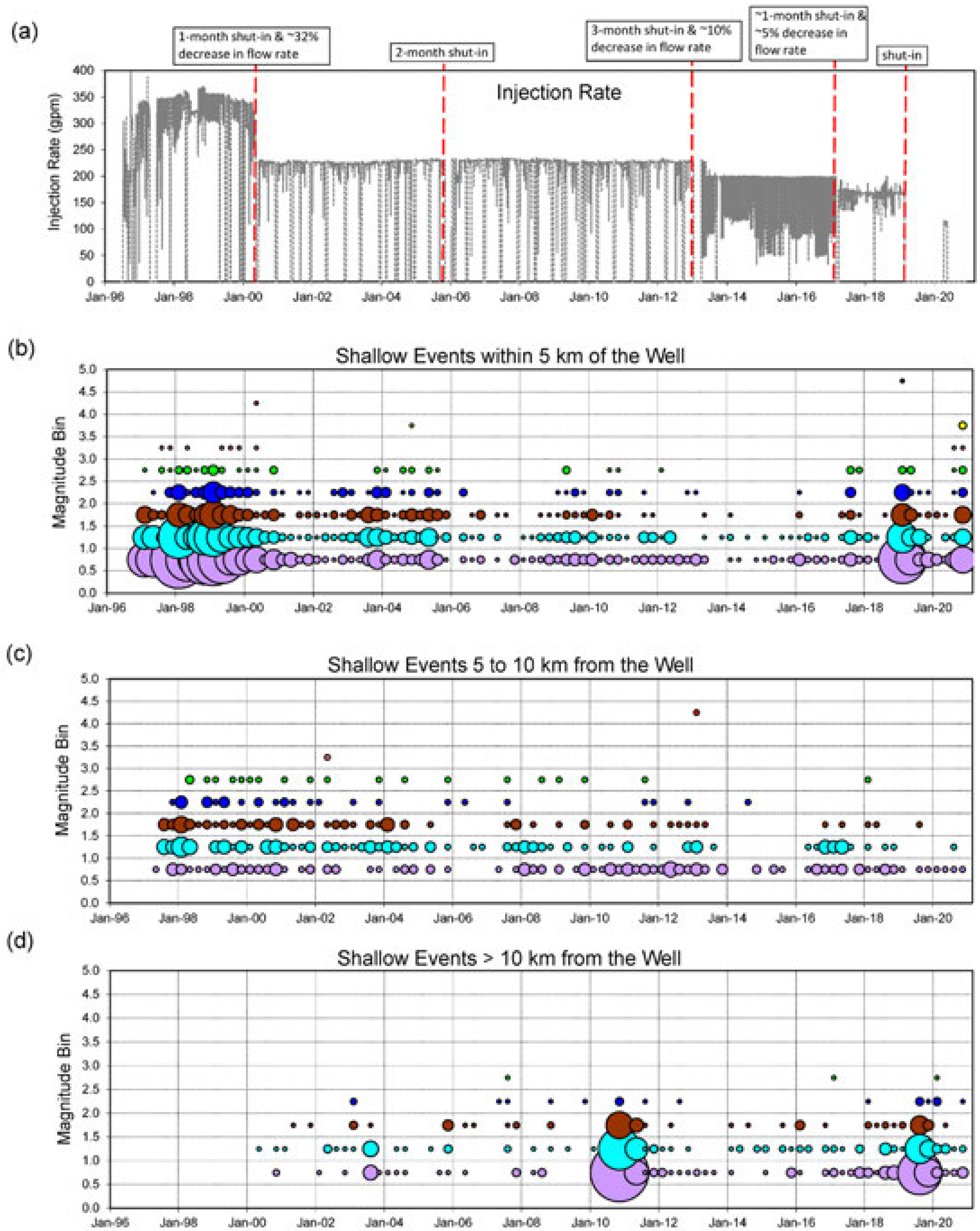

Figure IV-9: Injection flow rates (a) and occurrence of seismicity (depth ≤ 12 km) as a function of date and magnitude: within 5 km of the injection well (b), at distances of 5 to 10 km from the well (c), and more than 10 km from the well (d). In the seismicity plots, the area of each circle is scaled by the number of earthquakes in a given quarter-year and magnitude range; each plot is scaled independently. Duration magnitudes are used for events with M_D < 3.0, and moment magnitudes are used for larger events.

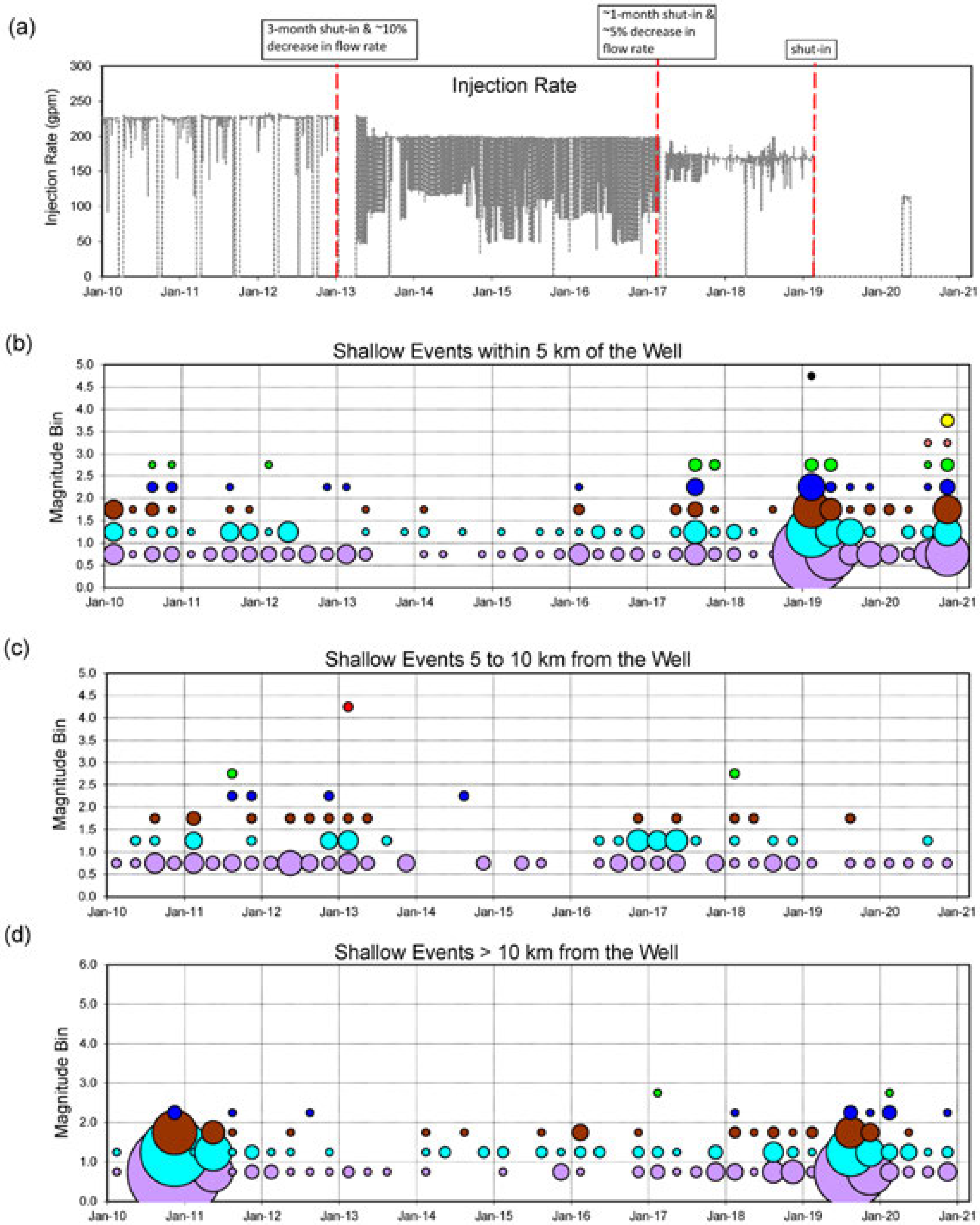

Figure IV-10: Same as Figure IV-9, but only showing data from 2010-2020.

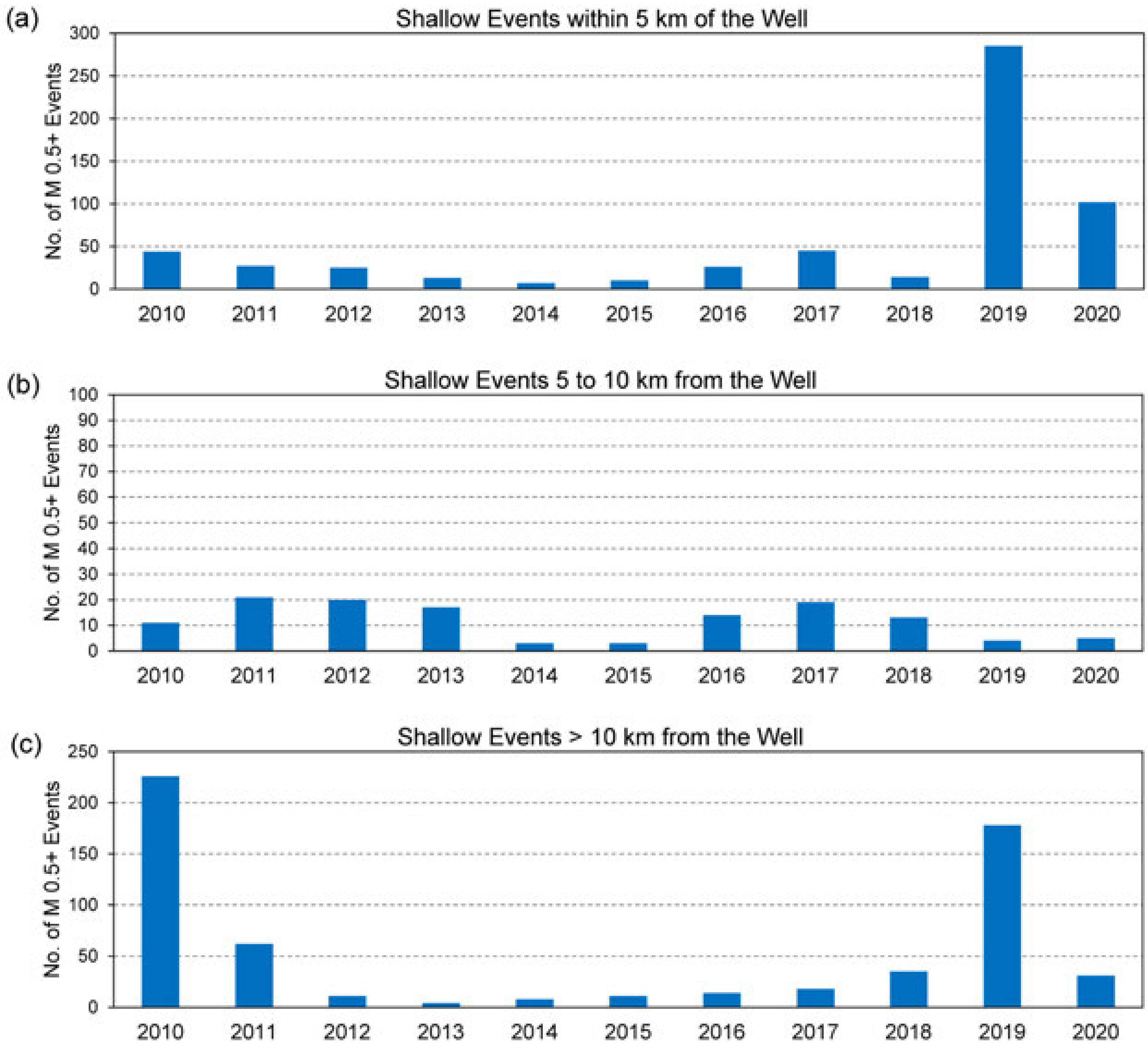

Figure IV-11: Annual numbers of earthquakes (depth ≤ 12 km) with M_D ≥ 0.5: within 5 km of the injection well (a), 5 to 10 km from the well (b), and more than 10 km from the well (c). Data from 2010 to 2020 are shown.

The annual rate of distant M 0.5+ events, those occurring more than 10 km from the injection well, increased from 2013 to 2019 (Figure IV-11c). The seismicity rate increased by an exceptionally large amount in 2019, due to an unusually strong swarm of seismic activity near the northern end of Paradox Valley (Block et al., 2020a). In 2020, the distant seismicity rate returned to about the same level as in 2018 (Figure IV-11c). The maximum magnitude of the distant induced earthquakes in 2020, M_D 2.5, was typical compared to historical trends (Figure IV-9d).

V. Conclusions

PVSN recorded 549 local earthquakes during 2020. The spatiotemporal seismicity trends observed since 1985 provide strong evidence that all but two of these events were induced by PVU brine injection. One of the remaining two earthquakes appears to be naturally occurring, while the other event is considered potentially induced.

Ten of the induced earthquakes recorded during 2020 have magnitudes ≥ M_D 2.5. This magnitude threshold is significant because it is the approximate minimum magnitude for ground shaking to be felt in the Paradox Valley area. Nine of these M_D 2.5+ earthquakes occurred within 3.5 km of the injection well, in the aftershock zone of the March 2019 M_W 4.5 induced earthquake. The remaining M_D 2.5+ earthquake occurred 12.1 km east of the PVU injection well, at a depth of approximately 6.3 km.

Near-well seismicity rates declined in 2020 compared to 2019, as the rate of aftershocks of the March 2019 M_W 4.5 earthquake decayed. However, an unusual swarm of near-well seismicity occurred during the last quarter of the year. This swarm occurred in a seismicity cluster that began forming within a few days of the March 2019 M_W 4.5 earthquake, ~700-1200 m southwest of the main shock rupture plane. Fourteen earthquakes occurred within this cluster during 2019 and were considered aftershocks of the M_W 4.5 earthquake. In 2020, 137 earthquakes occurred within this cluster, with 115 of them occurring in November and December. The earthquakes that occurred within this cluster during 2020 include eight events with magnitude ≥ M_D 2.5. Of these, four earthquakes have magnitude ≥ M_W 3.0. The largest of these earthquakes, with magnitude M_W 3.94, is the fourth largest PVU-induced earthquake to date. Seismicity rates within this cluster subsequently declined in January 2021.

Seismicity rates at distances of 5 to 10 km from the PVU injection well changed little in 2020 compared to the previous year. The seismicity rate and maximum magnitude (M_D 1.0) was low relative to historical trends.

The rate of induced seismicity at distances greater than 10 km from the well decreased substantially in 2020 compared to 2019 (91% overall decrease; 83% decrease in events with magnitude ≥ M_D 0.5). However, distant seismicity rates were not unusually low in 2020, but rather the 2019 rates were unusually high. The 2020 rates were fairly typical compared to historical trends. Seismicity either clearly or potentially related to PVU injection occurred at distances up to ~37 km from the injection well during 2020. Induced seismicity is occurring several km outside the perimeter of PVSN, decreasing the ability of the seismic network to detect and provide accurate locations for all of the induced earthquakes.

Despite travel restrictions imposed by the COVID-19 pandemic, extensive upgrades of the PVSN seismic stations were completed during two site visits conducted in 2020. New low-noise seismometers (Guralp model 3ESPCDE) were installed at 13 remote seismic stations, completing the network-wide broadband seismometer upgrade that was begun in 2018. New station electronics were also deployed, for compatibility with the new seismometers and improved station energy efficiency. In addition, new accelerometers (Silicon Audio 203V) and digitizers (Guralp Minimus) were installed at the three strong motion sites, and the data streams from these stations were integrated into PVSN's radio telemetry network and real-time data acquisition computer systems. PVSN performed well during 2020, with an annual network uptime of 99.4%.

VI. References

Block, L., Wood, C. K., Besana-Ostman, G., Schwarzer, J., Ball, J., and Kang, J. B., 2020a, *2019 Annual Report, Paradox Valley Seismic Network, Paradox Valley Unit, Colorado:* Technical Memorandum No. 86-68330-2020-07, Bureau of Reclamation, Denver, Colorado, 165 pp.

Block, L. V., Besana-Ostman, G., and Wood, C. K., 2020b, *Analysis of the March 4, 2019 Earthquake and Its Aftershocks:* Technical Memorandum No. 86-68330-2020-07, Bureau of Reclamation, Denver, Colorado, 149 pp.

Block, L. V., and Wood, C. K., 2009, *Overview of PVU-Induced Seismicity from 1996 to 2009 and Implications for Future Injection Operations: Technical Memorandum No. 86-68330-2009-22:* Technical Memorandum No. 86-68330-2009-22, Bureau of Reclamation, Denver, Colorado, 16 pp.

Block, L. V., Wood, C. K., Yeck, W. L., and King, V. M., 2014, The 24 January 2013 ML 4.4 Earthquake near Paradox, Colorado, and Its Relation to Deep Well Injection: *Seismological Research Letters*, v. 85, no. 3, p. 609-624.

Boore, D. M., 2001, Effect of baseline corrections on displacements and response spectra for several recordings of the 1999 Chi-Chi, Taiwan earthquake: *Bulletin of the Seismological Society of America*, v. 91, no. 5, p. 1199-1211.

-, 2010, Orientation-Independent, Nongeometric-Mean Measures of Seismic Intensity from Two Horizontal Components of Motion: *Bulletin of the Seismological Society of America*, v. 100, no. 4, p. 1830-1835.

Boore, D. M., Stephens, C. D., and Joyner, W. B., 2002, Comments on baseline correction of digital strong-motion data; examples from the 1999 Hector Mine, California, earthquake: *Bulletin of the Seismological Society of America*, v. 92, no. 4, p. 1543–1560.

Boore, D. M., Watson, L. J., and Abrahamson, N. A., 2006, Orientation-independent measures of ground motion: *Bulletin of the Seismological Society of America*, v. 96, no. 4a, p. 1502-1511.

Bozorgnia, Y., Abrahamson, N. A., Atik, L. A., Ancheta, T. D., Atkinson, G. M., Baker, J. W., Baltay, A., Boore, D. M., Campbell, K. W., Chiou, B. S. J., Darragh, R., Day, S., Donahue, J., Graves, R. W., Gregor, N., Hanks, T., Idriss, I. M., Kamai, R., Kishida, T., Kottke, A., Mahin, S. A., Rezaeian, S., Rowshandel, B., Seyhan, E., Shahi, S., Shantz, T., Silva, W., Spudich, P., Stewart, J. P., Watson-Lamprey, J., Wooddell, K., and Youngs, R., 2014, NGA-West2 Research Project: *Earthquake Spectra*, v. 30, no. 3, p. 973-987.

Bremkamp, W., and Harr, C. L., 1988, *Area of Least Resistance to Fluid Movement and Pressure Rise:* Report to the Bureau of Reclamation, 49 pp.

Envirocorp Services and Technology Inc., 1993, *Core Fluid Compatibility Test:* Report to the Bureau of Reclamation, 27 pp.

Gibbs, J. F., Healy, J. H., Raleigh, C. B., and Coakley, J., 1973, Seismicity in the Rangely, Colorado, Area: 1962-1970: *Bulletin of the Seismological Society of America*, v. 63, no. 5, p. 1557-1570.

Hsieh, P. A., and Bredehoeft, J. D., 1981, A reservoir analysis of the Denver earthquakes; a case of induced seismicity: *Journal of Geophysical Research. B*, v. 86, no. 2, p. 903-920.

Kharaka, Y. K., Ambats, G., Thordsen, J. J., and Davis, R. A., 1997, Deep well injection of brine from Paradox Valley, Colorado: Potential major precipitation problems remediated by nanofiltration: *Water Resources Research*, v. 33, no. 5, p. 1013-1020.

Mahrer, K., Ake, J., O'Connell, D., and Block, L., 2003, *2002 Status Report - Paradox Valley Seismic Network, Paradox Valley Project, Southwestern Colorado:* Technical Memorandum No. D8330-2003-009, Bureau of Reclamation, Technical Service Center, Denver, Colorado, 86 pp.

McKinley, R. M., 2001, *Comments on 19-Jun-2001 Mechanical Caliper Survey and 20-Jun-2001 Temperature Survey from Paradox Valley Injection Well #1*, 14 pp.

Nicholas, A., 2001, August 23rd Paradox Operations Meeting, Denver TSC, Internal Memorandum, Bureau of Reclamation, 4 pp.

Nicholson, C., and Wesson, R. L., 1990, *Earthquake Hazard Associated With Deep Well Injection - A Report to the U.S. Environmental Protection Agency:* Bulletin 1951, U.S. Geological Survey, 86 pp.

O'Connell, D. R. H., 2008, *Probabilistic Seismic Hazard Analysis, Hungry Horse Dam, Hungry Horse Project, Montana:* Technical Memorandum No. 86-68321-2008-12, Bureau of Reclamation, Technical Service Center, Denver, Colorado, 89 pp.

Power, M., Chiou, B., Abrahamson, N., Bozorgnia, Y., Shantz, T., and Roblee, C., 2008, An Overview of the NGA Project: *Earthquake Spectra*, v. 24, no. 1, p. 3-21.

Raleigh, C. B., Healy, J. H., and Bredehoeft, J. D., 1976, An Experiment in Earthquake Control at Rangely, Colorado: *Science*, v. 191, no. 4233, p. 1230-1237.

Subsurface Technology, 2001, *Report of Operations:* Report to the Bureau of Reclamation, Houston, 24 pp.

Walker, J. D., Geissman, J. W., Bowring, S. A., and Babcock, L. E., 2013, The Geological Society of America Geologic Time Scale: *GSA Bulletin*, v. 125, no. 3-4, p. 259-272.

Wood, C. K., Block, L. V., King, V. M., and Yeck, W. L., 2016, *The ML 4.4 Earthquake of January 24, 2013, Near Paradox, Colorado, and Implications for Near-term Injection Operation*, Bureau of Reclamation, Denver, Colorado, 150 pp.

Appendix A

2020 Site Visit Reports

Paradox Valley Seismic Network
Site Visit Report

Site Visit Number: PVSN-2020-1
Prepared by: Justin Schwarzer
Departure Date: 9/10/2020
Return Date: 9/19/2020
Personnel: Justin Schwarzer, Justin Ball

Primary Purpose: To perform preventive maintenance at the telemetered broadband seismic stations and install new seismometers at ten stations.

Details:
New Guralp model 3ESPCDE broadband seismometers were installed at stations PV03, 04, 05, 11, 13, 14, 15, 17, 21 and 22. These seismometers have improved sensitivity and noise characteristics compared to the previously installed Guralp CMG-40T seismometers. At each of these sites, DM24-BOBs were replaced with upgraded units. These new components were required for compatibility with the new seismometers.

New GPS antennas compatible with the 3ESPCDE seismometers where installed at PV04 and 10.

The GPS antenna was replaced at PV12 and a cable test performed.

Upgraded DM-24 BOBs were installed at PV02, 10, 12,19 and 20. Each of these sites have previously had 3ESPCDEs installed.

All sites received a new GPS-BOB chip flashed with the latest firmware.

At PV11, the vault was flooded with 2 inches of water and needed cleaning. Vault has concrete cracking and appears to have gone out of level. Dirt work was done on the surface to effect water flow away from vault.

Preventive maintenance work was performed at the data communication center at Hopkin’s Field consisting of standard antenna and radio testing, visual inspection of the tower and cabling, and generator diagnostics were run.

PVEF Guralp Minimus was reprogrammed with static IP address to fix telemetry issues.

Work by Site:

Site	Preventive Maintenance					Comments
	Checked Power System	Replaced Batteries	Tested Antennas and cables	Tested Radio(s)	Inspected Vault	
PV02	X		X			Replaced DM24-BOB and added new GPS chip. Chem rod refilled.
PV03	X		X		X	Replaced seismometer, GPS chip, and DM24-BOB.
PV04	X		X		X	Replaced seismometer, DM24-BOB, and GPS chip.
PV05	X	X	X		X	Replaced seismometer, GPS chip, DM24-BOB, and batteries.
PV10	X		X		X	Replaced DM24-BOB and GPS chip.
PV11	X		X		X	Replaced seismometer, DM24-BOB and GPS chip.
PV12	X		X		X	Replaced DM24-BOB and added new GPS chip. GPS antenna replaced and cable test ran. No issues found in wiring.
PV13	X	X	X		X	Replaced seismometer, DM24-BOB, GPS chip, and batteries.
PV14	X		X		X	Replaced seismometer, DM24-BOB and GPS chip.
PV15	X		X		X	Replaced seismometer, DM24-BOB and GPS chip.
PV17	X		X		X	Replaced seismometer, DM24-BOB and GPS chip.
PV19	X		X			Replaced DM24-BOB and added new GPS chip.
PV20	X		X			Replaced DM24-BOB and added new GPS chip.
PV21	X		X		X	Replaced seismometer, DM24-BOB and GPS chip.
PV22	X		X		X	Replaced seismometer, DM24-BOB and GPS chip.

Site	Preventive Maintenance					Comments
	Checked Power System	Replaced Batteries	Tested Antennas and cables	Tested Radio(s)	Inspected Vault	
Hopkins Field	X		X	X		

Abbreviations:

AP-1 – access point #1 antenna on the tower at the Hopkin's Field data communications center; receives radio data communications from individual stations PV01, PV07, and PV15

AP-2 – access point #2 antenna on the tower at the Hopkin's Field data communications center; receives radio data communications from radio repeater station PV02

AP-3 – access point #3 antenna on the tower at the Hopkin's Field data communications center; receives radio data communications from radio repeater stations PV04 and PV12

Chem rod – chemical ground rod that is part of the lightning protection grounding system at station PV02

DM24-BOB - seismic station electronics break-out-box located in enclosure; conditions power supply for the DM24 seismometer digitizer

GPS – refers to antenna that receives Global Positioning System satellite data to provide station timing

GPS-BOB - seismic station electronics break-out-box located in enclosure; serves as junction for dirty and clean power supplies and data communications

LVD - low-voltage disconnect

WAGO – refers to special tool needed for engaging (or disengaging) some electronics connections within station enclosure; manufactured by WAGO Corporation

Paradox Valley Seismic Network Site Visit Report

Site Visit Number: PVSN-2020-2
Prepared by: Lisa Block and Chris Wood
Departure Date: 10/14/2020
Return Date: 10/22/2020
Personnel: Chris Wood and Jong Kang

Primary Purpose: To upgrade instrumentation and to conduct preventive and remedial maintenance at broadband and strong motion seismic stations.

Details:
Instrumentation at the three strong-motion sites was upgraded to enable use of real-time data loggers, high-sensitive accelerometers, and continuous radio telemetry. At each of the three strong-motion sites (PVEF, PVPP, and PVCC), the obsolete Kinemetrics K2 data loggers and FBA-23 sensors were removed, along with modems, TMC-5s, and other now-superfluous ancillary equipment. New ground rods (three per site) and braided copper grounding cable were installed at each site. Existing interior equipment enclosures were relocated within the large fiberglass enclosures at PVPP and PVCC to be compatible with the positions of the new antenna masts. New Yagi antennas were installed on the masts and oriented towards the existing hub sites at PV04 or PV12, using azimuths determined from GIS and measurements using a Brunton compass and tripod. New Polyphaser RF surge suppressors and hardline Heliax transmission cables were installed. Lexan plates were epoxied to the concrete slabs at PVCC and PVPP. New Silicon Audio sensors were bolted to the Lexan plates at all three sites and oriented to within 0.2 degrees of true north using a Quadrans fiber-optic gyroscope system. Orientations of the old sensors were also measured using the Quadrans before being removed. New Guralp Minimus digitizers were installed at PVCC and PVPP and connected to new GE-MDS wireless bridges. The existing Minimus digitizer at PVEF was removed for factory repair. Continuous data streams were established for PVPP and PVCC. PVEF will be restored once the Minimus from that station can be replaced. New batteries were installed at all three sites.

New Guralp model 3ESPCDE broadband seismometers were installed at three remote sites (PV01, PV07, and PV16). These seismometers have improved sensitivity and noise characteristics compared to the previously installed Guralp CMG-40T seismometers, as well as a more capable digitizer that supports additional communications protocols. Standard preventive maintenance was also performed at these three sites, as well as at stations PV18 and PV23. At all five sites, the DM24-BOBs were replaced with re-engineered units having improved power efficiency and better compatibility with the new seismometers. These sites also received a new GPS-BOB chip flashed with the latest firmware.

The remaining broadband stations (PV02, PV03, PV04, PV05, PV10, PV11, PV12, PV13, PV14, PV15, PV17, PV19, PV20, PV21, and PV22) were visited briefly to perform an onsite upgrade of the DM24-BOB firmware to the latest version. This upgrade was needed to enable the units to restart if the stations experience any unexpected power failures.

A NetBotz environmental monitor was installed in the communications hub building at Hopkins Field.

Summary of Work by Site:

Site	Preventive Maintenance					Comments
	Checked Power System	Replaced Batteries	Tested Antennas and cables	Tested Radio(s)	Inspected Vault	
PV01	X		X		X	Upgraded seismometer, DM24-BOB, and GPS-BOB firmware
PV02						Upgraded DM24-BOB firmware
PV03						Upgraded DM24-BOB firmware
PV04						Upgraded DM24-BOB firmware
PV05						Upgraded DM24-BOB firmware
PV07	X		X		X	Upgraded seismometer, DM24-BOB, and GPS-BOB firmware
PV10						Upgraded DM24-BOB firmware
PV11						Upgraded DM24-BOB firmware
PV12						Upgraded DM24-BOB firmware
PV13						Upgraded DM24-BOB firmware
PV14						Upgraded DM24-BOB firmware

Site	Preventive Maintenance					Comments
	Checked Power System	Replaced Batteries	Tested Antennas and cables	Tested Radio(s)	Inspected Vault	
PV15						Upgraded DM24-BOB firmware
PV16	X		X		X	Upgraded seismometer, DM24-BOB, and GPS-BOB firmware
PV17						Upgraded DM24-BOB firmware
PV18	X		X			Installed re-engineered DM24-BOB; replaced GPS-BOB board
PV19						Upgraded DM24-BOB firmware
PV20						Upgraded DM24-BOB firmware
PV21						Upgraded DM24-BOB firmware
PV22						Upgraded DM24-BOB firmware
PV23	X		X			Installed re-engineered DM24-BOB; updated GPS-BOB firmware; removed SPM
PVCC		X	X			Upgraded strong motion instrumentation and communications equipment
PVEF		X	X			Upgraded strong motion instrumentation and communications equipment
PVPP		X	X			Upgraded strong motion instrumentation and communications equipment
Hopkins Field						Installed environmental monitor

Abbreviations:

AP-1 – access point #1 antenna on the tower at the Hopkin's Field data communications center; receives radio data communications from individual stations PV01, PV07, and PV15

AP-2 – access point #2 antenna on the tower at the Hopkin's Field data communications center; receives radio data communications from radio repeater station PV02

AP-3 – access point #3 antenna on the tower at the Hopkin's Field data communications center; receives radio data communications from radio repeater stations PV04 and PV12

Chem rod – chemical ground rod that is part of the lightning protection grounding system at station PV02

DM24-BOB - seismic station electronics break-out-box located in enclosure; conditions power supply for the DM24 seismometer digitizer

GPS – refers to antenna that receives Global Positioning System satellite data to provide station timing

GPS-BOB - seismic station electronics break-out-box located in enclosure; serves as junction for dirty and clean power supplies and data communications

LVD - low-voltage disconnect

SPM – station power monitor

WAGO – refers to special tool needed for engaging (or disengaging) some electronics connections within station enclosure; manufactured by WAGO Corporation

Appendix B

PVSN 2020 Local Earthquake Catalog

Table B-1: Local Earthquakes Recorded by PVSN During 2020

Date[1]	Time[1]	Latitude (deg.)	Longitude (deg.)	Elevation[2] (km)	Depth[3] (km)	Magnitude[4]		Horizontal Distance from Injection Well (km)
						M_D	M_W	
1/3/2020	17:19:00	38.4300	-108.9380	-6.2	7.8	0.2	1.0	15.3
1/4/2020	4:35:58	38.2821	-108.9078	-2.0	3.6	-0.4	1.0	2.0
1/4/2020	4:54:08	38.2821	-108.9079	-2.0	3.6	-0.4		2.0
1/4/2020	10:45:44	38.2858	-108.8989	-2.0	3.5	0.1	0.9	1.2
1/4/2020	15:50:19	38.3540	-108.6730	-9.1	10.7	0.5	1.3	20.4
1/5/2020	1:25:15	38.4036	-108.8708	-4.5	6.0	0.3	1.0	12.1
1/6/2020	5:41:22	38.2839	-108.9042	-1.9	3.4	-0.3	0.1	1.6
1/6/2020	18:24:30	38.2787	-108.9152	-2.6	4.1	-0.3	0.7	2.7
1/7/2020	20:04:49	38.2851	-108.9011	-2.0	3.5	-0.4		1.4
1/7/2020	22:16:26	38.2833	-108.9051	-1.9	3.5	0.0	0.6	1.7
1/9/2020	8:17:33	38.2849	-108.9014	-2.2	3.7	0.6	1.0	1.4
1/10/2020	6:52:41	38.4037	-108.8710	-4.5	6.0	0.0	0.7	12.1
1/10/2020	9:36:49	38.4036	-108.8713	-4.4	6.0	0.3	1.0	12.1
1/11/2020	5:35:22	38.2860	-108.8991	-2.0	3.5	-0.4	0.5	1.2
1/11/2020	16:26:06	38.2867	-108.8962	-2.1	3.7	0.3	0.9	1.1
1/12/2020	5:09:28	38.4016	-108.8694	-4.4	5.9	0.4	1.0	11.9
1/12/2020	5:13:21	38.3003	-108.8778	-3.9	5.4	1.5	1.3	1.6
1/12/2020	14:32:05	38.3110	-108.7347	-7.8	9.4	2.5	2.3	14.1
1/12/2020	18:24:50	38.3110	-108.7346	-7.8	9.4	0.5	1.2	14.1
1/12/2020	19:11:30	38.2828	-108.9062	-2.0	3.6	-0.1	0.9	1.8
1/12/2020	19:17:22	38.2827	-108.9063	-2.0	3.6	-0.5		1.8
1/12/2020	22:15:13	38.3112	-108.7344	-7.8	9.3	-0.2		14.1
1/13/2020	2:42:55	38.3110	-108.7357	-7.8	9.3	0.0	1.1	14.0
1/13/2020	3:26:52	38.2857	-108.8996	-2.0	3.5	-0.2	0.7	1.3
1/13/2020	10:06:00	38.3111	-108.7343	-7.8	9.3	1.2	1.6	14.1
1/13/2020	16:48:44	38.3109	-108.7352	-7.8	9.4	2.0	2.1	14.1
1/13/2020	17:19:02	38.2856	-108.8996	-2.1	3.6	-0.2	1.0	1.3
1/14/2020	8:39:41	38.2858	-108.8997	-2.0	3.5	-0.5	0.1	1.3
1/15/2020	12:58:06	38.3110	-108.7355	-7.8	9.3	0.3	1.3	14.0
1/16/2020	5:48:50	38.2790	-108.9012	-2.9	4.4	-0.1	0.7	2.0
1/16/2020	9:05:21	38.2838	-108.9041	-1.9	3.5	-0.4	0.6	1.6
1/16/2020	9:11:42	38.2838	-108.9043	-1.9	3.5	-0.5	0.8	1.6
1/16/2020	9:11:43	38.2837	-108.9043	-1.9	3.5	-0.1	1.0	1.6
1/16/2020	9:12:31	38.2839	-108.9044	-1.9	3.4	-0.7		1.6
1/16/2020	9:52:44	38.2833	-108.9061	-1.9	3.4	-0.1	0.6	1.8
1/19/2020	0:25:00	38.2852	-108.9006	-2.0	3.5	-0.4	0.1	1.4
1/20/2020	7:39:43	38.2828	-108.9058	-1.9	3.5	-0.3		1.8
1/21/2020	14:09:15	38.2695	-108.9220	1.1	0.4	0.9	1.0	3.8
1/21/2020	23:54:41	38.2837	-108.9045	-2.0	3.6	-1.2		1.7
1/21/2020	23:54:44	38.2833	-108.9059	-1.9	3.5	0.0	0.7	1.7

Date[1]	Time[1]	Latitude (deg.)	Longitude (deg.)	Elevation[2] (km)	Depth[3] (km)	Magnitude[4]		Horizontal Distance from Injection Well (km)
						M_D	M_W	
1/22/2020	1:28:05	38.2837	-108.9044	-1.9	3.5	-0.2	0.6	1.6
1/22/2020	1:42:33	38.2837	-108.9044	-2.0	3.5	0.0	1.0	1.6
1/22/2020	2:57:06	38.3220	-108.9820	-2.3	3.8	0.4	1.1	8.1
1/23/2020	5:18:56	38.2835	-108.9041	-2.0	3.5	-0.2	0.7	1.7
1/23/2020	14:16:21	38.2859	-108.8991	-2.0	3.5	0.2	1.1	1.2
1/23/2020	14:16:44	38.2860	-108.8993	-1.9	3.4	-1.2		1.2
1/23/2020	14:19:03	38.2861	-108.8992	-2.0	3.5	-0.2	0.8	1.2
1/23/2020	23:38:02	38.3500	-108.9065	-3.6	5.1	-0.4	0.6	6.0
1/25/2020	8:27:11	38.2859	-108.8986	-2.0	3.6	0.1	0.8	1.2
1/26/2020	15:50:27	38.2859	-108.8966	-2.3	3.8	-0.2	0.4	1.2
1/26/2020	18:00:08	38.2863	-108.8995	-1.9	3.4	-0.5		1.2
1/26/2020	20:29:15	38.2858	-108.8995	-2.0	3.6	-0.5	0.2	1.3
1/28/2020	5:16:05	38.2856	-108.9004	-2.0	3.6	-0.6		1.3
1/29/2020	2:11:19	38.2819	-108.9099	-2.0	3.5	0.2	1.0	2.1
1/29/2020	20:11:45	38.3109	-108.7357	-7.8	9.4	0.7	1.5	14.0
1/30/2020	18:51:47	38.2859	-108.8991	-2.0	3.5	-0.7		1.2
1/30/2020	23:05:37	38.2865	-108.7048	-6.6	8.1	0.2	1.3	16.7
1/31/2020	11:04:22	38.2855	-108.9003	-2.0	3.5	-0.4	0.8	1.3
1/31/2020	12:32:33	38.2858	-108.8990	-2.1	3.6	0.4	1.0	1.2
2/1/2020	1:20:54	38.2870	-108.7273	-3.8	5.3	0.9	1.3	14.7
2/1/2020	16:04:54	38.3109	-108.7363	-7.8	9.3	1.4	1.6	14.0
2/1/2020	21:00:27	38.2824	-108.9055	-2.3	3.9	-0.2		1.8
2/2/2020	3:12:12	38.2807	-108.9091	-2.2	3.8	-0.6	0.5	2.2
2/2/2020	10:51:08	38.3107	-108.7355	-7.9	9.4	0.8	1.4	14.0
2/3/2020	11:18:54	38.3110	-108.7362	-7.8	9.3	2.0	2.3	14.0
2/3/2020	11:59:45	38.3111	-108.7367	-7.7	9.2	2.3	2.4	13.9
2/3/2020	17:04:14	38.3111	-108.7360	-7.7	9.3	1.3	2.2	14.0
2/4/2020	3:08:38	38.3112	-108.7362	-7.7	9.2	0.2	1.0	14.0
2/4/2020	12:10:20	38.3570	-108.6780	-9.1	10.6	0.4	1.4	20.1
2/4/2020	17:22:45	38.2822	-108.9072	-2.2	3.7	-0.5	1.0	1.9
2/5/2020	1:40:42	38.3110	-108.7354	-7.8	9.3	0.3	1.5	14.1
2/6/2020	4:32:01	38.2862	-108.8964	-2.0	3.5	0.7	1.2	1.2
2/6/2020	5:45:16	38.2792	-108.8158	-2.8	4.3	0.0	1.0	7.2
2/6/2020	7:01:23	38.2844	-108.9036	-2.1	3.6	-1.5		1.5
2/7/2020	20:16:39	38.2817	-108.9074	-2.0	3.5	-0.3		2.0
2/12/2020	6:20:03	38.2777	-108.8280	-2.3	3.8	0.7	1.1	6.2
2/12/2020	20:02:47	38.2857	-108.9003	-2.0	3.5	-0.5	0.8	1.3
2/13/2020	3:41:32	38.2823	-108.9070	-2.2	3.8	-0.4	0.5	1.9
2/16/2020	4:51:03	38.2814	-108.9072	-2.0	3.5	0.1	0.9	2.0
2/17/2020	9:17:19	38.2837	-108.9044	-1.9	3.5	-0.1	0.6	1.6
2/18/2020	8:52:10	38.2830	-108.9053	-2.3	3.8	-0.2	0.5	1.8

Date[1]	Time[1]	Latitude (deg.)	Longitude (deg.)	Elevation[2] (km)	Depth[3] (km)	Magnitude[4]		Horizontal Distance from Injection Well (km)
						M_D	M_W	
2/18/2020	10:38:25	38.2852	-108.9014	-2.0	3.5	-0.7	1.1	1.4
2/20/2020	4:59:24	38.2764	-108.9013	-2.0	3.6	-0.2	0.8	2.3
2/21/2020	4:21:52	38.2822	-108.9077	-2.0	3.5	-0.6	0.7	1.9
2/21/2020	8:45:04	38.2732	-108.9275	-0.6	2.1	0.5	1.0	3.9
2/21/2020	8:50:01	38.2735	-108.9278	-0.4	1.9	0.0	1.0	3.8
2/21/2020	8:50:08	38.2742	-108.9268	-0.8	2.4	-0.3		3.7
2/21/2020	8:51:55	38.2733	-108.9273	-1.0	2.5	-0.7	0.6	3.8
2/21/2020	8:53:07	38.2732	-108.9272	-0.8	2.3	-0.1	0.6	3.8
2/21/2020	8:53:08	38.2737	-108.9260	-0.3	1.8	-0.2	0.8	3.7
2/22/2020	5:30:38	38.2791	-108.8981	-3.2	4.7	0.2	1.0	2.0
2/22/2020	8:41:54	38.4042	-108.8701	-4.5	6.0	0.3	1.0	12.1
2/22/2020	11:40:38	38.2859	-108.8984	-2.0	3.6	0.0	1.0	1.2
2/23/2020	7:00:54	38.2834	-108.9043	-2.0	3.6	0.6	1.1	1.7
2/23/2020	20:18:14	38.1452	-108.5155	-4.8	6.3	0.1		37.2
2/23/2020	23:16:18	38.4015	-108.8702	-4.3	5.9	0.0	0.8	11.9
2/25/2020	14:06:48	38.2860	-108.8992	-2.0	3.5	-0.4	0.9	1.2
2/26/2020	14:06:37	38.2821	-108.9075	-2.1	3.6	-0.5		1.9
2/26/2020	15:10:48	38.2860	-108.8989	-2.0	3.5	-0.1	0.8	1.2
2/26/2020	20:32:18	38.3116	-108.7405	-7.5	9.0	-0.6		13.6
2/26/2020	20:42:02	38.2821	-108.9074	-2.1	3.6	-0.3	0.6	1.9
2/26/2020	20:42:15	38.2787	-108.9027	-1.9	3.4	-1.2		2.1
2/26/2020	23:02:00	38.2822	-108.9077	-2.1	3.6	-0.8		1.9
2/27/2020	8:13:12	38.2853	-108.8932	-1.9	3.4	1.5	1.6	1.3
2/27/2020	19:39:55	38.2821	-108.9085	-1.9	3.5	-0.8		2.0
2/28/2020	13:21:47	38.2833	-108.8920	-2.8	4.3	-0.1	0.8	1.5
3/1/2020	1:02:38	38.2821	-108.9082	-2.1	3.6	-0.1	0.6	2.0
3/1/2020	7:48:10	38.2840	-108.8927	-2.6	4.1	-0.1	0.4	1.4
3/2/2020	10:14:34	38.2837	-108.9016	-2.4	3.9	0.1	1.0	1.5
3/2/2020	11:05:54	38.2840	-108.8927	-2.6	4.1	-0.4	0.7	1.4
3/3/2020	10:39:33	38.2825	-108.9055	-2.3	3.8	0.0	1.0	1.8
3/4/2020	9:34:36	38.2852	-108.9008	-2.0	3.5	-0.5		1.4
3/5/2020	2:54:02	38.2852	-108.9012	-2.2	3.7	0.4	1.1	1.4
3/6/2020	17:42:09	38.3109	-108.7376	-7.7	9.2	1.1	1.6	13.9
3/7/2020	18:06:23	38.2841	-108.9036	-1.9	3.5	-0.7	0.6	1.6
3/10/2020	11:10:50	38.2859	-108.8988	-2.0	3.5	0.1	1.0	1.2
3/10/2020	14:44:09	38.2829	-108.9062	-2.2	3.7	0.0	1.2	1.8
3/12/2020	20:22:25	38.2824	-108.9060	-2.2	3.7	0.7	1.2	1.8
3/14/2020	0:36:19	38.2862	-108.8969	-1.9	3.4	-0.2		1.2
3/14/2020	3:00:56	38.2857	-108.9001	-1.9	3.5	-0.6	0.9	1.3
3/14/2020	10:35:23	38.2863	-108.8969	-1.9	3.4	-0.5	0.5	1.1
3/16/2020	2:56:55	38.2816	-108.9066	-2.0	3.6	-0.4	0.6	1.9

Date[1]	Time[1]	Latitude (deg.)	Longitude (deg.)	Elevation[2] (km)	Depth[3] (km)	Magnitude[4]		Horizontal Distance from Injection Well (km)
						M_D	M_W	
3/19/2020	22:15:48	38.2854	-108.9015	-1.9	3.4	-0.4	0.5	1.4
3/20/2020	5:06:28	38.2834	-108.9048	-2.0	3.5	0.3	0.9	1.7
3/22/2020	6:57:01	38.2852	-108.9018	-2.1	3.7	-0.2	0.7	1.4
3/22/2020	17:56:46	38.2817	-108.9064	-2.0	3.6	-0.5	0.6	1.9
3/23/2020	0:53:00	38.2817	-108.9062	-2.1	3.6	-0.2	0.7	1.9
3/23/2020	16:18:25	38.2857	-108.8999	-2.0	3.5	-0.6		1.3
4/2/2020	21:56:23	38.2834	-108.9051	-1.9	3.5	-0.3		1.7
4/3/2020	11:23:43	38.2862	-108.8993	-1.9	3.4	-0.6		1.2
4/3/2020	22:49:46	38.2861	-108.8965	-2.0	3.5	1.0	1.2	1.2
4/4/2020	20:35:23	38.3110	-108.7378	-7.7	9.2	1.6	1.9	13.8
4/6/2020	18:07:31	38.4108	-109.0305	-3.2	4.7	-0.2	1.4	17.4
4/8/2020	13:16:52	38.2822	-108.9082	-1.9	3.4	-0.4		2.0
4/10/2020	3:06:18	38.2854	-108.9019	-2.0	3.5	-0.2		1.4
4/11/2020	1:09:46	38.2817	-108.9065	-2.0	3.6	-0.3	0.9	1.9
4/12/2020	3:42:29	38.4095	-109.0423	-4.6	6.1	1.3	1.4	18.0
4/12/2020	8:34:01	38.3109	-108.7382	-7.7	9.2	1.4	1.6	13.8
4/12/2020	9:31:30	38.2860	-108.8995	-2.0	3.5	-0.2		1.2
4/12/2020	19:20:13	38.2732	-108.8928	-0.9	2.5	0.3	1.2	2.6
4/14/2020	17:00:58	38.2817	-108.9065	-2.0	3.6	-0.7	0.8	1.9
4/17/2020	18:55:13	38.3153	-108.7413	-6.2	7.7	0.4	1.3	13.6
4/18/2020	4:44:49	38.2822	-108.9079	-2.0	3.5	-0.2		2.0
4/18/2020	10:15:10	38.2825	-108.9038	-2.3	3.8	1.0	1.0	1.7
4/20/2020	1:13:12	38.2818	-108.9054	-2.3	3.8	0.3	0.8	1.9
4/21/2020	21:24:06	38.2856	-108.9006	-1.9	3.4	-1.3	0.7	1.3
4/21/2020	22:04:31	38.2860	-108.8993	-2.0	3.5	-0.7		1.2
4/24/2020	3:01:57	38.2828	-108.9059	-1.9	3.5	-0.1	0.6	1.8
4/26/2020	20:07:36	38.2985	-108.9098	-6.3	7.9	0.1		1.3
4/26/2020	20:07:37	38.3000	-108.9162	-6.0	7.5	0.5		1.9
4/27/2020	2:41:36	38.2818	-108.9062	-2.1	3.6	1.5	1.6	1.9
4/27/2020	4:40:33	38.2816	-108.9067	-2.0	3.5	-0.4	0.6	1.9
4/28/2020	4:34:37	38.2818	-108.9065	-2.0	3.5	-0.7		1.9
4/30/2020	17:28:42	38.4072	-109.0065	-2.6	4.1	0.2	1.1	15.7
5/1/2020	2:44:19	38.2814	-108.9102	-1.8	3.4	0.4	1.1	2.1
5/1/2020	10:34:59	38.4040	-108.8702	-4.5	6.0	1.3	1.4	12.1
5/2/2020	14:51:08	38.3445	-108.7678	-4.1	5.6	0.3	1.3	12.3
5/6/2020	13:20:23	38.2860	-108.8999	-2.0	3.5	-0.6	1.0	1.3
5/6/2020	21:55:34	38.2857	-108.8994	-1.9	3.5	-0.1	1.0	1.3
5/13/2020	16:22:08	38.2842	-108.9021	-2.1	3.7	-0.2	1.1	1.5
5/16/2020	10:14:27	38.2713	-108.8950	-1.0	2.5	0.1	0.9	2.8
5/16/2020	13:24:49	38.2713	-108.8948	-1.0	2.5	-0.2		2.8
5/16/2020	15:42:16	38.2712	-108.8958	-1.4	2.9	-0.1		2.8

Date[1]	Time[1]	Latitude (deg.)	Longitude (deg.)	Elevation[2] (km)	Depth[3] (km)	Magnitude[4]		Horizontal Distance from Injection Well (km)
						M_D	M_W	
5/18/2020	5:47:41	38.2824	-108.9039	-2.3	3.8	-0.3		1.8
5/20/2020	4:42:02	38.2763	-108.8122	-2.0	3.5	-0.1		7.6
5/21/2020	1:01:00	38.2841	-108.9034	-1.9	3.4	-0.2		1.6
5/21/2020	12:25:18	38.2823	-108.9057	-2.1	3.6	0.5	1.0	1.8
5/22/2020	8:48:55	38.3109	-108.7377	-7.7	9.3	1.1	1.5	13.8
5/22/2020	21:34:43	38.2823	-108.9055	-2.0	3.6	0.2	0.9	1.8
5/22/2020	22:33:23	38.2823	-108.9055	-2.0	3.5	-0.8	0.6	1.8
5/24/2020	6:56:00	38.2764	-108.8894	-0.5	2.1	0.6	0.8	2.3
5/26/2020	11:45:48	38.2821	-108.9059	-2.0	3.6	-0.2		1.9
5/28/2020	2:46:08	38.2753	-108.9237	-0.7	2.2	0.0	0.7	3.4
5/28/2020	10:10:52	38.2735	-108.9252	-0.8	2.3	-0.4	0.6	3.7
5/28/2020	10:11:58	38.2763	-108.9222	-0.7	2.2	-1.1		3.3
5/29/2020	13:32:54	38.4014	-108.8699	-4.3	5.8	-0.1	0.7	11.8
5/29/2020	22:42:10	38.3292	-108.8613	-4.2	5.7	-0.3		4.7
5/29/2020	22:46:36	38.4210	-108.9775	-5.5	7.0	-0.3		15.6
5/30/2020	3:20:03	38.1857	-108.8308	-2.5	4.0	0.6		13.5
5/30/2020	3:20:07	38.1943	-108.8410	-0.9	2.4	0.3	0.9	12.3
6/1/2020	16:20:50	38.3515	-108.8807	-5.2	6.8	0.7	1.2	6.2
6/2/2020	3:45:47	38.2862	-108.8967	-1.9	3.5	-0.4	0.9	1.2
6/2/2020	5:47:25	38.2785	-108.8249	-2.4	4.0	0.1	1.0	6.4
6/2/2020	8:40:07	38.2856	-108.9003	-2.0	3.5	-0.1	0.8	1.3
6/2/2020	8:40:14	38.2856	-108.9003	-2.0	3.5	-0.6		1.3
6/2/2020	13:47:41	38.2854	-108.9017	-1.9	3.4	-1.0	0.9	1.4
6/3/2020	13:38:44	38.2860	-108.8982	-2.0	3.5	-0.1	0.8	1.2
6/3/2020	13:40:38	38.2845	-108.8935	-2.1	3.7	-0.9		1.3
6/9/2020	17:49:20	38.2735	-108.8940	-1.0	2.5	1.0	1.4	2.6
6/10/2020	16:16:35	38.2862	-108.8962	-2.0	3.5	0.2	1.1	1.2
6/15/2020	5:21:03	38.2840	-108.9035	-2.0	3.5	-0.4	0.5	1.6
6/17/2020	18:38:50	38.2825	-108.9066	-2.1	3.6	0.0	1.0	1.9
6/18/2020	4:40:31	38.2818	-108.9069	-2.1	3.6	-0.6		1.9
6/18/2020	8:48:20	38.2858	-108.9004	-2.0	3.5	-1.2		1.3
6/18/2020	8:48:31	38.2857	-108.8998	-2.1	3.6	0.0	0.9	1.3
6/20/2020	18:28:09	38.2842	-108.9030	-1.9	3.5	-0.1	0.9	1.5
6/21/2020	6:25:29	38.2819	-108.9068	-2.1	3.6	0.2	0.9	1.9
6/22/2020	2:57:46	38.4163	-108.9860	-5.1	6.7	0.7	1.2	15.5
6/22/2020	9:51:40	38.3105	-108.9465	-2.5	4.0	-0.3	0.6	4.8
6/22/2020	9:51:47	38.3105	-108.9465	-2.5	4.0	-0.5		4.8
6/22/2020	9:53:04	38.3106	-108.9465	-2.5	4.0	-1.6	0.4	4.8
6/22/2020	9:53:06	38.3105	-108.9464	-2.5	4.0	-0.2	0.6	4.8
6/22/2020	21:16:58	38.2837	-108.9044	-1.9	3.5	-0.4	0.5	1.6
6/24/2020	16:43:53	38.2861	-108.8986	-1.9	3.5	-0.9		1.2

Date[1]	Time[1]	Latitude (deg.)	Longitude (deg.)	Elevation[2] (km)	Depth[3] (km)	Magnitude[4]		Horizontal Distance from Injection Well (km)
						M_D	M_W	
6/26/2020	0:02:13	38.2774	-108.8304	-2.3	3.8	0.1	1.1	6.0
6/28/2020	12:08:31	38.2853	-108.9007	-2.2	3.7	-0.2	0.7	1.3
6/28/2020	15:33:55	38.2853	-108.8995	-2.2	3.7	-0.3	0.7	1.3
6/30/2020	12:50:52	38.2702	-108.9262	-0.7	2.2	-0.3	0.8	4.0
7/1/2020	11:14:37	38.2859	-108.8990	-2.0	3.5	0.1	1.0	1.2
7/3/2020	10:19:44	38.2837	-108.9042	-2.0	3.5	0.1	0.8	1.6
7/3/2020	11:35:05	38.2755	-108.9260	0.0	1.5	0.6	1.2	3.6
7/3/2020	14:53:16	38.2836	-108.9044	-1.9	3.4	-0.8		1.7
7/4/2020	4:46:51	38.2975	-108.8534	-4.2	5.7	-1.5		3.6
7/4/2020	4:46:56	38.2976	-108.8536	-4.2	5.7	-0.4		3.6
7/4/2020	4:47:06	38.3013	-108.8548	-3.7	5.2	-1.5		3.6
7/4/2020	4:47:10	38.3032	-108.8575	-3.6	5.1	-0.2		3.4
7/4/2020	4:47:16	38.2982	-108.8498	-3.0	4.5	-1.2		4.0
7/4/2020	4:47:40	38.3047	-108.8552	-4.4	5.9	-1.5		3.6
7/4/2020	4:49:40	38.2976	-108.8535	-4.2	5.7	-0.1	0.5	3.6
7/5/2020	9:35:03	38.2856	-108.8991	-1.9	3.5	-0.2	0.8	1.3
7/8/2020	1:10:01	38.2802	-108.8998	-3.1	4.6	-0.6		1.9
7/8/2020	13:50:50	38.2825	-108.9065	-2.0	3.5	-0.2	0.6	1.9
7/8/2020	18:18:58	38.2838	-108.8939	-2.6	4.1	0.8	1.4	1.4
7/10/2020	0:03:00	38.2771	-108.9150	-2.7	4.2	-0.2	0.7	2.8
7/10/2020	19:03:18	38.2804	-108.9064	-2.3	3.8	0.4	1.3	2.0
7/12/2020	0:50:37	38.2771	-108.9153	-2.7	4.2	2.7	2.8	2.8
7/12/2020	15:37:16	38.2953	-108.9278	-1.0	2.5	1.0	1.2	2.9
7/13/2020	13:27:53	38.2827	-108.9079	-2.1	3.6	0.0		1.9
7/13/2020	13:47:18	38.2827	-108.9079	-2.1	3.6	0.3	1.0	1.9
7/14/2020	17:51:53	38.2673	-108.8852	-0.3	1.8	-0.5	0.9	3.4
7/16/2020	13:04:05	38.2835	-108.9041	-2.0	3.6	-0.1	0.9	1.6
7/17/2020	10:12:58	38.2860	-108.8990	-2.0	3.5	0.5	1.1	1.2
7/17/2020	10:14:23	38.2862	-108.8990	-2.0	3.5	-0.2	0.6	1.2
7/17/2020	13:11:36	38.2770	-108.9159	-2.7	4.2	1.4	1.4	2.8
7/19/2020	0:17:08	38.3075	-108.8628	-5.1	6.6	-0.2	0.9	3.1
7/19/2020	0:39:31	38.3111	-108.7381	-7.7	9.2	0.2	1.0	13.8
7/19/2020	2:36:02	38.3052	-108.8632	-5.6	7.1	0.1		2.9
7/19/2020	17:41:22	38.2769	-108.9153	-2.8	4.3	0.3	1.1	2.8
7/21/2020	1:43:07	38.2793	-108.9055	-2.5	4.1	0.9	1.2	2.1
7/21/2020	21:24:26	38.2837	-108.9045	-2.0	3.5	0.0	0.9	1.6
7/21/2020	22:36:54	38.3143	-108.9616	-1.0	2.5	-0.3	0.9	6.2
7/22/2020	14:59:40	38.2835	-108.9046	-2.1	3.6	1.3	1.6	1.7
7/22/2020	16:25:27	38.2833	-108.9051	-2.1	3.6	0.0	0.9	1.7
7/22/2020	16:41:56	38.2833	-108.9050	-2.1	3.6	2.0	2.0	1.7

Date[1]	Time[1]	Latitude (deg.)	Longitude (deg.)	Elevation[2] (km)	Depth[3] (km)	Magnitude[4]		Horizontal Distance from Injection Well (km)
						M_D	M_W	
7/22/2020	16:42:43	38.2832	-108.9046	-2.1	3.7	-0.5		1.7
7/22/2020	16:44:07	38.2830	-108.9056	-2.1	3.6	-0.6		1.8
7/22/2020	16:44:14	38.2829	-108.9056	-2.0	3.6	-0.9		1.8
7/22/2020	16:59:55	38.2832	-108.9046	-2.1	3.6	-0.1		1.7
7/22/2020	18:17:15	38.2834	-108.9046	-2.0	3.6	-0.5		1.7
7/22/2020	21:16:38	38.2831	-108.9045	-2.1	3.6	0.5	1.1	1.7
7/22/2020	21:17:28	38.2833	-108.9044	-2.1	3.6	-0.5	0.5	1.7
7/22/2020	21:31:54	38.2831	-108.9058	-2.1	3.6	0.0	0.7	1.8
7/22/2020	22:09:31	38.2832	-108.9053	-2.1	3.6	0.5	1.1	1.7
7/22/2020	22:09:48	38.2834	-108.9052	-2.1	3.6	-0.7		1.7
7/22/2020	22:11:46	38.2833	-108.9042	-2.2	3.7	-0.4	0.6	1.7
7/23/2020	0:08:27	38.2831	-108.9062	-2.0	3.6	-0.5	0.7	1.8
7/23/2020	0:09:27	38.2829	-108.9064	-2.0	3.5	-0.9		1.8
7/23/2020	0:09:44	38.2829	-108.9065	-2.0	3.5	-0.8	1.2	1.8
7/23/2020	1:26:02	38.2819	-108.9063	-2.0	3.5	0.0	0.8	1.9
7/23/2020	3:53:58	38.2834	-108.9053	-2.1	3.6	-0.2	0.7	1.7
7/23/2020	4:56:07	38.3977	-108.8900	-2.5	4.1	-0.3		11.2
7/23/2020	5:58:55	38.2830	-108.9062	-2.0	3.6	-0.1	0.8	1.8
7/23/2020	6:00:21	38.2829	-108.9058	-2.1	3.6	0.8	1.2	1.8
7/23/2020	6:46:25	38.2828	-108.9065	-2.0	3.5	-0.1	0.7	1.8
7/24/2020	17:06:34	38.2818	-108.9064	-2.0	3.5	-0.5	0.7	1.9
7/28/2020	10:27:00	38.2857	-108.9009	-2.1	3.6	0.5	1.1	1.3
7/29/2020	0:51:57	38.2873	-108.8981	-2.1	3.6	-0.2	0.6	1.1
7/29/2020	2:41:08	38.2773	-108.9161	-2.7	4.2	0.5	1.0	2.8
7/29/2020	16:12:34	38.2822	-108.9082	-2.0	3.6	-0.6		2.0
7/29/2020	16:21:09	38.2816	-108.9104	-2.1	3.6	0.0	0.4	2.1
7/30/2020	5:45:23	38.2850	-108.9016	-2.1	3.6	-0.9		1.4
7/31/2020	14:17:50	38.2840	-108.9112	-2.3	3.8	-0.4	0.4	2.0
7/31/2020	14:35:42	38.2821	-108.9093	-1.9	3.5	-0.5		2.0
7/31/2020	14:43:50	38.2822	-108.9093	-2.0	3.5	0.2	0.9	2.0
8/1/2020	5:51:13	38.2774	-108.9162	-2.6	4.1	0.4	1.0	2.8
8/3/2020	12:23:06	38.2807	-108.9081	-2.3	3.8	-0.2	0.9	2.1
8/3/2020	12:57:21	38.2807	-108.9080	-2.3	3.8	-0.3	0.6	2.1
8/3/2020	15:50:29	38.2865	-108.9033	-2.5	4.0	-0.3		1.3
8/4/2020	6:13:27	38.2672	-108.8852	0.1	1.4	-0.5		3.4
8/5/2020	12:14:54	38.2831	-108.9040	-2.3	3.8	0.6	1.0	1.7
8/5/2020	14:41:13	38.2740	-108.9292	-0.2	1.8	0.1	0.4	3.9
8/6/2020	12:49:56	38.2829	-108.9061	-2.0	3.5	-0.4		1.8
8/7/2020	7:06:01	38.2892	-108.8974	-2.2	3.7	0.0	0.7	0.8
8/7/2020	18:23:13	38.2829	-108.9062	-2.0	3.5	0.3	1.2	1.8
8/7/2020	18:38:59	38.2829	-108.9062	-2.0	3.5	0.2	1.2	1.8

Date[1]	Time[1]	Latitude (deg.)	Longitude (deg.)	Elevation[2] (km)	Depth[3] (km)	Magnitude[4]		Horizontal Distance from Injection Well (km)
						M_D	M_W	
8/7/2020	18:40:19	38.2830	-108.9060	-2.0	3.5	0.2	0.9	1.8
8/7/2020	18:54:37	38.2828	-108.9063	-2.0	3.5	0.3	1.0	1.8
8/8/2020	2:29:28	38.2809	-108.9057	-2.3	3.8	-0.2	0.9	2.0
8/8/2020	3:45:22	38.2829	-108.9061	-2.0	3.5	-0.3		1.8
8/8/2020	7:39:20	38.2705	-108.9315	1.6	0.0	0.7	1.0	4.3
8/8/2020	19:16:08	38.2858	-108.9025	-2.3	3.9	-0.4	0.4	1.4
8/11/2020	15:51:08	38.2822	-108.9077	-2.0	3.5	-0.2	1.0	1.9
8/13/2020	1:51:08	38.2853	-108.9016	-2.0	3.5	-0.4	0.9	1.4
8/14/2020	4:53:15	38.3108	-108.7349	-7.8	9.4	1.2	1.4	14.1
8/20/2020	13:32:57	38.2819	-108.9079	-2.0	3.5	0.3	0.9	2.0
8/23/2020	3:48:08	38.2818	-108.9058	-2.3	3.8	-0.1	0.7	1.9
8/23/2020	10:29:50	38.2838	-108.8878	-2.7	4.2	0.3	0.8	1.6
8/23/2020	19:19:02	38.2836	-108.9041	-2.0	3.6	0.6	1.0	1.6
8/23/2020	19:19:34	38.2848	-108.9042	-2.1	3.6	-1.1	0.4	1.5
8/27/2020	3:15:38	38.2828	-108.9070	-2.1	3.7	0.0	1.0	1.9
8/27/2020	18:26:14	38.2836	-108.9056	-2.0	3.5	-0.1	0.6	1.7
8/27/2020	22:44:55	38.2820	-108.8703	-2.4	3.9	-0.2	0.9	2.7
8/30/2020	12:46:34	38.2768	-108.8340	-2.2	3.8	0.7	1.1	5.8
9/1/2020	11:51:44	38.1322	-108.5510	-3.1	4.6	0.9	1.1	35.2
9/2/2020	10:06:23	38.2730	-108.9213	-0.1	1.6	0.7	1.0	3.5
9/5/2020	5:17:21	38.3490	-108.9138	-4.2	5.7	-0.4		6.1
9/5/2020	23:48:12	38.2819	-108.9095	-1.9	3.4	-0.7	0.9	2.1
9/7/2020	2:46:21	38.4122	-108.9345	-5.9	7.4	-0.3		13.3
9/10/2020	8:14:34	38.3505	-108.9062	-3.5	5.0	1.0	1.2	6.1
9/11/2020	0:19:28	38.2846	-108.9027	-2.0	3.5	-0.4	0.8	1.5
9/12/2020	20:03:56	38.2830	-108.9052	-2.3	3.8	0.0	0.6	1.7
9/14/2020	12:36:36	38.2670	-108.9395	-0.6	2.1	-0.1	0.6	5.1
9/16/2020	9:18:52	38.4099	-108.9330	-4.8	6.3	0.5	1.1	13.0
9/16/2020	15:26:40	38.2785	-108.9045	-2.8	4.3	3.1	3.3	2.2
9/16/2020	18:13:39	38.2766	-108.9035	-2.6	4.1	-0.7		2.3
9/21/2020	6:35:16	38.2850	-108.9014	-2.2	3.7	-0.2		1.4
9/26/2020	13:08:21	38.2843	-108.9026	-2.0	3.6	0.3	0.9	1.5
10/2/2020	2:02:31	38.2859	-108.8987	-2.0	3.6	0.0	1.0	1.2
10/3/2020	7:47:21	38.2859	-108.8988	-2.0	3.6	1.0	1.2	1.2
10/5/2020	1:34:33	38.2825	-108.9058	-2.0	3.5	0.8	1.2	1.8
10/5/2020	3:22:13	38.2818	-108.9065	-2.1	3.7	1.5	1.4	1.9
10/5/2020	6:11:47	38.2826	-108.9060	-2.0	3.5	1.3	1.4	1.8
10/5/2020	6:12:19	38.2827	-108.9062	-1.9	3.4	-0.5		1.8
10/5/2020	7:06:32	38.2826	-108.9062	-2.0	3.5	1.2	1.3	1.8
10/5/2020	7:10:50	38.2827	-108.9064	-2.0	3.5	0.0	0.7	1.8
10/5/2020	10:27:45	38.2827	-108.9063	-2.0	3.5	0.3	0.9	1.8

Date[1]	Time[1]	Latitude (deg.)	Longitude (deg.)	Elevation[2] (km)	Depth[3] (km)	Magnitude[4]		Horizontal Distance from Injection Well (km)
						M_D	M_W	
10/5/2020	13:36:59	38.1660	-108.6187	-7.4	8.9	0.2		28.2
10/5/2020	13:37:37	38.1752	-108.6087	-9.0	10.5	0.1		28.5
10/6/2020	6:56:08	38.2805	-108.9148	-1.6	3.1	-0.4	0.3	2.5
10/8/2020	14:29:19	38.2821	-108.9075	-2.0	3.6	-0.1	0.5	1.9
10/8/2020	23:46:13	38.2848	-108.9022	-1.9	3.4	-0.4	1.2	1.4
10/10/2020	3:22:13	38.2771	-108.9171	-2.6	4.1	-0.5	1.1	2.9
10/10/2020	7:09:29	38.2825	-108.9063	-2.2	3.7	2.1	1.8	1.8
10/10/2020	17:28:49	38.2771	-108.9171	-2.6	4.1	-0.3	1.0	2.9
10/12/2020	19:06:37	38.2827	-108.9062	-2.0	3.5	-0.2		1.8
10/12/2020	21:30:21	38.2831	-108.9040	-2.2	3.8	-0.5	0.7	1.7
10/14/2020	5:11:55	38.4785	-108.9477	-12.8	14.3	0.1	1.0	20.7
10/15/2020	18:29:45	38.2854	-108.8915	-2.2	3.7	-0.1	1.1	1.3
10/16/2020	22:48:37	38.2856	-108.8970	-2.1	3.6	0.5	1.2	1.2
10/16/2020	22:53:23	38.2856	-108.8977	-2.0	3.5	-1.3		1.2
10/16/2020	22:57:08	38.2856	-108.8973	-2.1	3.6	-0.5		1.2
10/16/2020	23:06:49	38.2856	-108.8972	-2.0	3.6	-0.8	0.7	1.2
10/16/2020	23:40:41	38.2856	-108.8971	-2.1	3.6	0.5	1.2	1.2
10/16/2020	23:41:32	38.2857	-108.8972	-2.1	3.6	-0.7		1.2
10/16/2020	23:44:44	38.2856	-108.8970	-2.1	3.6	1.5	1.6	1.2
10/17/2020	0:45:07	38.2857	-108.8971	-2.0	3.6	-0.4	0.5	1.2
10/17/2020	1:08:06	38.2857	-108.8975	-2.1	3.6	-0.9	0.5	1.2
10/17/2020	1:12:55	38.2856	-108.8973	-2.1	3.6	-0.2	0.6	1.2
10/17/2020	3:04:45	38.2855	-108.8970	-2.1	3.6	0.8	1.2	1.2
10/19/2020	2:03:11	38.3112	-108.7321	-7.9	9.4	0.5	1.1	14.3
10/26/2020	9:53:02	38.2861	-108.8990	-2.0	3.5	-0.5	1.1	1.2
10/28/2020	21:18:38	38.3458	-108.8946	-4.3	5.8	-0.2	1.0	5.5
10/29/2020	5:20:48	38.2856	-108.8998	-1.9	3.5	-0.7		1.3
10/29/2020	14:48:33	38.2819	-108.9083	-2.0	3.5	-0.6	0.9	2.0
10/31/2020	22:36:59	38.4388	-109.0023	-1.7	3.2	0.7	1.2	18.4
11/1/2020	2:42:09	38.4725	-109.0243	-3.6	5.1	0.3	0.8	22.6
11/3/2020	0:03:48	38.2680	-108.9350	0.0	1.5	0.7	1.1	4.7
11/3/2020	0:40:25	38.2856	-108.8996	-1.9	3.4	-0.7	0.6	1.3
11/6/2020	13:47:12	38.4427	-109.0372	-3.2	4.7	1.4	1.5	20.4
11/6/2020	22:52:47	38.2856	-108.8974	-2.1	3.6	0.5	1.4	1.2
11/6/2020	22:53:06	38.2855	-108.8973	-2.1	3.6	-0.3	1.5	1.2
11/7/2020	14:03:02	38.4492	-109.0355	-3.7	5.2	0.6	1.5	20.9
11/7/2020	17:51:20	38.2856	-108.8974	-2.1	3.6	0.8	1.3	1.2
11/7/2020	18:43:36	38.4415	-109.0220	-2.0	3.5	0.6	1.1	19.5
11/7/2020	20:35:02	38.4717	-109.0492	-2.2	3.7	0.5	1.5	23.6
11/8/2020	3:18:53	38.2707	-108.8885	-1.4	2.9	0.0	1.3	2.9
11/8/2020	11:19:57	38.2766	-108.9180	-2.7	4.3	3.0	3.6	3.0

Date[1]	Time[1]	Latitude (deg.)	Longitude (deg.)	Elevation[2] (km)	Depth[3] (km)	Magnitude[4]		Horizontal Distance from Injection Well (km)
						M_D	M_W	
11/8/2020	12:08:56	38.2754	-108.9183	-3.1	4.6	-0.4	1.1	3.1
11/8/2020	13:05:54	38.2753	-108.9167	-2.9	4.4	-0.3	0.9	3.0
11/8/2020	13:32:35	38.2769	-108.9188	-2.6	4.1	2.5	2.7	3.0
11/8/2020	13:39:14	38.2758	-108.9198	-2.8	4.4	0.3	1.3	3.2
11/8/2020	13:42:49	38.2766	-108.9193	-2.7	4.2	2.5	2.8	3.1
11/8/2020	13:49:53	38.2758	-108.9198	-2.9	4.4	-0.3	0.9	3.2
11/8/2020	14:07:24	38.2760	-108.9197	-2.8	4.3	-0.3	0.9	3.1
11/8/2020	14:10:19	38.2762	-108.9193	-2.8	4.3	1.2	1.7	3.1
11/8/2020	15:13:03	38.2770	-108.9164	-2.7	4.2	-0.3	0.8	2.9
11/8/2020	16:45:54	38.2771	-108.9185	-2.6	4.1	-0.2	0.9	3.0
11/8/2020	20:47:05	38.2775	-108.9171	-2.5	4.0	0.7	1.5	2.9
11/9/2020	6:28:41	38.2751	-108.9183	-3.2	4.7	0.3	1.1	3.1
11/9/2020	6:29:21	38.2752	-108.9183	-3.2	4.7	-0.2	0.7	3.1
11/9/2020	9:37:43	38.2760	-108.9196	-2.8	4.3	0.7	1.2	3.1
11/9/2020	9:54:33	38.2773	-108.9184	-2.5	4.0	0.2	0.9	3.0
11/9/2020	14:08:43	38.2767	-108.9167	-2.8	4.3	1.2	1.6	2.9
11/10/2020	1:22:57	38.2772	-108.9185	-2.5	4.1	-0.5	0.7	3.0
11/10/2020	5:42:33	38.2821	-108.9086	-2.0	3.6	-0.6		2.0
11/10/2020	14:13:47	38.2767	-108.9200	-2.6	4.1	0.1	0.9	3.1
11/10/2020	19:29:12	38.3552	-108.7017	-9.0	10.6	0.4	1.2	18.1
11/10/2020	23:23:47	38.2767	-108.9200	-2.6	4.1	-0.1	0.8	3.1
11/11/2020	1:36:48	38.2757	-108.9208	-2.8	4.3	-0.5		3.2
11/11/2020	3:57:07	38.2762	-108.9196	-2.7	4.3	2.2	2.0	3.1
11/11/2020	4:20:02	38.2761	-108.9200	-2.8	4.3	-0.3		3.1
11/12/2020	3:40:18	38.2768	-108.9199	-2.6	4.1	0.3	1.0	3.1
11/12/2020	8:15:39	38.2775	-108.9179	-2.5	4.0	1.3	1.3	2.9
11/12/2020	23:40:31	38.2776	-108.9176	-2.5	4.0	0.4	1.2	2.9
11/13/2020	0:22:16	38.2775	-108.9174	-2.5	4.0	1.7	1.7	2.9
11/13/2020	6:26:22	38.2756	-108.9208	-2.8	4.4	0.3	1.1	3.2
11/13/2020	6:26:37	38.2757	-108.9208	-2.8	4.3	-0.5		3.2
11/13/2020	14:30:20	38.2823	-108.9087	-2.0	3.5	-1.0		2.0
11/13/2020	20:33:17	38.2776	-108.9175	-2.5	4.0	0.4	1.1	2.9
11/14/2020	4:57:39	38.2757	-108.9208	-2.8	4.3	-0.6	0.8	3.2
11/14/2020	6:45:40	38.2715	-108.9360	-0.3	1.8	0.3	0.9	4.5
11/14/2020	7:38:11	38.2838	-108.9023	-2.0	3.5	-0.2	0.8	1.6
11/14/2020	7:55:40	38.2757	-108.9208	-2.8	4.3	-0.2	1.0	3.2
11/14/2020	12:47:18	38.4037	-108.8711	-4.4	5.9	0.2	1.4	12.1
11/14/2020	14:48:29	38.4037	-108.8712	-4.4	5.9	0.2	0.7	12.1
11/14/2020	14:55:54	38.4035	-108.8712	-4.4	5.9	-0.1		12.1
11/14/2020	15:24:40	38.4038	-108.8712	-4.4	5.9	0.3	1.1	12.1
11/15/2020	7:54:28	38.3112	-108.7322	-7.9	9.4	0.1	1.2	14.3

Date[1]	Time[1]	Latitude (deg.)	Longitude (deg.)	Elevation[2] (km)	Depth[3] (km)	Magnitude[4]		Horizontal Distance from Injection Well (km)
						M_D	M_W	
11/15/2020	10:08:09	38.2771	-108.9193	-2.5	4.1	1.5	1.5	3.0
11/15/2020	13:49:22	38.3225	-108.8568	-5.1	6.6	0.7	1.1	4.4
11/15/2020	22:17:26	38.2825	-108.9000	-2.6	4.1	-0.1	1.3	1.6
11/17/2020	6:11:08	38.2757	-108.9209	-2.8	4.3	0.9	1.3	3.2
11/18/2020	14:11:16	38.2857	-108.9001	-2.0	3.5	-0.1		1.3
11/20/2020	5:45:36	38.2849	-108.9021	-1.7	3.2	-1.0	1.0	1.4
11/20/2020	12:54:23	38.2774	-108.9181	-2.5	4.0	0.3	1.0	2.9
11/20/2020	17:55:30	38.2836	-108.9044	-1.9	3.5	-1.0		1.7
11/20/2020	20:36:29	38.2837	-108.9042	-1.9	3.4	-0.6		1.6
11/21/2020	3:35:07	38.2781	-108.9157	-2.4	3.9	0.1	0.8	2.7
11/21/2020	4:15:34	38.2775	-108.9194	-2.4	3.9	1.3	1.4	3.0
11/21/2020	4:29:07	38.2760	-108.9204	-2.8	4.3	-0.2	0.8	3.2
11/21/2020	4:34:06	38.2836	-108.9045	-1.9	3.5	-0.5		1.7
11/21/2020	10:27:12	38.2845	-108.9020	-2.1	3.6	0.3	0.9	1.5
11/22/2020	7:07:24	38.2851	-108.9002	-1.9	3.4	-0.1	0.5	1.3
11/22/2020	18:02:48	38.2856	-108.8976	-2.1	3.6	-0.5		1.2
11/23/2020	10:15:51	38.2819	-108.9077	-2.0	3.5	-0.5		2.0
11/23/2020	14:59:32	38.2778	-108.9186	-2.4	3.9	0.0	0.8	2.9
11/24/2020	5:33:30	38.2837	-108.9045	-1.9	3.4	-0.1		1.7
11/25/2020	8:52:54	38.2849	-108.9012	-1.8	3.4	-0.9		1.4
11/25/2020	8:53:05	38.2852	-108.9010	-2.0	3.5	-1.0	0.7	1.4
11/26/2020	6:16:48	38.3082	-108.9249	-2.8	4.3	0.7	1.1	2.9
11/26/2020	10:55:12	38.2838	-108.9034	-2.2	3.7	0.0	0.6	1.6
11/27/2020	9:43:34	38.2850	-108.9014	-2.2	3.8	-0.7	0.5	1.4
11/28/2020	6:59:06	38.2828	-108.8975	-1.9	3.4	0.7	0.9	1.5
11/30/2020	9:52:00	38.2779	-108.9176	-2.4	3.9	1.3	1.4	2.9
12/1/2020	23:43:07	38.2772	-108.9183	-2.5	4.1	-1.1	1.4	3.0
12/2/2020	2:02:36	38.2778	-108.9172	-2.4	4.0	0.3	1.3	2.8
12/2/2020	20:41:37	38.2776	-108.9195	-2.4	3.9	-0.2	0.8	3.0
12/3/2020	0:08:50	38.2859	-108.8990	-2.0	3.5	-0.5	0.7	1.2
12/4/2020	4:49:45	38.2778	-108.9176	-2.4	3.9	0.4	1.0	2.9
12/4/2020	13:15:13	38.2818	-108.9079	-2.0	3.5	0.6	1.0	2.0
12/4/2020	22:11:50	38.2853	-108.9008	-1.9	3.5	-0.4		1.4
12/5/2020	5:51:08	38.2861	-108.8988	-2.0	3.6	-0.2	0.8	1.2
12/5/2020	23:19:56	38.3107	-108.7348	-7.9	9.4	0.4	0.9	14.1
12/5/2020	23:40:26	38.2778	-108.8279	-2.3	3.8	0.7	1.2	6.2
12/6/2020	10:13:25	38.2780	-108.9181	-2.4	3.9	0.2	0.8	2.9
12/6/2020	11:09:39	38.2837	-108.9045	-2.0	3.5	-0.4		1.7
12/8/2020	3:23:50	38.2771	-108.9186	-2.5	4.1	0.7	1.2	3.0
12/8/2020	19:32:29	38.2860	-108.8983	-2.0	3.5	0.3	0.9	1.2
12/8/2020	22:53:42	38.2769	-108.9157	-2.7	4.3	3.0	3.5	2.8

Date[1]	Time[1]	Latitude (deg.)	Longitude (deg.)	Elevation[2] (km)	Depth[3] (km)	Magnitude[4]		Horizontal Distance from Injection Well (km)
						M_D	M_W	
12/8/2020	23:39:37	38.2776	-108.9183	-2.4	4.0	-0.3	0.8	2.9
12/8/2020	23:41:07	38.2769	-108.9193	-2.6	4.1	0.8	1.2	3.1
12/9/2020	0:12:22	38.2778	-108.9163	-2.5	4.1	-0.1	0.9	2.8
12/9/2020	0:30:46	38.2777	-108.9184	-2.4	4.0	0.5	1.1	2.9
12/9/2020	2:01:04	38.2778	-108.9190	-2.4	3.9	1.9	1.8	3.0
12/9/2020	2:23:09	38.2776	-108.9198	-2.4	3.9	1.8	1.7	3.0
12/9/2020	2:40:59	38.2775	-108.9193	-2.4	4.0	0.6	1.1	3.0
12/9/2020	2:49:01	38.2778	-108.9177	-2.4	3.9	0.4	1.2	2.9
12/9/2020	3:51:10	38.3388	-108.8585	-2.6	4.1	-0.3		5.7
12/9/2020	4:46:19	38.2774	-108.9198	-2.4	3.9	0.5	1.1	3.0
12/9/2020	6:23:04	38.4437	-109.0205	-3.7	5.2	2.4	2.1	19.7
12/9/2020	9:07:06	38.3127	-108.8690	-3.0	4.5	-0.5		2.9
12/9/2020	12:01:11	38.2648	-108.9247	-3.1	4.7	-0.2		4.4
12/9/2020	13:49:35	38.2778	-108.9190	-2.4	3.9	0.5	1.1	3.0
12/10/2020	5:59:51	38.2854	-108.9005	-1.9	3.4	-0.6	0.1	1.3
12/10/2020	20:54:43	38.2757	-108.9210	-2.8	4.3	0.4	1.2	3.2
12/11/2020	11:18:14	38.2780	-108.9183	-2.4	3.9	1.7	1.7	2.9
12/12/2020	8:27:10	38.2774	-108.9200	-2.4	4.0	1.2	1.3	3.1
12/12/2020	10:45:55	38.2856	-108.8999	-2.0	3.6	0.0	0.6	1.3
12/12/2020	10:51:15	38.2774	-108.9200	-2.4	4.0	-0.1	0.7	3.0
12/12/2020	13:47:52	38.2771	-108.9204	-2.5	4.0	1.2	1.5	3.1
12/12/2020	14:48:27	38.2770	-108.9189	-2.5	4.1	0.0	0.9	3.0
12/12/2020	15:09:45	38.2774	-108.9191	-2.4	4.0	1.4	1.5	3.0
12/12/2020	20:43:13	38.2773	-108.9196	-2.5	4.0	2.4	2.3	3.0
12/12/2020	23:21:16	38.2777	-108.9198	-2.4	3.9	0.8	1.4	3.0
12/13/2020	6:57:20	38.2845	-108.9088	-2.2	3.7	-1.2	0.4	1.8
12/13/2020	11:34:27	38.2830	-108.9045	-2.1	3.6	-0.3	0.6	1.7
12/13/2020	14:51:21	38.2780	-108.9179	-2.4	3.9	0.0	0.9	2.9
12/13/2020	15:57:40	38.2827	-108.8940	-2.8	4.4	-0.3	1.0	1.5
12/13/2020	17:50:47	38.2776	-108.9195	-2.4	3.9	0.5	1.0	3.0
12/14/2020	5:06:44	38.2781	-108.9146	-2.4	3.9	0.0	0.8	2.7
12/14/2020	9:51:29	38.4538	-109.0375	-4.2	5.7	0.4	1.1	21.4
12/14/2020	11:08:39	38.2767	-108.9204	-2.5	4.1	0.1	0.8	3.1
12/14/2020	12:57:19	38.2770	-108.9211	-2.5	4.0	0.6	1.1	3.2
12/15/2020	8:13:56	38.2773	-108.9200	-2.4	4.0	-0.6	0.7	3.1
12/15/2020	19:52:23	38.2779	-108.9174	-2.4	3.9	0.5	1.1	2.8
12/15/2020	23:24:08	38.2771	-108.9202	-2.5	4.0	1.9	1.9	3.1
12/16/2020	16:27:47	38.2780	-108.9176	-2.4	3.9	-0.7		2.9
12/17/2020	10:25:12	38.2817	-108.9073	-2.0	3.6	1.9	1.8	2.0
12/17/2020	20:24:30	38.2772	-108.9190	-2.5	4.0	1.7	1.7	3.0
12/18/2020	17:38:19	38.4592	-109.0068	-3.0	4.5	1.2	1.4	20.5

Date[1]	Time[1]	Latitude (deg.)	Longitude (deg.)	Elevation[2] (km)	Depth[3] (km)	Magnitude[4]		Horizontal Distance from Injection Well (km)
						M_D	M_W	
12/19/2020	0:12:33	38.2776	-108.9201	-2.4	3.9	-0.3	1.0	3.0
12/19/2020	2:38:08	38.2775	-108.9203	-2.4	3.9	0.3	0.9	3.1
12/19/2020	10:14:30	38.3303	-108.8873	0.5	1.0	-0.5		3.8
12/19/2020	21:47:20	38.2833	-108.9047	-2.0	3.5	0.0	0.7	1.7
12/20/2020	1:53:43	38.2777	-108.9182	-2.4	4.0	3.0	3.3	2.9
12/20/2020	2:05:24	38.2779	-108.9194	-2.3	3.9	-0.1	0.7	3.0
12/20/2020	2:11:06	38.2757	-108.9206	-2.8	4.3	3.2	3.9	3.2
12/20/2020	2:24:19	38.2770	-108.9212	-2.5	4.0	-0.9	0.5	3.2
12/20/2020	2:33:31	38.2776	-108.9203	-2.4	3.9	0.0	0.8	3.1
12/20/2020	2:40:44	38.2745	-108.9215	-3.1	4.6	-0.2	0.5	3.4
12/20/2020	2:54:37	38.2780	-108.9195	-2.3	3.8	2.0	2.0	3.0
12/20/2020	2:55:13	38.2779	-108.9193	-2.3	3.9	-0.4	1.4	3.0
12/20/2020	3:10:31	38.2761	-108.9183	-2.9	4.4	1.7	1.6	3.1
12/20/2020	3:29:05	38.2750	-108.9233	-2.9	4.4	-0.7	0.8	3.4
12/20/2020	4:08:58	38.2747	-108.9232	-3.0	4.5	0.0	0.8	3.5
12/20/2020	4:11:38	38.2787	-108.9183	-2.0	3.5	-1.2	0.4	2.8
12/20/2020	5:45:04	38.2779	-108.9197	-2.3	3.8	1.2	1.2	3.0
12/20/2020	6:11:42	38.2779	-108.9203	-2.3	3.8	-0.3	0.6	3.0
12/20/2020	8:50:07	38.2782	-108.9207	-1.2	2.7	-1.0	0.2	3.0
12/20/2020	10:57:30	38.2783	-108.9181	-2.2	3.8	-0.5	0.3	2.9
12/20/2020	12:10:39	38.2779	-108.9201	-2.3	3.8	0.6	1.1	3.0
12/20/2020	12:16:23	38.2783	-108.9181	-2.2	3.8	0.1	0.8	2.9
12/20/2020	12:39:47	38.2755	-108.9239	-2.7	4.3	-0.5	0.5	3.4
12/20/2020	14:26:43	38.2856	-108.9003	-2.0	3.5	-0.1	0.5	1.3
12/20/2020	16:45:27	38.2767	-108.9204	-2.5	4.0	0.8	1.3	3.1
12/20/2020	17:34:21	38.2776	-108.9205	-2.4	3.9	0.5	1.1	3.1
12/20/2020	20:31:40	38.2751	-108.9242	-2.9	4.4	0.6	1.2	3.5
12/20/2020	20:40:46	38.2775	-108.9207	-2.4	3.9	1.5	1.5	3.1
12/20/2020	20:48:28	38.2747	-108.9206	-3.1	4.6	-0.2	0.4	3.3
12/20/2020	21:01:14	38.2768	-108.9213	-2.5	4.0	2.7	2.5	3.2
12/20/2020	22:24:04	38.2855	-108.9001	-2.0	3.5	-1.0		1.3
12/20/2020	22:25:24	38.2855	-108.9023	-0.7	2.3	-1.2		1.4
12/20/2020	22:26:04	38.2856	-108.9001	-2.0	3.6	-0.9		1.3
12/20/2020	23:58:23	38.2781	-108.9169	-2.4	3.9	1.3	1.4	2.8
12/21/2020	0:37:52	38.2754	-108.9183	-3.1	4.7	-0.7		3.1
12/21/2020	12:11:24	38.2810	-108.9139	-1.5	3.0	-0.5		2.4
12/22/2020	6:46:49	38.2840	-108.9035	-1.9	3.5	-0.7		1.6
12/22/2020	11:03:31	38.2839	-108.9036	-2.0	3.5	-0.5		1.6
12/23/2020	8:40:06	38.2836	-108.9045	-1.9	3.5	-0.7		1.7
12/23/2020	13:28:13	38.2769	-108.9174	-2.7	4.3	-0.3	0.8	2.9
12/23/2020	16:58:02	38.2752	-108.9243	-2.9	4.4	0.1	1.1	3.5

Date[1]	Time[1]	Latitude (deg.)	Longitude (deg.)	Elevation[2] (km)	Depth[3] (km)	Magnitude[4]		Horizontal Distance from Injection Well (km)
						M_D	M_W	
12/24/2020	22:51:14	38.2818	-108.9069	-2.1	3.6	-0.6		1.9
12/25/2020	13:31:37	38.2748	-108.9237	-2.9	4.5	0.5		3.5
12/25/2020	14:28:37	38.2749	-108.9232	-3.0	4.5	-0.2		3.5
12/25/2020	16:33:12	38.2839	-108.9036	-2.0	3.5	-0.4	1.2	1.6
12/25/2020	21:40:12	38.2849	-108.9015	-2.2	3.7	-0.2	0.5	1.4
12/26/2020	6:41:56	38.2835	-108.9051	-1.9	3.5	-0.2	0.5	1.7
12/26/2020	14:58:34	38.2778	-108.9153	-2.5	4.0	0.5	1.0	2.7
12/26/2020	15:58:05	38.2827	-108.9064	-1.9	3.4	-0.5		1.8
12/26/2020	16:25:20	38.2775	-108.9133	-2.6	4.1	-0.5		2.7
12/26/2020	20:02:22	38.3032	-108.8838	-1.6	3.1	-0.8	1.2	1.2
12/27/2020	5:11:53	38.2780	-108.9200	-2.3	3.8	0.9	1.2	3.0
12/28/2020	8:43:41	38.2789	-108.8992	-3.1	4.7	1.8	1.4	2.0
12/28/2020	13:25:50	38.2780	-108.9199	-2.3	3.8	0.1	0.9	3.0
12/29/2020	20:58:34	38.2682	-108.8750	-1.0	2.5	-0.2	0.5	3.6
12/30/2020	0:35:18	38.2751	-108.9228	-2.9	4.4	-0.2		3.4
12/30/2020	1:49:16	38.2767	-108.9175	-2.7	4.3	0.2	0.9	3.0
12/30/2020	2:55:10	38.2752	-108.9241	-2.9	4.4	-0.1	0.8	3.5
12/30/2020	3:03:35	38.2808	-108.9070	-2.3	3.8	-0.5	0.7	2.0

[1] Date and time listed are in Coordinated Universal Time, UTC (Mountain Standard Time = UTC – 7 hours; Mountain Daylight Savings Time = UTC – 6 hours)
[2] Elevation is given with respect to mean sea level.
[3] Depth is referenced to the surveyed ground surface elevation at the injection wellhead, 1.524 km.
[4] M_D = duration magnitude; M_W = moment magnitude. All magnitudes computed using only PVSN data.